GEO-3900

MASTER'S THESIS IN GEOLOGY

---

# Geology, mineralogy and geochemistry of the Holmsletfjella Au-As occurrence, West Spitsbergen Fold Belt, Svalbard


Håvard Kvåle Simonsen


May 2012


FACULTY OF SCIENCE AND TECHNOLOGY

DEPARTMENT OF GEOLOGY

University of Tromsø

GEO-3900

MASTER'S THESIS IN GEOLOGY

# Geology, mineralogy and geochemistry of the Holmsletfjella Au-As occurrence, West Spitsbergen Fold Belt, Svalbard

Håvard Kvåle Simonsen

May 2012

## Acknowledgement

I wish to thank my supervisors, associated professor Kåre Kullerud from the University of Tromsø, professor (professor II at the University of Tromsø) Krister Sundblad from the University of Turku and Dr. Juhani Ojala from Store Norske Gull, for all their help with my thesis. I also whish to thank Harald Hansen for the help with the cross-section of the drill holes and the aerial photo. Store Norske Gulls exploration group; Morten Often, Dr. Juhani Ojala, Harald Hansen and Hannu Ahola is also to thanked for whom made this thesis possible.

Most of all my beloved Ane for her encouragement and support throughout this thesis.

Tromsø, May 2012

Håvard K. Simonsen

## Abstract

Holmsletfjella is situated on the southern side of St. Jonsfjorden on the archipelago of Svalbard. The drill core herein studied is part of an exploration program by Store Norske. Chemical analysis of the drill cores in combination with the geological history have reviled the Holmsletfjella Formation and the Ultramafic Vestgötabreen Complex to have been altered by fluids migrating through the rocks during the formation of the Caledonian mountain chain. These fluids were sourced from VAMSNAZ (V, As, Mo, Se, Ni, Ag and Zn) shales, which is an excellent source of gold. At the same time as the fluids were migrating the serpentinites of the Ultramafic Vestgötabreen Complex underwent listwanite alteration that resulted in partial alteration of the serpentinites into listwanites. Possible gold deposits may have been displaced or remobilised during the generation of the West Spitsbergen Fold Belt thereby making the work locating the gold deposits harder.

## Contents

# 1 – Introduction

## 1.1 – Context of the study

Gold prices have risen with a factor of about 4 in the last 10 years. This rise in gold price is partly due to the recession where moving assets into a stable markets has been a way to secure the assets. Before the recession in 2008 gold prices had already started to rice so there is at least another factor involved. As pointed out by (McKeith et al., 2010) fewer high-quality discoveries are being made and the cost per ounce gold discovered continues to rice.

With the incentive of the gold prices Store Norske Gull AS started with preliminary prospecting along the west coast of Spitsbergen in 2008. From the preliminary prospecting the south shore of St. Jonsfjorden were chosen for an additional two weeks of fieldwork in 2009 which gave the foundation a drilling program in the winter/spring of 2010. By the end of August 2010 another two weeks of fieldwork had been conducted in the surrounding areas of St. Jonsfjorden. Bureaucracy in 2011 blocked further work so that no fieldwork or drilling was done. Continued work in the region is planed for 2013.

Very little work has been done in this region in terms of gold prospecting. Gaining an understanding of the area in relation to gold mineralizations is key in order to optimize the prospecting methods and making educated assessments of the results.

## 1.2 – Purpose of the study

The purpose of the study is to provide geological, structural, metamorphic, petrographic and geochemical information on the gold mineralisation in the Holmsletfjella target in the St Jonsfjorden area. Through the use of the data gain an understanding of the structural, metamorphic and hydrothermal history of the deposit and the relationship of the gold mineralisation to the geological history. From applying the data and the history of the deposit develop a genetic model for the gold mineralisation.

## 1.3 – Geography of the Study Area

The area of study is located on the island of Spitsbergen, which is the largest island of the Svalbard Archipelago. Spitsbergen is situated between approximately 77°N and 80°N. The study area is positioned at the mountain of Holmsletfjella along the west coast on the southern side the St. Jonsfjorden (Fig. 1.1 and 1.2). From Longyearbyen (Fig. 1.1) the area is accessible by snowmobile and helicopter during winter, and boat and helicopter during summer. The terrain is alpine with glaciers separating some of the ridges. Scree and glaciers are the main reasons for limited exposures in the area.


**Figure 1.1:** Overview of Svalbard and Svalbard's location in the right hand corner. The red shaded area marks the location of figure 1.2. Modified from (Polarinstitutt, 2011).


**Figure 1.2:** Overview of the St. Jonsfjorden, with the red circle marking the study area on Holmsletfjella. Modified from (Polarinstitutt, 2011).

## 1.4 – Regional Geology

The Pre-Devonian basement (Fig. 1.3) on Svalbard is separated into three different terrains: the Northeastern (Nordaustlandet), Northwestern and Southwestern (Fig. 1.4). In post Silurian time the three terrains were accumulated into forming Svalbard (Fig. 1.4). From Devonian time up trough Cenozoic time the main accumulation of new rock has been from deposition of sediments. (Harland et al., 1974, Harland and Wright, 1979, Harland et al., 1997)

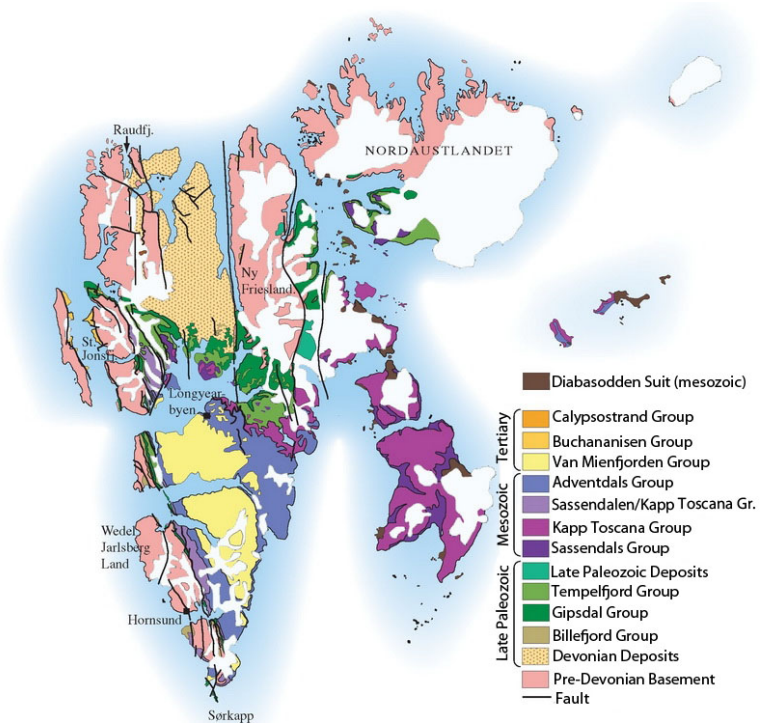


**Figure 1.3:** Regional geology of Svalbard with the different groups and their spatial distribution. Modified from (Fossen et al., 2007).

### 1.4.1 – Northeastern Terrain (Nordaustlandet)

Between 1200 and 960 Ma the Northeastern Terrain was a basin of alternating deposition of lava and sediments. The Svekonorwegian orogenic event resulted in folding of the volcanic and sedimentary rocks, and intrusions of granites at about 950 Ma. Elevation and erosion followed the Svekonorwegian orogenic event, and the erosion surface was superimposed by a late Proterozoic sedimentary package of basal conglomerate, schist, quartzite and carbonate. The sedimentation continued until the Caledonian Orogeny interrupted it with folding and granite intrusions. (Harland and Wright, 1979, Dallmann and Ohta, Birkenmajer, 1981, Harland et al., 1997)

### 1.4.2 – Northwestern Terrain

The Northwestern Terrain is composed of schists, migmatites and marble likely of Mid-Proterozoic age that has been intruded by granitic plutons ca. 960 Ma ago. Diabase dykes related to rifting in late Precambrian cut the Precambrian bedrock. (Harland and Wright, 1979, Dallmann and Ohta, Birkenmajer, 1981, Harland et al., 1997)

### 1.4.3 – Southwestern Terrain

Neoproterozoic sediments make up the Southwestern Terrain that has been strongly influenced by Caledonian deformation. The Caledonian deformation resulted in a 2-5 kilometres wide and a least 50 kilometres long zone of serpentinites, eclogites, blue schist and flysch. Some areas have been affected by the Svekonorwegian event and later superimposed by late Proterozoic sediments. (Harland and Wright, 1979, Dallmann and Ohta, Birkenmajer, 1981, Harland et al., 1997)

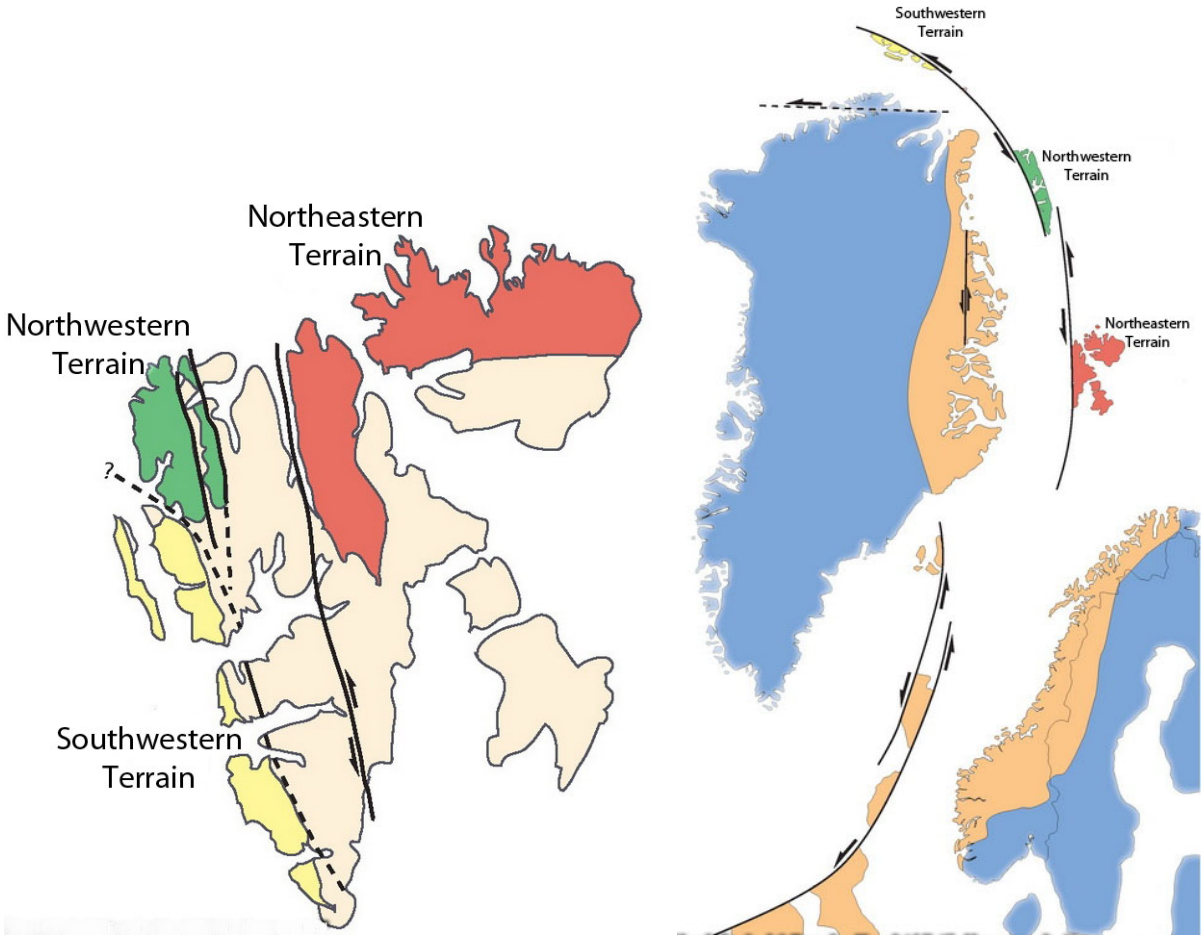


**Figure 1.4:** Placement and accumulation of the different terrains in post Silurian time as proposed by (Harland et al., 1974). Modified from (Fossen et al., 2007).

### 1.4.4 – Devonian

Most of the Devonian deposits (Old Red Sandstone) are located on the northern part of Spitsbergen between the Northwestern and Northeastern Terrain. On Svalbard the Devonian deposits represent a molasse basin, which was created by the collapse of the Caledonian mountain chain. The Svalbardian event has affected the Devonian but not the Carboniferous rocks; the deformation was related to deep and penetrating fault zones that were reactivated with transpression. (Harland and Wright, 1979, Dallmann and Ohta, Birkenmajer, 1981)

### 1.4.5 – Carboniferous

Greyish sandstones, dark mudstones, coal and plant fossils were deposited in isolated basins in early Carboniferous. The sediments were of continental origin. Movement along the Paleo-Hornsund fault resulted in the formation of narrow basins along the west coast of Spitsbergen, with thick deposits of sand and gravel (Fig. 1.5). (Dallmann and Ohta, Birkenmajer, 1981, Dallmann, 1999)

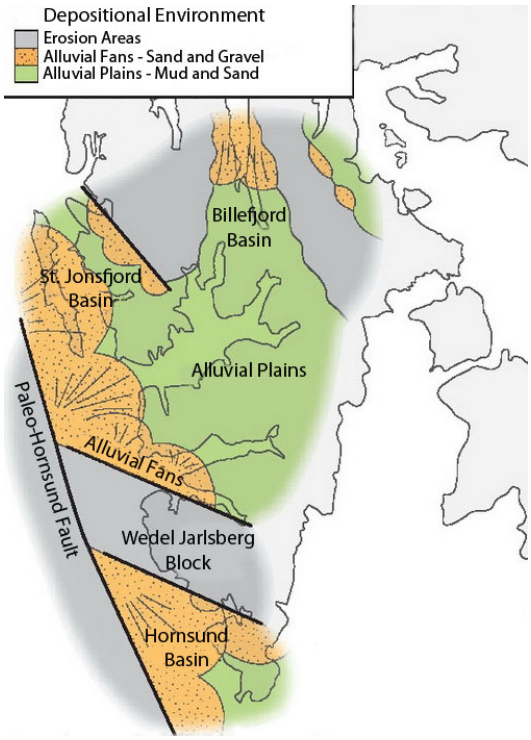


**Figure 1.5:** Carboniferous depositional environment. Modified from (Nøttvedt and Worsley, 2007).

Mid-Carboniferous climate resulted in the deposition of thick evaporite layers. In combination with the evaporate layers, red sand and mudstones make up the Gipsdalen Group. (Dallmann and Ohta, Birkenmajer, 1981, Dallmann, 1999)

Late Carboniferous subsidence resulted in the formation of shallow marine environment where dolomite, anhydrite and chalk were deposited on different surfaces from Precambrian to Early Carboniferous. (Dallmann and Ohta, Birkenmajer, 1981, Dallmann, 1999)

### 1.4.6 – Permian

The sedimentation from late Carboniferous continued through Permian with alternating sea levels. (Dallmann and Ohta, Birkenmajer, 1981, Dallmann, 1999)

### 1.4.7 – Triassic

Alternating transgressive and regressive stratigraphy composed of mudstone, siltstone and sandstone represents Early Triassic. Rivers from the west deposited sand as deltas along the west coast of Spitsbergen; today these deposits are known as Vardebukt Formation and Tvillingodd Formation. The expansion of the deltas continued into Mid-Triassic with somewhat finer fractions. In the central and eastern part of Spitsbergen marine mudstone was deposited during Mid-Triassic. (Dallmann and Ohta, Birkenmajer, 1981, Dallmann, 1999)

During Late Triassic the Northeastern Svalbard was elevated, resulting in the development of large delta plains towards the south and west. (Dallmann and Ohta, Birkenmajer, 1981, Dallmann, 1999)

### 1.4.8 – Jurassic

The delta plains from Late Triassic continued into Early and Mid-Jurassic adding alternating layers of sandstone and mudstone to the Kapp Toscana Group from Late Triassic. A shallow marine platform with very little influx of sediments covered the western part of Svalbard in Early and Mid-Jurassic. (Dallmann and Ohta, Birkenmajer, 1981, Dallmann, 1999)

During Late Jurassic the entire Svalbard region was flooded and several hundred metres of marine clay and silt were deposited. (Dallmann and Ohta, Birkenmajer, 1981, Dallmann, 1999)

### 1.4.9 – Cretaceous

Dark marine mudstone was deposited during Early Cretaceous in a shallow marine environment, by Mid-Cretaceous Svalbard was covered by a shallow marine environment and thick layers of sand and mud were deposited. (Dallmann and Ohta, Birkenmajer, 1981, Dallmann, 1999)

Northern Svalbard was elevated in Late Cretaceous, which resulted in increasing erosion in the north; hence the Cretaceous package is more than one kilometre thick in the south and only about 300 metres thick in the north. (Dallmann and Ohta, Dallmann, 1999)

### 1.4.10 – Paleogene

As a result of the transform plate boundary between Svalbard and North-Greenland the mountain chain structure, West Spitsbergen Fold Belt, was formed from 65 My to 40 My. The West Spitsbergen Fold Belt runs along the west coast of Spitsbergen until Ny Ålesund (Fig. 1.1) where it turns west out into the Greenland Sea and at Sørkapp (Fig. 1.1) it continues south out into the Barents Sea. Eroded material from the West Spitsbergen Fold Belt has been deposited in the central parts of Spitsbergen together with peat, that today make up the commercial coal seams. The West Spitsbergen Fold Belt has been eroded down and the mountain chain visible today is due to elevation during the last 10 My. Svalbard was elevated in Oligocene as a result of the opening of the Greenland Sea and magmatic intrusions, and isostatic rebound after the last ice age in Pliocene. (Dallmann and Ohta, Dallmann, 1999)

## 1.5 – St. Jonsfjorden Region

The western province of Svalbard has been subjected to Mid-Paleozoic and Mid-Cenozoic deformation. The deformation in Mid-Paleozoic occurred during the Caledonian Orogeny. During Mid-Cenozoic the West Spitsbergen Fold Belt was formed. The tectogenesis of the Caledonian Orogeny resulted in low and medium grade metamorphism, and recumbent structures that has been overfolded from the east to the west. The West Spitsbergen Fold Belt was on a smaller and more superficial scale, characterized by folding and thrusting to the east. (Harland, 1985)

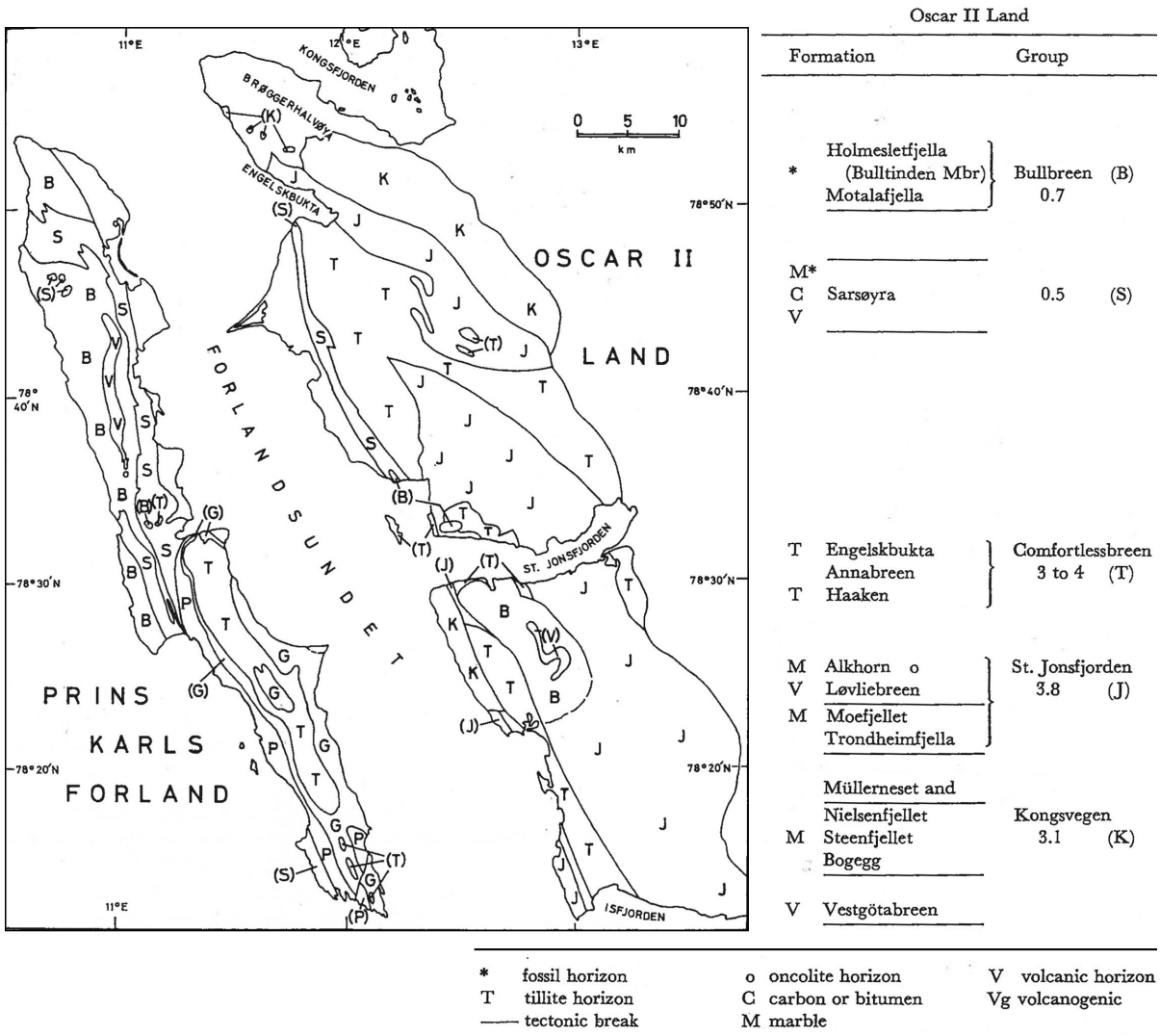


**Figure 1.6:** Geological map of the St. Jonsfjorden region showing larger outcrop areas of the stratigraphic groups as described below. The letters in brackets used in the table serve as key to unites on the geological map. Modified from (Harland et al., 1979).

### 1.5.1 – Bullbreen Group

The Bullbreen Group is outcropping at the western end of St. Jonsfjorden (Fig. 1.6). Despite being strongly folded and foliated, the Bullbreen Group shows only slight metamorphism. Because of this, fossils and sedimentary structures are well preserved. The Bullbreen Group contains fossils of Paleozoic age. The group contains two formations; the Holmsletfjella and the Motalafjella. In a small klippe at Ankerfjella (Fig. 1.2), north of St. Jonsfjorden, the whole group appears as overthrust sheets. The group appears more extensively around Bullbreen in the south. (Harland et al., 1979)

#### *1.5.1.1 – Holmsletfjella Formation*

The uppermost unit contains calcareous siltstone, argillites and polymict conglomerates. Weathering of the siltstones has resulted in a pale buff colour, often with gray bands. The siltstones contain various sedimentary structures including graded bedding, ripple marks and trace fossils. Massive conglomerates occur but are variable in composition and thickness. On Ankerfjella (Fig. 1.2) two separate conglomerate beds occur while on Motalafjella (Fig. 1.2) there is only one single unit. The conglomerate unit on Motalafjella is several hundred meters thick with thin limestone intercalations. Due to the fauna the conglomerate has been designated the Bulltinden Conglomerate Member for convenience. To the SE of Holmsletfjella (Fig. 1.2) occurs a thin horizon of tilloid associated with conglomerates. A stratigraphic conformity between the Holmsletfjella and Motalafjella Formation is apparent. (Harland et al., 1979)

The Bulltinden conglomerate member forms a substantial part of the Holmsletfjella Formation but the conglomerates are variable. Holtedahl's description from 1913 of the conglomerate member related it to Bulltinden and he found oolitic boulders of the Alkhorn Formation on it. Fossils collected from the conglomerates in Motalafjella (Fig. 1.2) yielded an age of Late Ordovician or Early Silurian. Samples taken at a later stage from a slightly different facies of slumped limestone gave a less diversified fauna. The two collections have been examined and the fossils from the conglomerate have been considered to be of Silurian aspect and probably of either Wenlock or Ludlow age. (Harland et al., 1979)

Clasts of marble lithology within the Bulltinden conglomerate member are similar to the Alkhorn Formation varieties. Some of the marble clasts have been folded prior to inclusion in the Bulltinden conglomerate member. Dolomite clasts are less common in the Bulltinden conglomerate member and it contains no stromatolites compared to the Comfortlessbreen tillites. No granite clasts have been found but one or two pebbles of retrogressed schist have been found similar to those of Vestgötabreen Formation. The absence of extra-basinal lithologies and the closely packed and well-sorted distribution of clasts offer no support to the interpretation of the Bulltinden conglomerate member as a tillite. The formation of the conglomerates is considered to have been in a shallow

marine environment during a phase of Silurian faulting, possibly with metamorphism and folding. (Harland et al., 1979)

#### *1.5.1.2 – Motalafjella Formation*

The Motalafjella formation consist of a 200 metre thick, pale gray, massive limestone, has been well exposed in an overturned nappe structure on Motalafjella. Here it structurally overlies the Vestgötabreen Formation of coarse-grained glaucophane schist and metamorphosed basic intrusives. "An unfaulted lower boundary has not been found and mapping suggests that this horizon has acted as a zone of décollement, with the limestone becoming more crystalline and dolomitic towards this zone". (Horsfield, 1972, Harland and Wright, 1979)

#### *1.5.1.3 – Sarsøyra Formation*

The marbles and argillites of the Sarsøyra Formation borders the Forlandsundet Fault Complex both its upper and lower relationships are probably tectonic. It is not clear whether the constituent units are an unbroken sequence or not. It is assumed one formation, that is at least 500m thick and four members are recognized. (Harland et al., 1979)

The uppermost member has been strongly sheared and grade into dark gray calcareous shales, there has not been observed any dolomitization. Based on the lack of dolomitization the calcareous shales are not correlated to the dolomites north of Engelskbukta (Fig. 1.6) (the Motalafjella Formation). (Harland et al., 1979)

Black, purple and green cleaved argillites, some with a soapy feel suggesting chlorite or talc make up the upper member. They are less metamorphosed than the pelites of Comfortlessbreen Group. (Harland et al., 1979)

Calcareous conglomerates and breccias form the next member with clasts that are small and show considerable flattening. Clasts of quartzites, dolomites and limestone are found in the calcareous matrix. Fossils found in the limestone clasts indicate a possible Ordovician or Silurian age. (Harland et al., 1979)

Associated with the lowermost member are semi-pelites and greenstones. (Harland et al., 1979)

### 1.5.2 – Comfortlessbreen Group

The Comfortlessbreen Group (Fig. 1.6) is characterized by tillite formations. Three unites have been distinguished and so define the group; in descending order Engelskbukta (tillite) Formation, Annabreen (quartzite) Formation and Haaken (tillite) Formation. (Harland et al., 1979)

The sequence is in places thickened by folding and elsewhere reduced by faulting but the whole sequence appears to be 3 to 4 kilometres thick. The upper and lower tillite has some characteristics in common, namely: they are thick, calcareous and clastic possibly flyschoid turbidites with dispersed stones of varied composition and up to a metre or more in diameter but more commonly only a few centimetres across. The clasts are usually of dolomite, limestone, quartzite or granite, here listed in decreasing order of frequency. (Harland et al., 1979)

#### *1.5.2.1 – Engelskbukta Formation*

The name Engelskbukta Formation is used to distinguish this upper unit from the lower unit named Haaken. Restricted to the Engelskbukta Formation are bands up to a metre thick of unsorted ortho-conglomerates. (Harland et al., 1979)

#### *1.5.2.2 – Annabreen Formation*

Annabreen Formation consists of massive pink, brown and white weathering quartzites with no clasts. The granular texture of Annabreen Formation typifies the kind of metamorphism associated with presumed Precambrian rocks. Fine compositional banding may show up in quartzites and semi-pelites. (Harland et al., 1979)

#### *1.5.2.3 – Haaken Formation*

Common in the Haaken Formation are dolomitic boulders, including stromatolitic and oncolitic structures. Larger clasts, including quartzites, are more evident than in the Engelskbukta Formation. (Harland et al., 1979)

### 1.5.3 – St. Jonsfjorden Group

Two pairs of formations constitute the St. Jonsfjorden Group (Fig. 1.6). The upper pair consists of Alkhorn Formation and Løvliebreen Formation. Moefjellet Formation and Trondheimfjella Formation make up the lower pair. The lower pair of formations are isolated by faults and inferred into position with breaks of unknown magnitude above and below. The group is unified on the basis of that the two pairs of formations has been confused, and that the tillites above and the more highly metamorphosed rocks of the Kongsvegen Group beneath, are distinct. (Harland et al., 1979)

#### *1.5.3.1 – Alkhorn Formation*

The Alkhorn Formation is essentially a limestone formation that underlies the Haaken tillites of the Comfortlessbreen Group and the contact between the two formations is sedimentary. The limestone of Alkhorn Formation overlies quartzites of the Løvliebreen Formation. The Alkhorn Formation contains a wide range of lithologies but very little dolomite; this characteristic feature distinguishes it clearly from the lower Moefjellet Formation. Present in the Alkhorn Formation is banded pale and dark marbles of a distinctive variety, also fine grained tinted marbles, calc-argillites, grits, breccias and conglomerates. Stromatolites have not been observed but oolitic and pisolitic textures, which may be algal (oncolites), are common. Typically they are visible as dark spots where chert has replaced the oncolites. (Harland et al., 1979)

#### *1.5.3.2 – Løvliebreen Formation*

The name of the formation is taken from the glacier on the southern side of the St. Jonsfjorden. The Løvliebreen Formation corresponds to the dark quartzites at the bottom of Alkhornet sequence, described by (Holtedahl, 1913) and to the massive quartzite bodies, of (Weiss, 1953), occurring in the eastern part of Holmsletfjella and in

Gunnar Knudsenfjella. Both localities, Holmsletfjella and Gunnar Knudsenfjella (Fig. 1.2), show interbedded pelites and volcanic rocks. The formation occurs in a recumbent syncline south of St. Jonsfjorden, the thickness is estimated to be a 1000 meters, this might be to small since the base of the formation is not seen. (Harland et al., 1979)

Two members of the Løvliebreen Formation are distinguished:
The upper member is characterized by massive quartzites with intercalated pelites. Cutting the dark quartzites are white quartz veins. In thin sections the quartz veins are equigranular and pure with rounded or sutured outlines. (Harland et al., 1979)

Volcanic rocks make up the lower member and their weathering colours are dark brown, green and purple. The rocks are fine-grained and contain amygdules, but they do not contain any glassy shards, crystallites or spherulites and no pillow lava structures. The extensive occurrence of these metavolcanics in glacial moraines makes it likely that they are widespread in the inland areas of Oscar II Land (Fig. 1.1). (Harland et al., 1979)

#### *1.5.3.3 – Moefjellet Formation*

Massive dolomite constitute the Moefjellet Formation, the dolomite is uniform, unfoliated and difficult to subdivide. The weathered surface of the rock is typically of a cream-weathering bluish gray colour with a gritty or sandy texture. On weathered surfaces veining and internal small-scale brecciation are often visible. Small-scale banding may result from alternating cream and gray dolomitic or cherty layers in dolomite. No organic structures have been observed in the Moefjellet Formation. Shallow water deposition with algae mats has been proposed as the origin of the formation. At Trondheimfjella, in the bay of Engelskbukta (Fig. 1.6), the Moefjellet Formation lies above the Trondheimfjella Formation, but the upper relationship to Moefjellet Formation is faulted. The lower relationship is inferred due to that there are no brakes in the sequence Comfortlessbreen-Alkhorn-Løvliebreen. Interjacent strata may be missing. Thrusting has produced an outcrop of variable width and a minimum thickness of 800 metres is suggested for the Moefjellet Formation. North and south of Engelskbukta the formation outcrops and it is possible that the marbles at Eidempynten, southwest of Motalafjella, and Daudmannsodden, at the opening of Isfjorden (Fig. 1.1 and 1.6), are correlative. (Harland et al., 1979, Harland et al., 1997)

#### *1.5.3.4 – Trondheimfjella Formation*

The formation is a mix of interbedded marbles, quartzites and pelites with a calcareous conglomerate towards the base. Along the northeast face of Trondheimfjella the formation is well exposed, and the Trondheimfjella Formation passes concordantly upward into the Moefjellet Formation, but the lower boundary of Trondheimfjella Formation is faulted. The thickness of the formation is no less than a 1000 metres. Faulting has brought its lower boundary in close contact with rocks of Carboniferous age. The Trondheimfjella Formation has been divided into three members. (Harland et al., 1979)

The lower member is about 200 metres thick and consists of orange-weathering bands of calcareous conglomerates in a sequence of quartzites, psammites and massive dolomites. (Harland et al., 1979)

The middle member is approximately 300 metres thick and is composed of dark phyllitic semi-pelites and psammites with minor quartzites and calcareous beds. (Harland et al., 1979)

The top member is 500 metres thick and is made up of marble flags. (Harland et al., 1979)

Although it is suggested that the Trondheimfjella Formation overlies the Kongsvegen Group the basal conglomerate of Trondheimfjella Formation do not contain typical Kongsvegen-type clasts. (Harland et al., 1979)

### 1.5.4 – Kongsvegen Group

The Kongsvegen Group (Fig. 1.6) is inverted so that the first formation would be the youngest, as (Orvin, 1934) proposed it. He set up 11 units where units 1-9 was named "Quartzite and Mica Schist series"; 10 the "Steenfjell Dolomite"; and 11 the "Bogegg Mica Schist", underlain by "Dolomites and limestones at Forlandsundet". The inverted order of Orvin was confirmed by (Harland et al., 1966) and (Challinor, 1967) due to the overturned Carboniferous unconformity. The name Nielsenfjellet Formation was

introduced for the units 1 to 9, unit 10 the "Steenfjell Dolomite" has been given the name Steenfjellet Formation and unit 11 the "Bogegg Mica Schist" has been named the Bogegg Formation. Orvin's fourth unit "Dolomites and limestones at Forlandsundet" has been identified with the Trondheimfjella Formation, described above. Included into this group is also the Müllerneset Formation from the south of St. Jonsfjorden, which is correlated with the Nielsenfjellet Formation. The Kongsvegen Group forms a distinct mountain range extending 30 kilometres as the backbone of Brøggerhalvøya (Fig. 1.6), it is overthrust from the south and a fundamental fault could be concealed there. (Orvin, 1934, Harland et al., 1966, Challinor, 1967, Harland et al., 1979)

#### *1.5.4.1 – Nielsenfjellet Formation*

Southeast of Ny-Ålesund in dark mountain ridges the Nielsenfjellet Formation can be seen. The formation is comprised of monotonous dark phyllitic semi-pelites interspersed with paler, dolomitic quartzite bands. A 1500 metres thickness is derived from southeast of Brøggerhalvøya that has a relatively constant width. On the other hand the Müllerneset Formation is correlated to the Nielsenfjellet Formation, and the Müllerneset Formation is no less than 2000 metres, so a 2000 metres estimate for the Nielsenfjellet Formation is reasonable. (Harland et al., 1979)

#### *1.5.4.2 – Steenfjellet Formation*

The Steenfjellet Formation constitutes a 100-metre band of gray and creamy-orange marbles that separates the Bogegg and Nielsenfjellet Formation. It is coarse-grained with a slight foliation and it has a well-developed internal passive folding. Thrusting cuts the formation locally. Parallel muscovite and differential weathering of quartz-dolomite and calcite rich layers accentuates the foliation of the marble. (Harland et al., 1979)

#### *1.5.4.3 – Bogegg Formation*

Schistose and gneissose psammites, pelites, semi-pelites, pale dolomitic marbles, pink feldspathites and dark amphiboles make up the varied sequences of the Bogegg Formation. In the Edithbreen area, in the bay of Engelskbukta (Fig. 1.6), the formation is

well exposed and forms dark ridges with occasional thin paler bands. The Bogegg Formation has been divisible into three members. (Harland et al., 1979)

The lowermost member is composed of pelites and semi-pelites with intercalated orange-weathering quartzites, marbles and psammites. The pelites and semi-pelites are biotite schists that contain quartzo-feldspathic bands and lenses, and occasional small garnets. Coarse-grained and gritty marbles with a slight muscovite schistosity comprise half the bulk of the 500 metre thick member. (Harland et al., 1979)

The middle member is about 400 metres thick and consists of dark feldspathic and garnetiferous semi-pelite with quartzo-feldspathic bands. Characteristics of this member are large quartzo-feldspathic segregations up to 2 metres in diameter, with muscovite, and ptygmatic structures. (Harland et al., 1979)

The top member has a thickness of approximant 600 metres and is composed of gneissose porphyroblastic feldspathites and semi-pelites with schistose garnetiferous pelites, subordinate dolomites and impersistent concordant amphiboles. Weathering of the feldspathites result in a greenish-gray colour and typically develop and augen structure. (Harland et al., 1979)

Coarser schistosity and more prominent deformation of the Bogegg Formation relative to the structurally lower Nielsenfjellet Formation support the view that Bogegg Formation is the oldest of the three formations. (Harland et al., 1979)

#### *1.5.4.4 – Müllerneset Formation*

Phyllitic and schistose pelites and semi-pelites with psammites and white quartzites make up the Müllerneset Formation which is 2000 metres thick. Typically it is visible around Müllerneset (Fig. 1.2), south of St. Jonsfjorden, and occupies the Svartfjellstranda costal plain west of the thrust strip of Carboniferous and Permian rocks. The Müllerneset Formation was correlated with the Nielsenfjellet Formation since the tectonic setting is similar to that at Kulmodden west of Brøggerhalvøya. (Harland et al., 1979)

#### *1.5.4.5 – Vestgötabreen Formation*

Vestgötabreen Formation is a suite of metamorphic rocks of blue schist facies, of which some lithologies at least are derived from basic igneous rocks. The occurrence is narrow, about a few hundred metres wide and it extends some 10 kilometres parallel to the regional NW-SE strike. These rocks are located on Motalafjella and on ridges to the north of Vestgötabreen (Fig. 1.2). Along the zone, which these outcrops run is associated with considerable brecciation, and iron and copper mineralization. Parallel to this zone several low angle faults that dip to the west also run. West of the Vestgötabreen Formation lies sheared marbles and east lies metamorphosed greenstones. This suite of rocks have not been correlated but they are probably older than the Bulltinden conglomerates, and probably underwent metamorphism at around 470 M.y.; however, since their occurrence is restricted to the area of Bullbreen Group rocks they may well originally have been Paleozoic rocks. (Harland et al., 1979)

### 1.5.5 – Formations in a Historical Perspective

Other well-known glaucophane schist occurrences around the world correspond with the mineral assemblages of the Vestgötabreen suite. Resulting from chemical analyses and field evidence it is clear that some lithologies at least are metamorphosed basic igneous rocks. (Horsfield, 1972)

Radiometric and stratigraphic evidence indicate a Caledonian age, with little or no recrystallization during Tertiary. There is a similar age between the Vestgötabreen glaucophane schists and metamorphic rocks elsewhere in Spitsbergen. Around the world, several authors have noted a close correlation between glaucophane schist belts and former compressive plate boundaries (Blake, 1969, Ernst, 1970, Coleman, 1971). If the correlation between glaucophane schist belts and compressive plate boundaries was valid during the Caledonian Orogeny, then a compressive plate boundary may have existed in the Oscar II Land region at this time. At least one of the two colliding plates may have been of oceanic composition due to the associated serpentinites and gabbroic rocks, though small in volume. Large-scale faulting might be expected in the vicinity of a plate boundary, but although the outcrops occur close to a low angle fault, this appears to be little more than 10 kilometres in length, and may be entirely Tertiary in age.

Tertiary faulting could have displaced the glaucophane schists from their original location. (Horsfield, 1972)

Two structural units that are separated by a thrust fault represent the high-pressure metamorphic complex around Motalafjella. The lower unit is made up of metabasic rocks with lawsonite-pumpellyite-epidote assemblages within a matrix of variably arenaceous pelitic phyllites. The upper structural unit has blocks of garnet-glaucophane schist, eclogite and, lenses of schistose micaceous marble in a matrix of garnet-chloritoid-muscovite schist. On the basis of Fe-Mg partitioning between coexisting garnet and omphacite, the Mg-content of chloritoid, and of the observed mineral assemblages, an estimate of the peak metamorphic conditions was made to about 575 to 645°C and 17 to 24 kb (Hirajima et al., 1988). Growth of large idiomorphic crystals of glaucophane and a lack of retrograde alteration of high-pressure minerals suggests a rapid post-metamorphic uplift from initial metamorphic depths. Crystals of glaucophane indicate a prolonged maintenance of the lower temperature conditions that characterize the glaucophane stability field during uplift. Phengites from rocks within the upper init record variably discordant $^{40}Ar/^{39}Ar$ age spectra that show well defined, intermediate- and high-temperature plateaus of approximant 460 to 470 Ma. These results are interpreted to date post-metamorphic cooling through the temperatures required for intracrystalline retention of argon, the estimated retention interval is 314 to 405°C (Sisson and Onstott, 1986). Spectra discordancy seems to reflect a ca. 380 to 400 Ma thermal overprint that effect minor volume-diffuse losses of radiogenic $^{40}Ar$ form the phengite grains. (Dallmeyer et al., 1989, Ohta et al., 1989)

The flyschoid metasedimentary rocks of Caradocian and Early Wenlockian age are folded into regional recumbent folds that resulted in the development of locally penetrative, axial planar cleavage in the more pelitic rocks. Whole-rock samples of cleaved slate display internally discordant $^{40}Ar/^{39}Ar$ age spectra, which indicate cleavage formation occurred at about 400 Ma and was followed by a significant early Tertiary thermal overprint. (Ohta et al., 1989)

The results from the $^{40}Ar/^{39}Ar$ studies clearly indicate that two separate Caledonian tectonothermal events are recorded in the metamorphic rocks of Motalafjella. These, in

combination with petrologic characteristics suggest: first, subduction of an oceanic crust in Early to Middle Ordovician, with resultant high-pressure metamorphism. Secondly, uplift and deposition of flysch took place from the Caradocian to the Early Wenlockian. And thirdly Late Wenlockian folding, thrusting and low-grade metamorphism of the flysch and older sequences came about. (Ohta et al., 1989)

Lower U/Pb zircon intercept age of 476±30 Ma supports the ages mentioned above, indicating a high-pressure metamorphic occurred about 475 Ma ago. (Bernard-Griffiths et al., 1993)

### 1.5.6 – Tectonic

#### *1.5.6.1 – Caledonian Orogeny*

The Caledonian Orogeny i.e. the succession of events related to the closure of the Iapetus Ocean in Early to Middle Paleozoic time, has affected all rocks of Pre-Devonian age on Svalbard, though in many places under low-grade, locally reaching to amphibolite facies metamorphic conditions. Reconstructing the overall regional Caledonian structure is difficult due to later disconfiguration by folds and faults. (Ohta et al., 1997)

Similar to the Caledonides of Scandinavia and the Appalachian Mountains the development of the Caledonian structures of Svalbard can be divided into two phases. (Ohta et al., 1997)

The Mid-Ordovician event is exposed in Motalafjella with ENE-vergent, recumbent folding and complex thrust duplexes that are associated with blue-schists, eclogites, oceanic basic pyroclastics, dyke swarms and pelagic sediments. These structures are interpreted as allochthonous fragments of possible Early-Caledonian subduction zone that has a post-metamorphic cooling-age of 460 to 470 Ma and a metamorphic age of 475 Ma (Dallmeyer et al., 1989, Bernard-Griffiths et al., 1993). (Ohta et al., 1997)

Granitic intrusions are associated with the second Caledonian phase of folding. Along the west coast of Spitsbergen this resulted in the folding of Late Ordovician to Mid-Silurian flyschoid sediments into E-vergent overturned structures. (Ohta et al., 1997)

Marking the boundary between the traditionally “basement” and “cover successions” is the Post-Caledonian angular unconformity with the overlaying Devonian and Carboniferous rocks that is widely exposed in Svalbard. (Ohta et al., 1997)

#### *1.5.6.2 – Tertiary Tectonics*

##### 1.5.6.2.1 – Vegardfjella Thrust Complex

A northeast-directed thrust stack involving basement rocks and platform cover strata up into Triassic age units has been documented through detailed mapping in the St. Jonsfjorden area. Three major thrusts occur and are briefly described below from the structurally lowest to highest, collectively they are referred to as the Vegard thrust complex. (Maher and Welbon, 1992)

##### *1.5.6.2.2 – The Lower Vegardfjella Thrust*

At the lower levels on Vegardfjella’s northwestern slope the thrust outcrops with a variable NE dip and becomes subsurface before the terminus of the Vegardbreen glacier (Fig. 1.2). The Lower Vegardfjella Thrust southwest termination is the Upper Vegardfjella Thrust. Where exposed the Lower Vegardfjella Thrust cuts up-section to the northeast. For most of its exposed length the Lower Vegardfjella Trust is subparallel to foliation and lithologic layering in basement rocks of the hanging wall. On the northern slopes of Vegardfjella (Fig. 1.2), in the immediate hanging wall, a Carboniferous fault, subparallel to the Tertiary thrust, juxtaposes Tårnkanten Formation strata (Carboniferous, Gipsdalen Group) against basement rocks. The thrust is inferred subsurface to cut up-section until it forms a flat in the Gipshuken Formation (Permian, Gipsdalen Group), which is a common detachment level in west-Spitsbergen. A flat in the footwall of Nordenskiöldbreen Formation (Carboniferous-Permian, Gipsdalen Group) has local complexities that can be explained as local distribution by down-to-the-west Carboniferous normal faults. Approximate 2 kilometres of displacement for the Lower Vegardfjella Thrust in indicated by Nordenskiöldbreen cut-offs. Though other thrusts may join the Lower Vegardfjella Thrust in the subsurface to the east and increase displacement in that direction. (Maher and Welbon, 1992, Welbon and Maher Jr, 1992)

#### *1.5.6.2.3 – The Upper Vegardfjella Thrust*

The Upper Vegardfjella Thrust can be traced within basement rocks from the southern part of Vegardfjella to Vegardbreen, where it is interpreted to have a leading edge termination against the roof thrust, Vegardbreen Thrust. At the southwestern end of the Upper Vegardfjella Thrust, a SW-dipping hanging wall and footwall foliation flat occurs within basement. Complicated geometry of hanging wall and footwall cut-offs presents itself to the northeast. These cut-offs generate a major ramp, with minor flats, that climb up to the Bravaisberget Formation (Triassic, Sassendalen Group) where the Upper Vegardfjella Thrust joins a major flat, reactivating the Vegardbreen Thrust flat. Footwall repetition is due to the Lower Vegardfjella Thrust, but apart from this the stratigraphic climb of the Upper Vegardfjella Thrust is clearly to the NE for both the hanging wall and the footwall. As a part of the thrust stack, the Upper Vegardfjella Thrust is also folded. (Maher and Welbon, 1992, Welbon and Maher Jr, 1992)

#### *1.5.6.2.4 – The Vegardbreen Thrust*

In terms of extent and amount of movement the Vegardbreen Thrust is the most noticeable. Geometry of the thrust is complex, with notable flats occurring within the Nordenskiöldbreen and Bravaisberget Formation. Truncated overturned fold limb with abundant minor structures occurs in the eastern hanging wall. In the eastern part an overall northeast dip is due to rotation above underlying thrusts as the highest exposed thrust in the stack. This implies a foreland-propagating thrust sequence, with some 2,5-3,2 kilometres offset without unfolding hanging wall structures. (Maher and Welbon, 1992, Welbon and Maher Jr, 1992)

#### *1.5.6.3 – Affects of Tectonics*

During the Tertiary shortening, Caledonian basement foliation and subparallel lithological contacts, Mid-Carboniferous dip-slip and possibly strike-slip faults and folds were either reactivated or acted as stress risers. Hence the thrust stack formed in conjunction with a westward thickening Carboniferous basin with several fault steps, and represents basin inversion. A major Carboniferous fault that is the common basement root of the Upper and Lower Vegardfjella Thrust, defines this basin margin. (Welbon and Maher Jr, 1992)

Change in structural style along strike is a result of the southerly structural plunge that exists in the St. Jonsfjorden region. (Welbon and Maher Jr, 1992)

The structures of the St. Jonsfjorden fold and thrust belt are largely northeast vergent with a change in tectonic style from basement imbrication in the hinterland to thin-skinned tectonics in platform cover strata towards the foreland. Kinematics of the St. Jonsfjorden area correlates with a model of decoupling of the entire continental margin. Tertiary transpressional motion between Spitsbergen and Greenland is decoupled into shortening across western Spitsbergen and strike-slip components. The strike-slip components acted on major faults elsewhere in the transpression zone, whereas the shortening components formed the West Spitsbergen Fold Belt. (Welbon and Maher Jr, 1992)

E-ENE-verging folds and thrust nappes has effected the Carboniferous to Triassic rocks of the inner part of St. Jonsfjorden. The nappes these rocks exhibit has been overthrusted from the west by a thick pile of nappes dominated by the Caledonian complex. Underlying basement and Carboniferous to Triassic rocks are stacked into two or possibly three folded thrust nappes. Approximately 13 kilometres of shortening is indicated by the 10 kilometres wide cross-section of these nappes. (Welbon and Maher Jr, 1992, Lyberis and Manby, 1993)

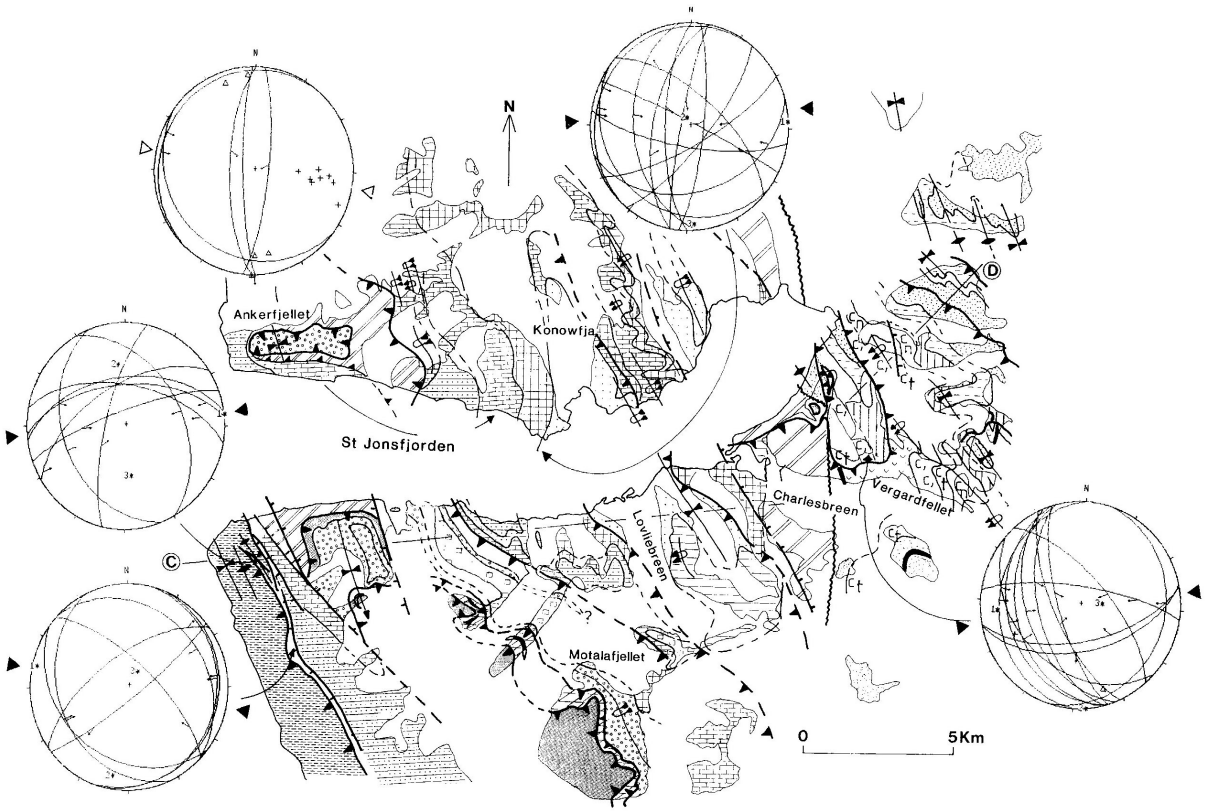


**Figure 1.7:** Geological sketch-map of St. Jonsfjorden area with the trace for the cross-section in figure 1.8 marked between C and D. (Lyberis and Manby, 1993)

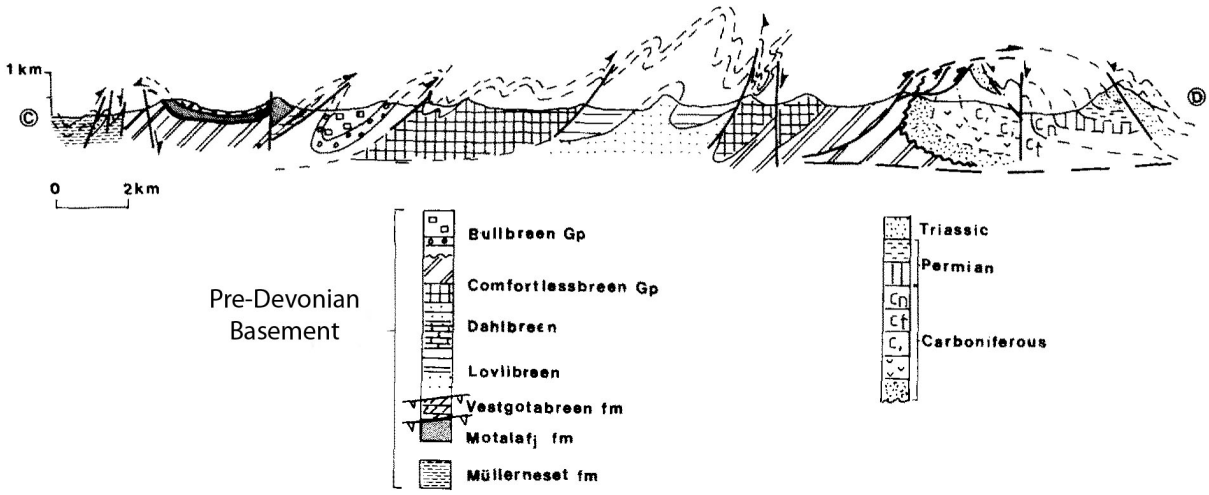


**Figure 1.8:** Cross-section of southern St. Jonsfjorden with legend. Modified from (Lyberis and Manby, 1993).

Above, a 20 kilometres cross-section (Fig. 1.8) along the southern shore of St. Jonsfjorden show a stack of E-verging imbricated thrust nappes. Post-metamorphic folding and pressure solution cleavages produced during thrusting has overprinted the Caledonian fabric within the thrust nappes. These structures indicate that Caledonian rocks were actively involved in the formation of the West Spitsbergen Fold Belt. Determining the exact shortening from the cross-section above is not possible, but it has been estimated in the range of 20 to 30 kilometres. Stress patterns has been calculated from fault planes in the St. Jonsfjorden area with a compression orientations between 70° and 90°, which is perpendicular to the thrust front (Fig. 1.7). (Lyberis and Manby, 1993)

Permo-Carboniferous rocks have been imbricated and strongly sheared together with the phyllitic and tillitic Caledonian rocks in the southwestern part of the St. Jonsfjorden area. Above these imbricated sequences there has been found large scale E-vergent folds in the basement. To the east and beneath the imbricates, a thick Post-Caledonian unmetamorphosed conglomeratic sequence has been effected by E-vergent thrusts, the rocks themselves display a well-developed pressure solution cleavage, axial planar to folds with N-S-striking axis. Below this conglomeratic sequence, SW-vergent Caledonian fold nappe structures has been affected by E-vergent folds and thrusts. Post-Caledonian unmetamorphosed conglomerates south of the St. Jonsfjorden has been overthrusted and imbricated with blue-schist-facies rocks of Early Caledonian age. Based on the above-mentioned relationships there is a strong indication that the basement has been involved with the deformation of the fold belt. (Horsfield, 1972, Lyberis and Manby, 1993)

## 1.6 – Gold Deposit- and Source-Rock Models

### 1.6.1 – Orogenic gold deposits

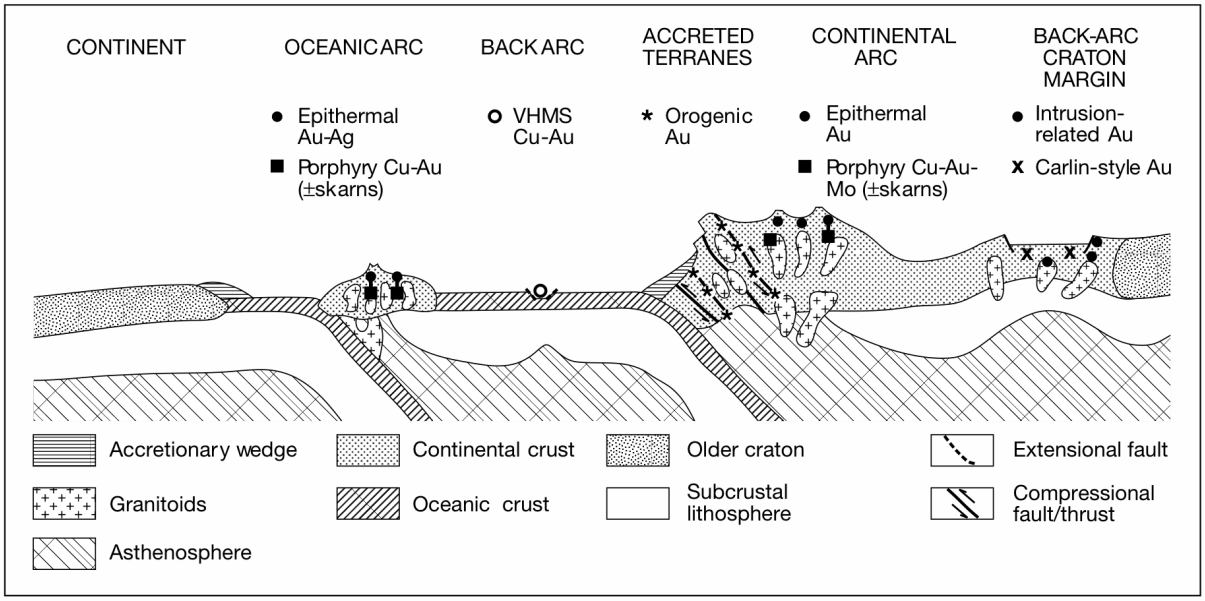


**Figure 1.9:** Tectonic settings of epigenetic gold mineral deposits. Vertical scale is exaggerated to allow schematic depth. Abbreviations: VHMS = volcanic-hosted massive sulphide. From (Groves et al., 2003).

Through the review of the nomenclature for gold deposits in metamorphic belts (Groves et al., 1998), emphasized the overall similarities in tectonic setting, structural controls, geochemistry of alteration, ore-element association, and fluid and isotopic composition. This was done in the most abundant Au-dominant (Au > Ag, low Cu-Pb-Zn) deposits in metavolcanic rock (greenstone) and turbidite/slate (accretionary prism) terrains. Following (Bohlke, 1982), (Groves et al., 1998) used “orogenic gold deposit” as a unifying term to describe these types of deposits. Orogenic gold deposits are widely interpreted to form late in the orogenic cycle, from metamorphic fluids originating at mid- to lower-crustal levels, although deeply sourced magmatic fluids might also be a possibility (Groves et al., 2003).

Orogenic gold deposits (Fig. 1.9) develop typically in terrains that have experienced moderate to high temperatures and low to moderate pressure during metamorphism, as a consequence large volumes of granitic melts are generated. Hence, a distal spatial relationship with certain intrusions is to be expected of these deposits. (Groves et al., 2003)

Typical element association of gold-bearing veins in orogenic deposits exhibit enrichments in As, B, Bi, Hg, Sb, Te and W; Cu, Pb and Zn concentrations are generally only slightly elevated above regional backgrounds (Groves et al., 1998). Base metals, Fe, Mg and Mn are rarely mobile in settings of orogenic gold deposits (Eilu and Groves, 2001). Orogenic gold deposits may be overprinted as there are gold-bearing deposits in metamorphic belts, which include some cited as intrusion-related deposits, gold-rich volcanic-hosted massive sulphide or gold-overprinted volcanic-hosted massive sulphide, and deformed Cu ± Au ± Mo porphyry deposits. Anomalous and controversial deposits hosted in metamorphic belts may be the result of overprinting of one ore system on a preexisting alteration or on a different type of ore system, or even local remobilization of preexisting mineralization during deformation and metamorphism. Given the complex and lengthy (~100–200 M.y.) evolution of metamorphic belts along active continental margins, diversity is not to be unexpected. The orogenic gold deposits are likely to be preserved in these belts unless the orogen is eroded down to their high-grade metamorphic roots. (Goldfarb et al., 2001, Groves et al., 2003)

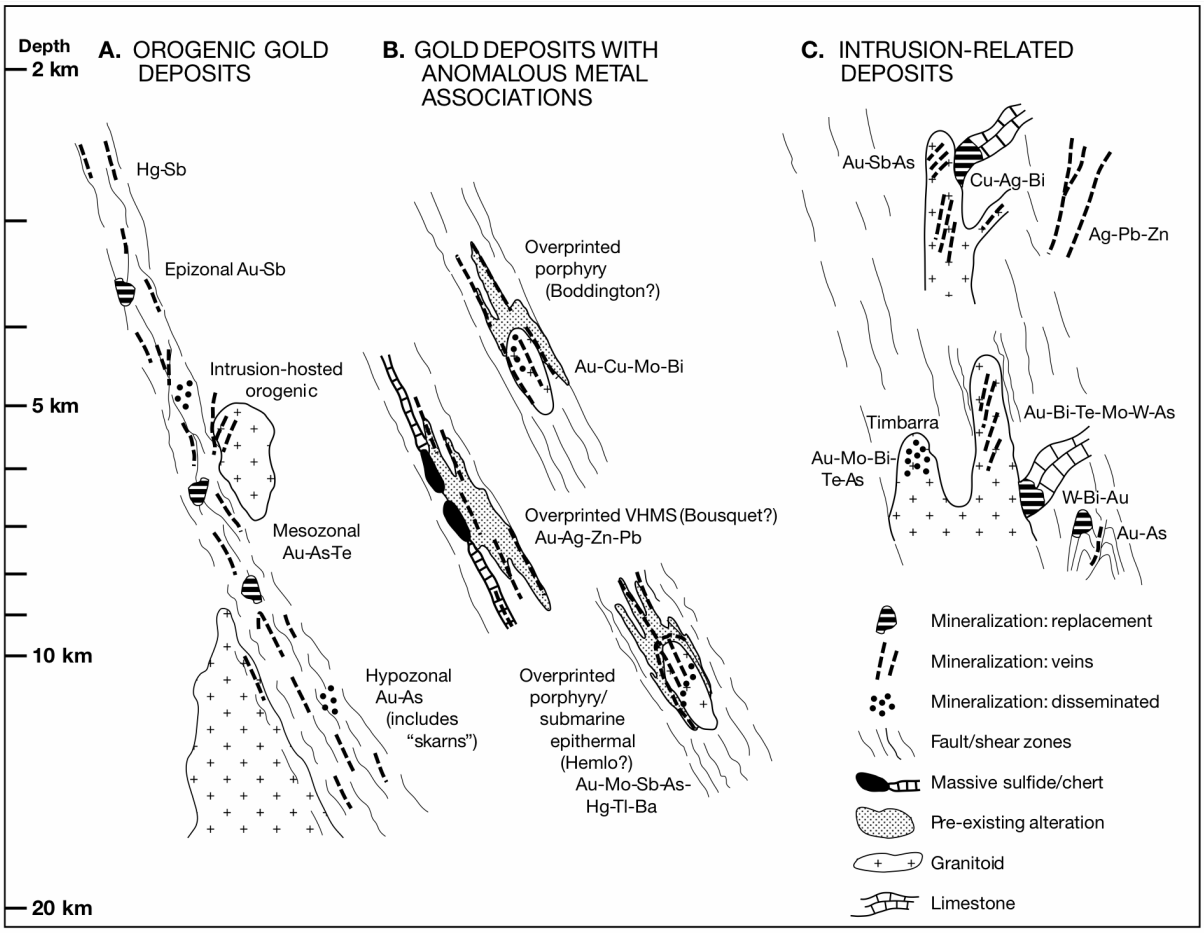


**Figure 1.10:** Orogenic gold deposits presented in a schematic crustal environments with anomalous metal associations, and intrusion-related gold deposits, in terms of depth of formation and structural setting. Abbreviations: VHMS = volcanic-hosted massive sulphide. From (Groves et al., 2003).

Orogenic gold deposits were by (Groves et al., 1998) defined to include those deposits previously referred to as mesothermal. Orogenic gold deposits were also classified in terms of the ore associations; gold-only, host sequences; greenstone-hosted, slate-belt style or turbidite-hosted and their form; lode, quartz-carbonate vein, or disseminated deposits. To describe the specific depth of the orogenic gold system epizonal <6 kilometers, mesozonal from 6 to 12 kilometers, and hypozonal >12 kilometers are used (Fig 1.10). (Groves et al., 1998, Groves et al., 2003)

Orogenic gold deposits form along convergent margins during terrain accretion, translation, or collision. Typically they form in the latter part of the deformational-metamorphic-magmatic history of the orogen. The regional metamorphism commonly

generates country rocks into belts of greenschist through lower amphibolite facies. Ores developed synkinematically, with at least one stage of the main penetrative deformation of the country rocks. Resulting in that the country rock has a strong structural control involving faults, shear zones, folds, and zones of competency contrast. Orogenic gold deposits may have as much as 1 to 2 km vertical extent, with only subtle metal zoning, and lateral zonation of wall-rock alteration, which normally involves addition of K, As, Sb, LILE, CO2, S and Na or Ca in specific cases, particularly in deposits sited in amphibolite-facies rocks. Variation in the temperature of the hydrothermal systems results in that the proximal wall-rock alteration assemblages typically vary from high crustal levels of sericite-carbonate-pyrite, through biotite-carbonate-pyrite, to biotite-amphibole-pyrrhotite and biotite/phlogopite-diopside-pyrrhotite at deeper crustal levels. Quartz ± carbonate veins are ubiquitous and are commonly gold bearing. Although many systems show the sulfidized, high Fe/Fe + Mg + Ca, wall rocks adjacent to the veins contain most ore. (Hodgson, 1989, Groves et al., 2000, Groves et al., 2003)

When it comes to localizing orogenic gold deposits crustal-scale deformation zones, particularly those hosting swarms of felsic porphyry intrusions, serpentinized ophiolite fragments, and/or lamprophyre dikes, play an important role. On a regional scale, bends or jogs in deep-crustal structural zones and their interaction with lower-order shear zones, major competency contrasts in lithostratigraphic sequences, anticlinal or uplifted zones, and irregularities along granitoid contacts may all influence the creation of low minimum or mean stress zones into which ore fluid could be focused. (Groves et al., 2000, Groves et al., 2003)

All orogenic gold ore bodies show strong structural control at deposit scale, although variations in that control are found both within and between provinces. Faults with a reverse component of shear are more commonly mineralized compared to those with a dominant normal or strike-slip shear component. Host rocks are extremely variable, but the overall trend is of volcanic rock-hosted or intrusion-hosted deposits in Archean provinces to sedimentary rock-hosted deposits in Paleoproterozoic to Tertiary provinces. (Sibson et al., 1988, Groves et al., 2003)

### 1.6.2 – Carlin-Type Deposits

Carlin-type ores mirror several of the features of orogenic gold deposits but they are classified separately due to one notable feature. While linked to orogenic activity (Fig. 1.9) and hosted along deep-crustal features, they are not related to compression as orogenic gold deposits but formed after the onset of extensional forces that follows earlier subduction-related processes. (Robb, 2005)

Carlin-type ore is characterized by Au-bearing and trace element-rich disseminated pyrite, which occurs within replacement bodies in the carbonate host rocks. Ore bodies varies in form due to local zones of porosity and permeability which again results from favourable lithologic features such as, high- and low-angle faults, and especially intersections of these features. Features controlling the permeability are high-angle faults, thrust faults, low-angle normal faults, hinge zones of anticlines, lithologic contacts, reactive carbonate units, debris-flow deposits, facies changes, brecciated zones between rocks of differing lithology and contacts of sedimentary rocks with metamorphic aureoles related to intrusions. Aquitards include structures and less permeable rocks such as shales and intrusive rocks. (Cline et al., 2005)

Domes or anticlines are often where he best ore grades are, here high-angle structures acted as feeders in a style similar to that of petroleum reservoirs. (Cline et al., 2005)

The association of Au with As, Sb, Tl, and Hg in preference to base metals and Ag are reflected in the mineralogy and geochemistry. Most of the Au is deposited with main ore-stage minerals that include Au-bearing arsenian pyrite and marcasite, quartz, kaolinite, dickite and illite. These minerals are typically fine-grained and volumetrically minor in comparison to the relict host-rock minerals, which are quartz, micas, clay minerals, dolomite, calcite, pyrite, and various forms of C. Late ore-stage minerals are generally dominated by calcite, pyrite and/or marcasite, quartz, orpiment, realgar, and stibnite, with realgar and calcite typically having precipitated last. The late ore-stage minerals generally are macroscopic and precipitated in voids or crosscutting fractures as hydrothermal systems collapsed and cooled. (Arehart et al., 1993, Arehart, 1996, Cline et al., 2005)

In addition to being sulfidized and enriched with Au and As, the host rocks are typically decarbonatized, argillized and variably silicified. The reactions that formed alteration minerals are generally not the same reactions that form Au-bearing pyrite. Ore and alteration zoning within the deposits generally is irregular. This lack of a spatial relationship, along with the fine-grained nature and sparse abundance of ore and alteration minerals, limits the use of alteration to identify ore. (Hofstra et al., 1991, Cline et al., 2005)

### 1.6.3 – Porphyry, Epithermal and Volcanic-Hosted Massive Sulphide Deposits

Porphyry Cu-Au ± Mo and epithermal Ag-Au deposits are generated at relatively shallow levels in the volcanoplutonic arcs and back arcs (Fig. 1.9). Typically these deposits are less likely to be preserved in metamorphosed sequences, since they form prior to the major phase(s) of orogenesis. During the major phase(s) of orogenesis, involving compressional to transpressional deformation, regional metamorphism, and postvolcanic granitoid magmatism, orogenic gold deposits form. In these main phases of orogenesis, the porphyry, epithermal, and volcanic-hosted massive sulphide deposits commonly (Fig. 1.9) are deformed and weakly metamorphosed, during uplift of the orogen following crustal thickening they typically are eroded. (Kerrich et al., 2000, Groves et al., 2003)

### 1.6.4 – Source-Rock Model for Carlin-Type and Orogenic Gold Deposits

A number of unresolved questions remain on the aspect of orogenic- and Carlin-type gold deposits. (Groves et al., 2003)

When it comes to the questions of where the gold-rich fluids are derived from, what is the source of the gold and when is the gold introduced, there are now new evidence that challenge the current views related to orogenic gold deposits. (Large et al., 2011)

1, Current view: Au-rich fluids are derived from deep metamorphic processes or from crustal granites.
Challenging view: Au is sourced in the sedimentary basin. (Large et al., 2011)

2, Current view: Organic-rich sediments are traps for Au.

Challenging view: Organic-rich sediments are excellent source rocks for Au and a variety of other elements (As, Zn, V, Mo, Ag, Ni, Se, Te). (Large et al., 2011)

3, Current view: Au is introduced late, i.e. syn- of posttectonic.
Challenging view: Au is introduced early, i.e. syndiagenetic, and remobilized and concentrated locally on a scale of metres to kilometres during syntectonic and/or synmagmatic fluid flow. (Large et al., 2011)

Common host rocks for orogenic and Carlin type gold deposits are carbonaceous sediments, with organic carbon content from 0.2 to over 2.0 wt. %. Mean values for black shales are 7 ppb Au and 30 ppb As, whereas the mean crustal concentrations of gold and arsenic in shales are 2 ppb Au and 10 ppm As and mean average of crustal rocks are 1.8 ppb Au and 1 to 1.8 ppm As. Gold content of the mantle are estimated at around 1 ppb Au. This data results in that average black shales have a Au and As enrichment factor of about 3 compared to average shales. If the gold and arsenic required to form orogenic and Carlin style Au-As deposits have the same source rock, then gold-arsenic-enriched carbonaceous shales of this type is a very strong candidate. (Boyle and Jonasson, 1973, Wedepohl, 1995, Ketris and Yudovich, 2009, Large, 2010)

Syngenetic gold-bearing shales are enriched in a suite of other trace elements, in particularly, V, As, Mo, Se, Ni, Ag and Zn, enrichment in additional elements such as U, Cu, Pb, Te, Bi and Cr may occur. (Large, 2010) coined the term VAMSNAZ shales for carbonaceous black shales that contain such a suite of elements, and for which Eq. 1.1 is forfilled. (Large, 2010, Large et al., 2011)

**Equation 1.1:**
VAMSNAZ score = V + Mo + Ni + Zn > 250 ppm. (Large, 2010, Large et al., 2011)

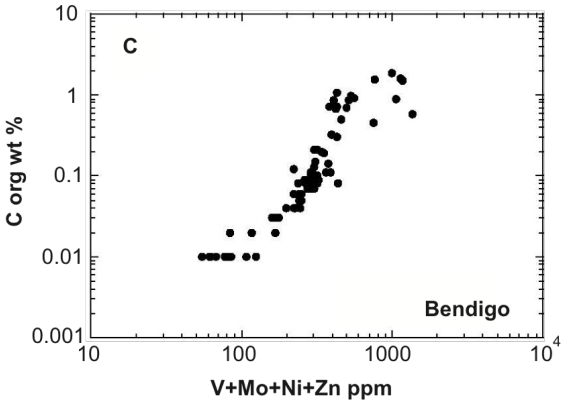


**Figure 1.11:** Plot of V-score (V+Mo+Ni+Zn) vs. organic carbon (C), for carbonaceous sedimentary host rocks at Bendigo. (Large, 2010)

Most of the trace element suite in the VAMSNAZ shales are redox-sensitive, in particular, Mo, V, U, Zn, Ni, Cr, As, Cu and Pb, this is indicative of reducing, anoxic to euxinic marine condition, under which organic-rich black mudstones are deposited. The correlation between organic carbon and V-score (V + Mo + Ni + Zn) at Bendgo clearly shows the enrichment of the V-score elements in the organic carbon-bearing sediments (Fig. 1.11). Common to all these trace elements is that they form organometallic complexes with humic substances and are readily reduced and trapped in organic matter on the seafloor. Gold and PGE may also be concentrated in organic matter on the seafloor in a similar manner, by forming organometallic bonds; if present in the seawater, or contributed from detrital clay material during sedimentation. (Calvert and Pedersen, 1993, Wood, 1996, Hu et al., 2000, Algeo and Maynard, 2004, Rimmer, 2004, Tribovillard et al., 2006, Large, 2010, Large et al., 2011)

During sedimentation and early diagenesis the invisible gold trapped in arsenian pyrite of carbonaceous shales, gradually become released and reconcentrated as free gold associated with later generations of pyrite, minor pyrrhotite and quartz veinlets, over the period of early diagenesis to late metamorphism. (Large, 2010, Large et al., 2011)

During diagenesis some of the early framboidal pyrite and porous aggregates and microcrystalline forms of pyrite are during diagenesis recrystallised to form small euhedral crystals (< 0.1 mm), or larger euhedral aggregates with porous pyrite cores. This process appears to take place during diagenetic monazite growth, before the

development of a metamorphic fabric in the shales. Early syn-sedimentary to diagenetic pyrite (py1) has more invisible gold than middle to late diagenetic pyrite (py2), suggesting that some gold is partitioned into the diagenetic fluid during the py1 to py2 conversion. This gold is then available for concentration in diagenetic fluid escape channels and related trap sites. (Large, 2010, Large et al., 2011)

When the pyrites in the sediments are subjected to greenschist facies metamorphism and deformation, it continues to recrystallise resulting in coarser grained pyrite aggregates. Py3 develops before peak deformation, whereas py4 and py5 develop post peak deformation, after the shales have a strong metamorphic fabric. From py3 to py5 the content of invisible gold in the pyrite decreases, however within the ore body these later generations contain inclusions of free gold and gold tellurides in the cores of the pyrite aggregates. During the progression from py1 to py4 over 90% of the invisible gold is lost from the arsenian pyrite. Over this paragenetic transition the pyrite does not lose As, but rather gains As progressively, albeit at a decreasing rate from py1 to py4. Through the paragenesis, from py3 to py5, the gradual conversion of pyrite to pyrrhotite is considered to be a key element in enabling the stage 2 gold up-grading processes by the release of arsenic and gold from the sediments to the metamorphic fluid. During greenschist to amphibolite facies metamorphism the conversion of pyrite to pyrrhotite in carbonaceous shales, with constant whole-rock iron, is most likely represented by the equations 1.2 and 1.3. (Ferry, 1981, Large, 2010, Large et al., 2011)

**Equation 1.2:** $2FeS_2 + 2H_2O + C\ (graphite) = 2FeS + 2H_2S + CO_2$. (Ferry, 1981, Large, 2010)

For diagenetic arsenian pyrite with 0.0999 mole % As and 0.0001 mole % Au the equation becomes:

**Equation 1.3:** $(Fe_{0.9}As_{0.0999}Au_{0.0001})S_2 + C + 2.1498H_2O + 0.1249O_2 = 0.9FeS + 0.0001Au(HS)^{2-} + 0.0999H_3AsO_4 + 1.998H_2S + CO_2 + 0.0001H^+$. (Ferry, 1981, Large, 2010)

Under reducing near neutral conditions where $H_2S$ is the dominant aqueous phase of sulfur, equation 1.3 indicates that through the conversion of pyrite to pyrrhotite, gold and arsenic are released as soluble complexes. Recrystallization of diagenetic arsenian pyrite to metamorphic arsenian pyrite releases over 90% of invisible gold and none of the arsenic, whereas the conversion of diagenetic pyrite to pyrrhotite (Eq. 1.3) releases all of the gold and all of the arsenic to the metamorphic fluid. Recrystallization of diagenetic pyrite, during early metamorphism, is accompanied by pyrite being partially replaced by pyrrhotite and the release of invisible Au, Cu, Pb and Zn from the structure of diagenetic pyrite to form discrete inclusions of gold, chalcopyrite, galena and sphalerite in the metamorphic pyrite. Peak conversion of arsenian pyrite to pyrrhotite (Eq. 1.2), and consequent loss of all structurally bound gold and arsenic in diagenetic pyrite to metamorphic fluid, probably occurs with the generation of metamorphic biotite, at around 375 to 400$^{o}$C, during middle greenschist facies metamorphism. (Bucher and Frey, 2002, Large, 2010, Large et al., 2011)

Micro nuggets of free gold in the matrix of the carbonaceous shales will likely dissolve during metamorphism and deformation. Through the generation of a $CO_2$-$H_2S$-bearing metamorphic fluid the micro nuggets are dissolved, contributing more gold to the fluid, for the eventual concentration in structural sites to form the orogenic ores. Arsenic is also likely added to the fluids from the organic matter in the shales. (Large, 2010, Large et al., 2011)

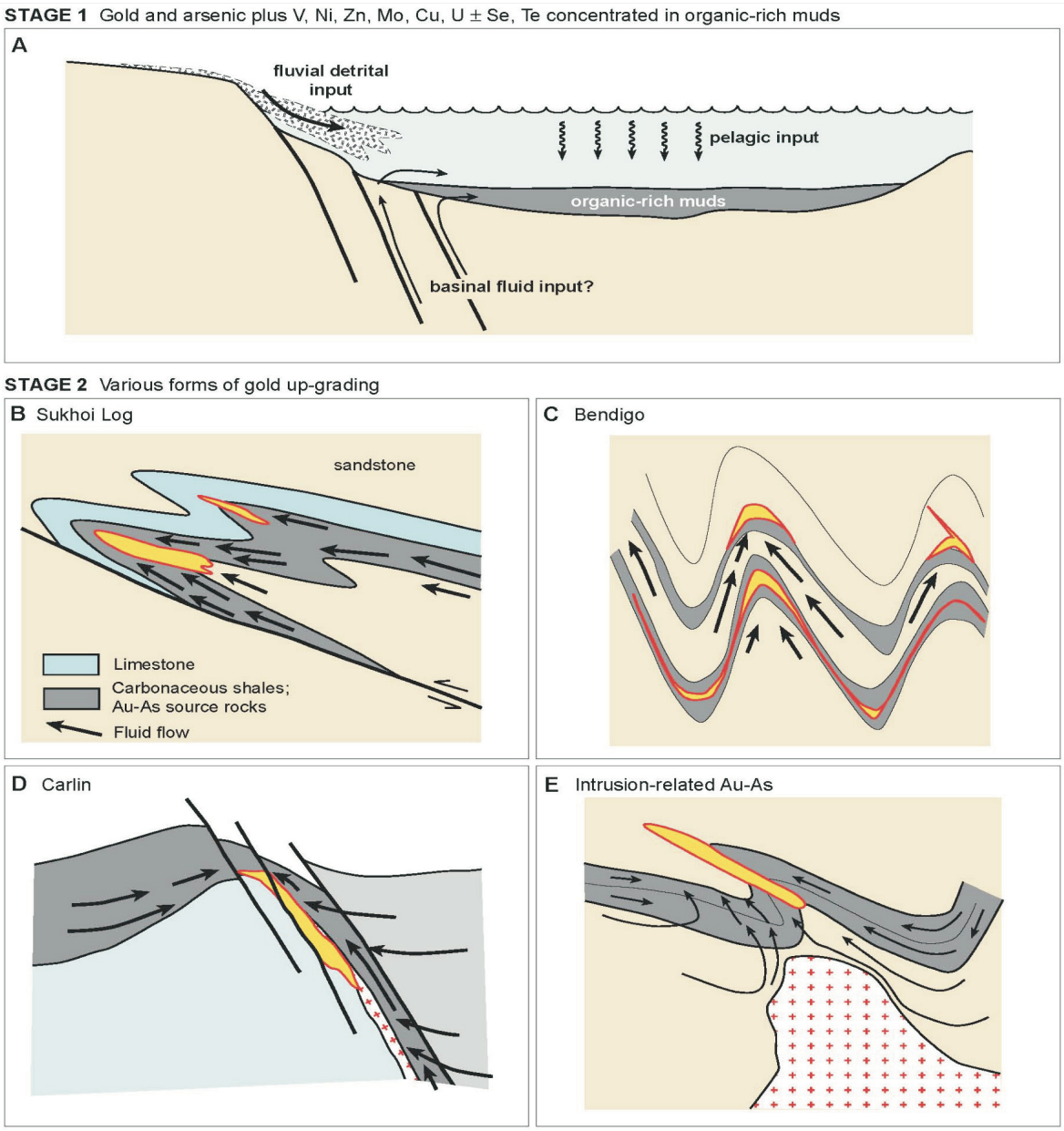


**Figure 1.12:** "Model for the two-stage concentration of gold and arsenic in orogenic and Carlin style deposits hosted by carbonaceous shales. (A) Stage 1: accumulation of gold and arsenic in continental margin sediments by normal sedimentary and diagenetic processes. (B) Stage 2: Sukhoi log Model – mobilisation of gold and arsenic from black shales, siltstones and sandstones into anticlinal core zones for concentration to ore grades. (C) Stage 2: Bendigo Model – mobilisation of gold and arsenic from black shales, siltstones and sandstones into anticlinal core zones for concentration in saddle reef structures to ore grades. (D) Stage 2: Carlin Model – gold and arsenic mobilisation during deformation of carbonaceous shales, with concentration in favourable structural sites. (E) Mobilisation of gold and arsenic from shales associated with felsic intrusions to become concentrated in favourable structural sites." (Large, 2010)

"… A two-stage process of gold and arsenic concentration is viable and likely for sediment-hosted, orogenic Au-As and Carlin style deposits (Fig. 1.12). A consequence of this model is that gold and arsenic are not sourced from deep fluids at the base of the crust, the mantle or the core as proposed by previous workers, but are derived from pre-concentrated carbonaceous sedimentary rocks, in the same basin as the Au-As ores. The relationship of gold in the ores and surrounding sediments to a suite of trace elements, termed the VAMSNAZ suite (V, As, Mo, Se, Ni, Ag, Zn), provides strong evidence that the gold and arsenic were initially pre-concentrated by normal sedimentary and diagenetic processes involving adsorption onto organic matter and incorporation into diagenetic pyrite (Fig. 1.12 A). LA- ICPMS analyses of organic matter and diagenetic pyrite confirms that these pre-concentration processes have taken place in the host sediments at Sukhoi Log, in the north Carlin Trend and the Victorian Goldfields. A second stage of gold upgrading takes place during deformation metamorphism and/or granite intrusion, associated with basin inversion (Fig. 1.12 B to E). Recrystallization of diagenetic pyrite and maturation of organic matter leads to release of gold from the sediments to the metamorphic fluid. The process of progressive replacement of sedimentary pyrite by metamorphic pyrrhotite at higher metamorphic grades, between middle to upper greenschist facies, results in the complete release of both gold and arsenic to the metamorphic fluid. Focussing of the metamorphic/hydrothermal fluids into structural sites such as anticlinal zones, breccia zones or shear zones results in the orogenic and Carlin style Au-As deposits." (Large, 2010)

### 1.6.5 – Listwanites Associated Gold Deposits

Listwanite is a term used to describe carbonate ± sericite ± pyrite altered ophiolitic mafic and ultramafic rocks that are veined by hydrothermal quartz ± carbonate. (Boyle and Canada, 1979, Ash et al., 2001)

"The main characteristic of listwäentinization is the conversion of serpentinite into talc and/or carbonates. The chemical composition of listvenite is variable and is controlled by zonal factors and the composition of the host rocks. In general there is an introduction of K, Ca, Al, $CO_2$ and $H_2O$ and an abstraction of $SiO_2$." (Boyle and Canada, 1979)

A point of confusion is the inclusion of quartz as a component of listwanite. Quartz would not be included if listwanite is regarded strictly to be a hydrothermal alteration product of mafic and ultramafic rocks. (Lindgren, 1896) recognized the absence of silica as an alteration component in these alteration systems. (Ash et al., 2001)

"Replacement by silica is not among the processes here recognized. It should be borne in mind that a rock shattered and filled with quartz seams is not an evidence of metasomatic replacement by quartz, nor is such a rock a quartz vein in process of formation. In a mineral water containing carbon dioxide, sulphureted hydrogen, carbonates and silica, the former three compounds will vigorously attack, by chemical processes, the minerals of any ordinary rock and form new compounds, while the silica is inert and plays a passive role". (Lindgren, 1896, cited in: Ash et al., 2001)

Later (Johnston and Thorpe, 1940) reiterated this feature and confirmed, as earlier pointed out by (Lindgren, 1896), that hydrothermal solutions introduced three principal classes of minerals into the rocks – carbonate, sericite and sulphides. (Ash et al., 2001)

"Quartz rarely replaces the wall rocks, although it commonly fills small fractures adjacent to veins, in many places of such great complexity as to suggest large-scale replacement when viewed in place or in hand specimens. Under the microscope, however, the quartz of the veinlets is in sharp contact with the carbonatized and sericitized country rock, and evidence of encroachment upon the rock minerals is wanting." (Johnston and Thorpe, 1940, cited in: Ash et al., 2001)

Therefore a listwanite is not entirely an altered rock but a combination of altered rock and, quartz and carbonate fracture-filling veins. (Ash et al., 2001)

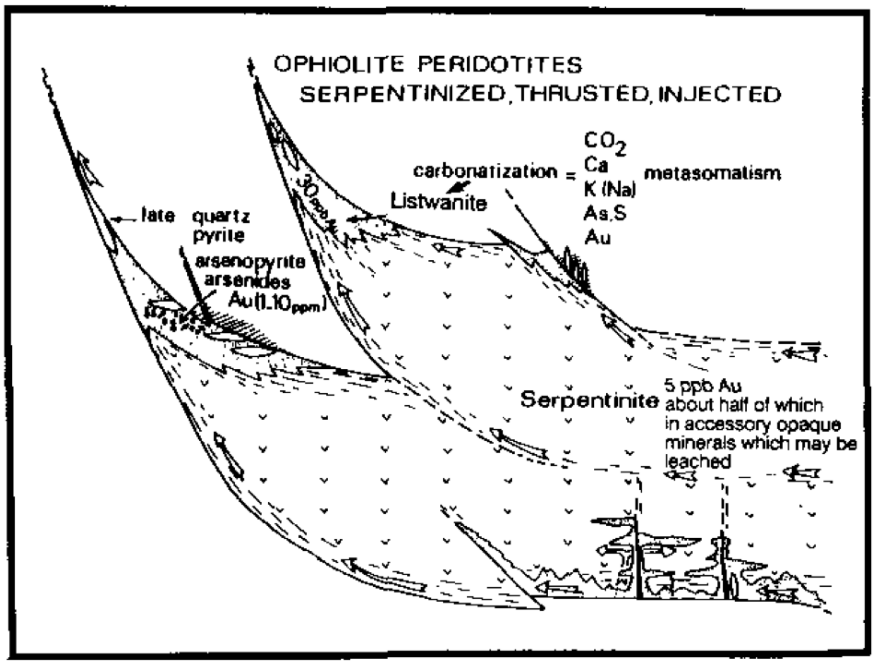


**Figure 1.13:** Generalized listwanitic alteration model, invoking carbonatization of serpentinized ultramafic rocks and the development of gold-bearing veins in and above the thrust. (Ash and Arksey, 1990)

Gold deposition in and around listwanites invoke low-salinity hydrothermal fluids rick in $CO_2$ which carry gold as $Au(HS)_2$. Figure 1.13 show how listwanite zones form along major faults that cut or are marginal to the serpentinized ophiolite peridotites. A distinctive alteration halo (Table 1.1) is generated by the alteration being most intense within and above the mineralized structure. Here iron magnesite/mariposite rocks are generally sheared and cut by a network of quartz-carbonate veins, whereas outwards from the faults the intensity of the carbonatization of the serpentinized ultramafic rocks are zoned. (Ash and Arksey, 1990)

| Increase in Intensity of Alteration → | | | |
|---|---|---|---|
| **HOST** | | | **FAULT** |
| Serpentinite | Talc<br>Carbonate | Quartz (veinlets)<br>Talc<br>Carbonate | Quartz<br>Carbonate<br>Mariposite<br>Au, Ag<br>Sulphides |

**Table 1.1:** Characteristic alteration assemblage of listwanite. (Ash and Arksey, 1990)

# 2 – Previous Work

The shortwave infrared (SWIR) mineralogical survey was ordered by Store Norske Gull A/S to detect alteration patterns in spatial relation to mineralizations. By analyzing the core, with the analytical spectral device (ASD) Terra Spec, one creates a pattern in relation to known mineralization. Applying this pattern to surveys on outcrops and cliff faces will give a valuable tool in focusing further prospecting work.

## 2.1 – SWIR Mineralogical Survey

The ASD Terra Spec can be applied to measure the composition and abundance of a variety of alteration minerals. Through a hand held light source the rock is subjected to light in the visible to SWIR range. By measuring reflected light from the rock in the short wavelength infrared region of the light spectrum between 350 and 2500 nanometres, chemical bonds in minerals absorb energy corresponding to particular wavelengths different. This generates a different absorption features, and on the basis of this it is possible to discriminate different phases of the same mineral, based on variations in composition and/or crystallinity. Absorption in the SWIR range is due to water, hydroxyl bonds, carbonates and sulphates. (GeoPool, 2008, Halley, 2012)

### 2.1.1 – Results of SWIR Mineralogical Survey at Holmsletfjella

Figure 2.1 show immobile element plots. Most igneous rocks plot around 6 to 9% Al. This is due to that they all have around the same amount of feldspar, either plagioclase in mafic rocks or alkali feldspar in felsic rocks. Carbonate rocks plot with low Al, because they are calcite dominant and lack feldspar. The various shales have low Al, this is most likely caused by an origin from quartz-rich sediments. The few analyses of Sc-rich rocks are from mafic rocks. The cataclasite is dominantly within a field of felsic composition. (Halley, 2012)

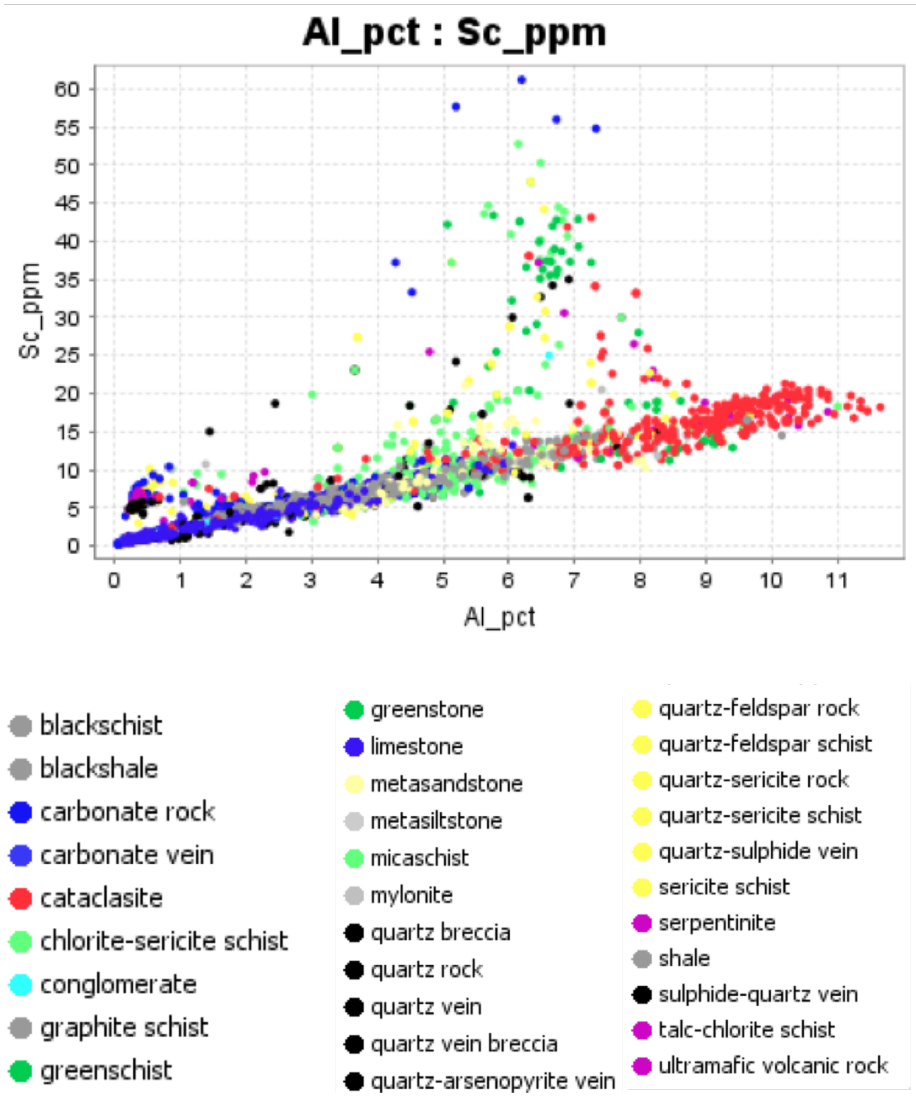


**Figure 2.1:** Immobile trace element plots, coloured by logged rock types. Modified from (Halley, 2012)

The spectra from the drill samples were classified into mineralogical groups (Fig 2.3). These are Sericite, Chlorite, Sericite-Chlorite, Carbonate, Talc and Null. (Halley, 2012)

A significant number of the limestone and shale samples have yielded “aspectral” results; the reason for this is that the spectra are too dark to give a recognizable mineral signature and has therefore been assigned to the “Null” group (Fig2.3). (Halley, 2012)

Figure 2.4 is the same plot as figure 2.2, only figure 2.4 has been coloured by the mineralogy interpreted from the ASD spectra (Fig 2.3). The mafic rocks (high Sc) in figure 2.4 are shown to be predominantly chloritic. The chlorite-sericite schists and the "cataclasite" have similar mineralogy, but a little different geochemistry. (Halley, 2012)

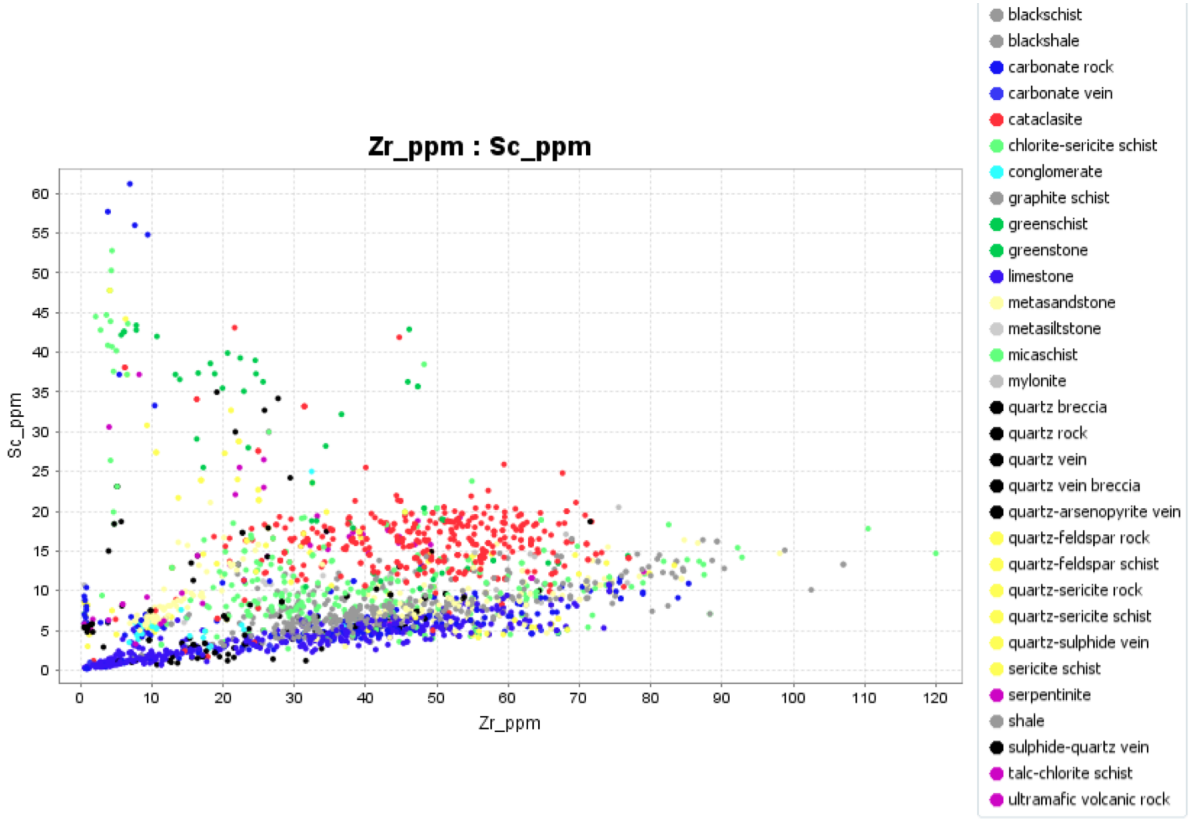


**Figure 2.2:** Highlighting correlations between logged lithologies (logging codes) and trace element compositions through Sc vs. Zr plot, from (Halley, 2012).

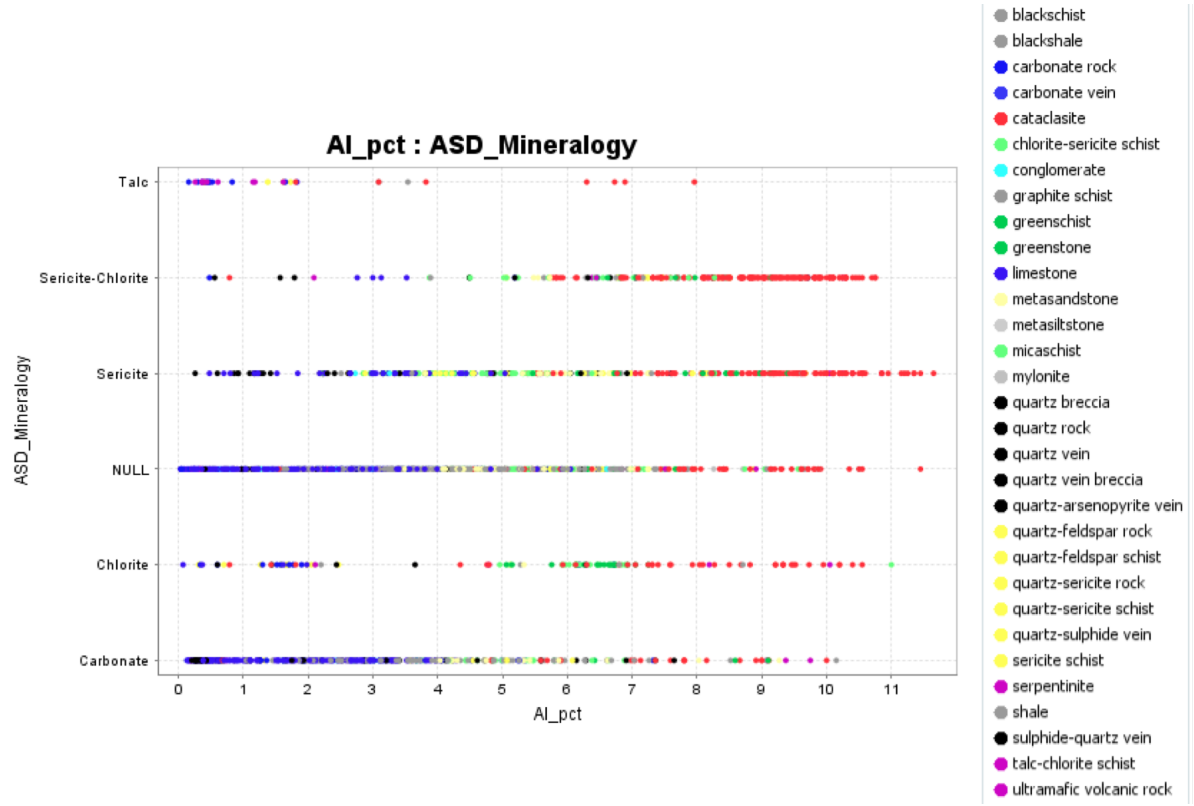


**Figure 2.3:** ASD_Mineralogy vs. Al coloured by logging codes, from (Halley, 2012)

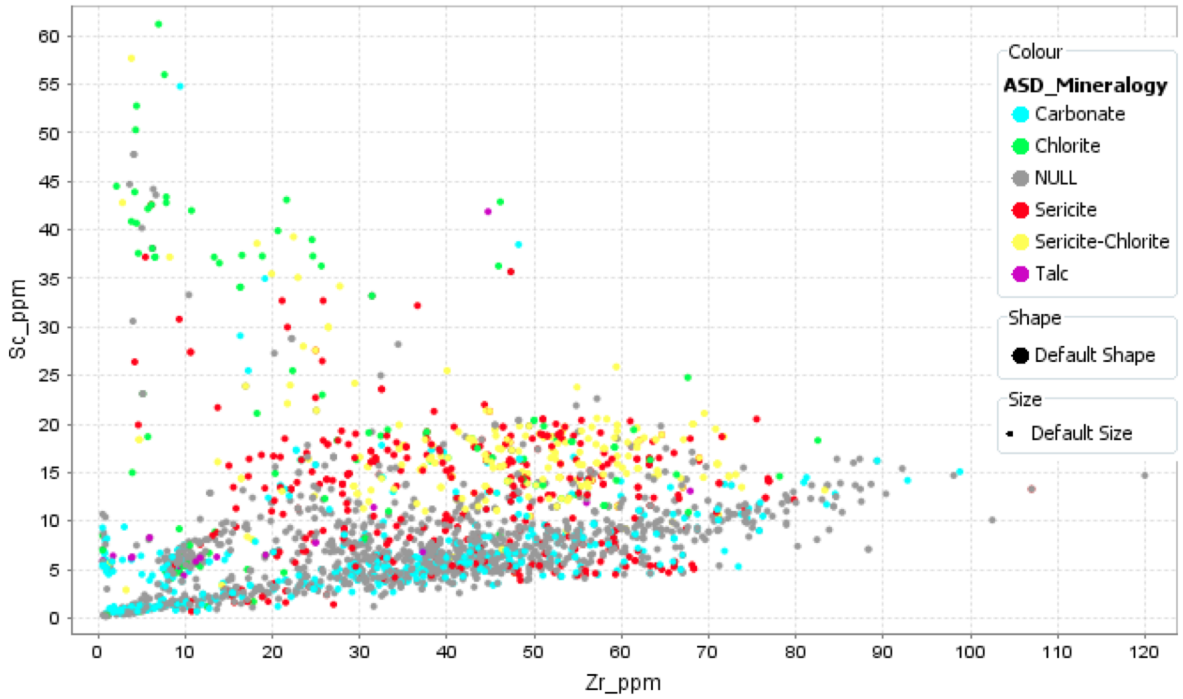


**Figure 2.4:** Sc vs. Zr plot, coloured by ASD mineralogy, from (Halley, 2012).

Note the three distinct clusters of data in figure 2.5 and partly 2.6, the carbonate rich rocks, the shales and the cataclasite. The tightly clustered rocks on an alteration plot, indicates that the majority of the samples have not had significant losses or gains of alkali elements. This suggests that alteration has not been widespread and/or very intense. (Halley, 2012)

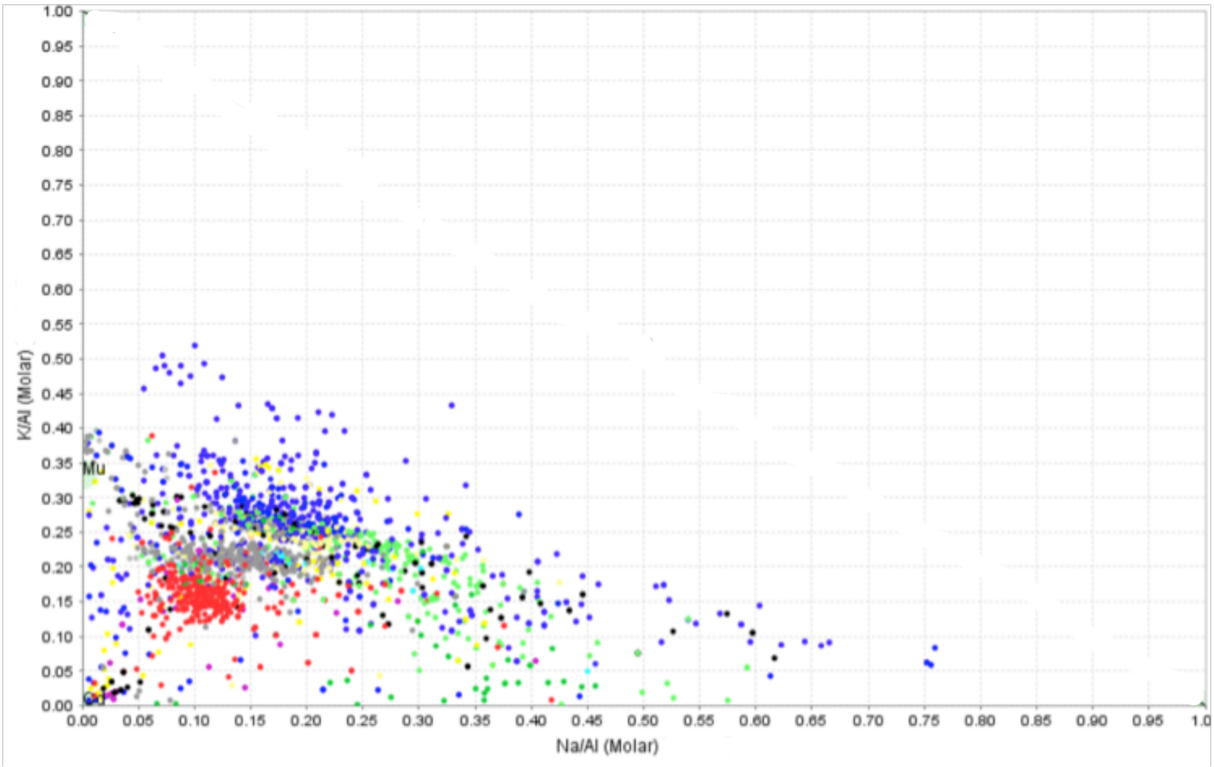


**Figure 2.5:** K/Al vs. Na/Al molar ratio plot. Points have been coloured by the logging codes. Refer to figure 2.3 for legend. Modified from (Halley, 2012)

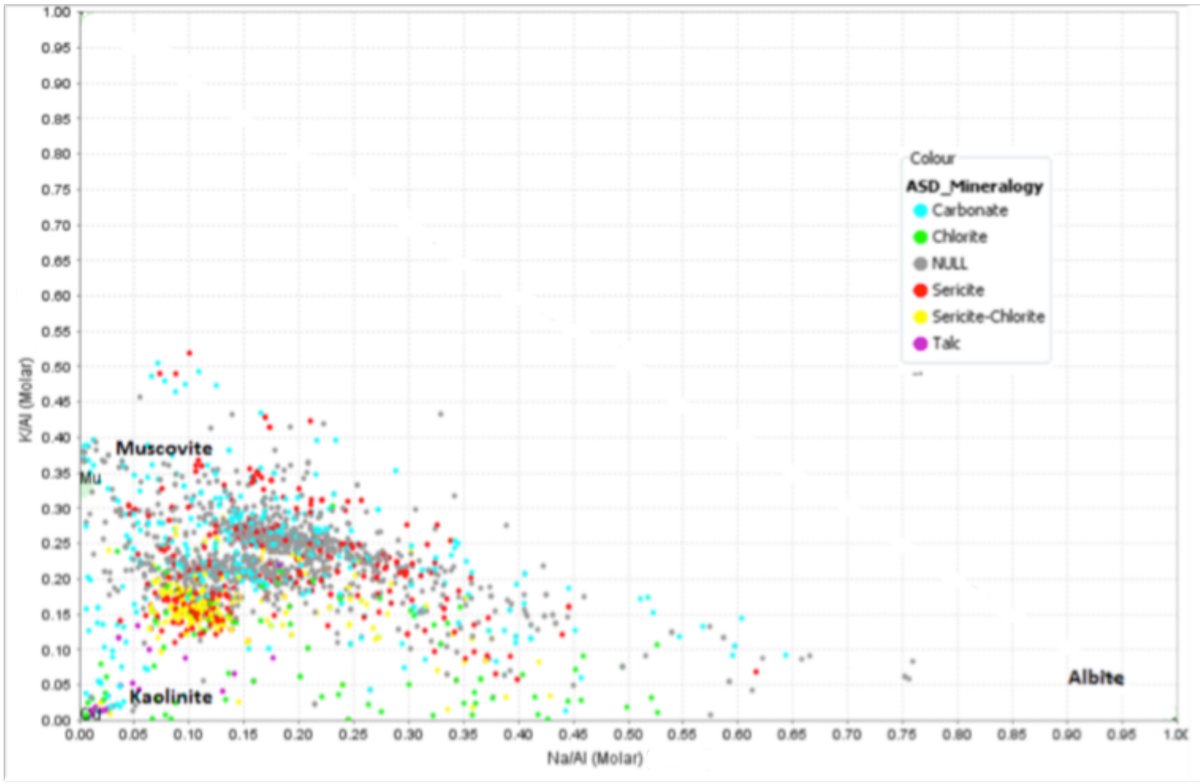


**Figure 2.6:** K/Al vs. Na/Al molar ratio plot, same as figure 2.5, only figure 2.6 has been coloured by the ASD mineralogy, modified from (Halley, 2012)

Figure 2.7 shows the points plotting on or above the muscovite-albite tie line have the longest wavelengths. Points lying below the tie line shift progressively towards shorter wavelengths, with increasing distance from the tie line. This reflects that long wavelength micas are phengitic in composition; where they have Fe or Mg replacing Al, thereby these points plot with a higher K/Al ratio. Micas with shorter wavelengths are muscovitic in composition. (Halley, 2012)

**Equation 2.1:**

$2KAl_2(AlSi_3)O_{10}(OH)_2$ (musc) + $K^+$ + $1.5Fe^{2+}$ + $4.5SiO_2$ + $3H_2O$ ⇔

$3KFe_{0.5}Al_{1.5}(Al_{0.5}Si_{3.5})O_{10}(OH)_2$ (phen) + $4H_+$

Note the pH term included in this reaction. Acid conditions favour muscovite (Al-rich), and alkaline conditions favour phengite (Al-poor). (Halley, 2012)

Figure 2.8 is a view of the drill holes with the data from figure 2.7, in 3D; this shows that the mica compositions are zoned spatially. The blue surface modelled in figure 2.8 shows the boundary between phengitic micas (below), and muscovite (above). The alteration seem to have been rock buffered, i.e. low water to rock ratio. If so the carbonate in the lower part of the sequence has worked as a buffer, and buffered the pH in the system to create a more alkaline environment where phengite has been stable (see equation 2.1). Without the carbonate, the micas are stable with a muscovitic composition. Rather than a zonation in the hydrothermal system, the mica zonation appears to be reflecting a host rock control. (Halley, 2012)

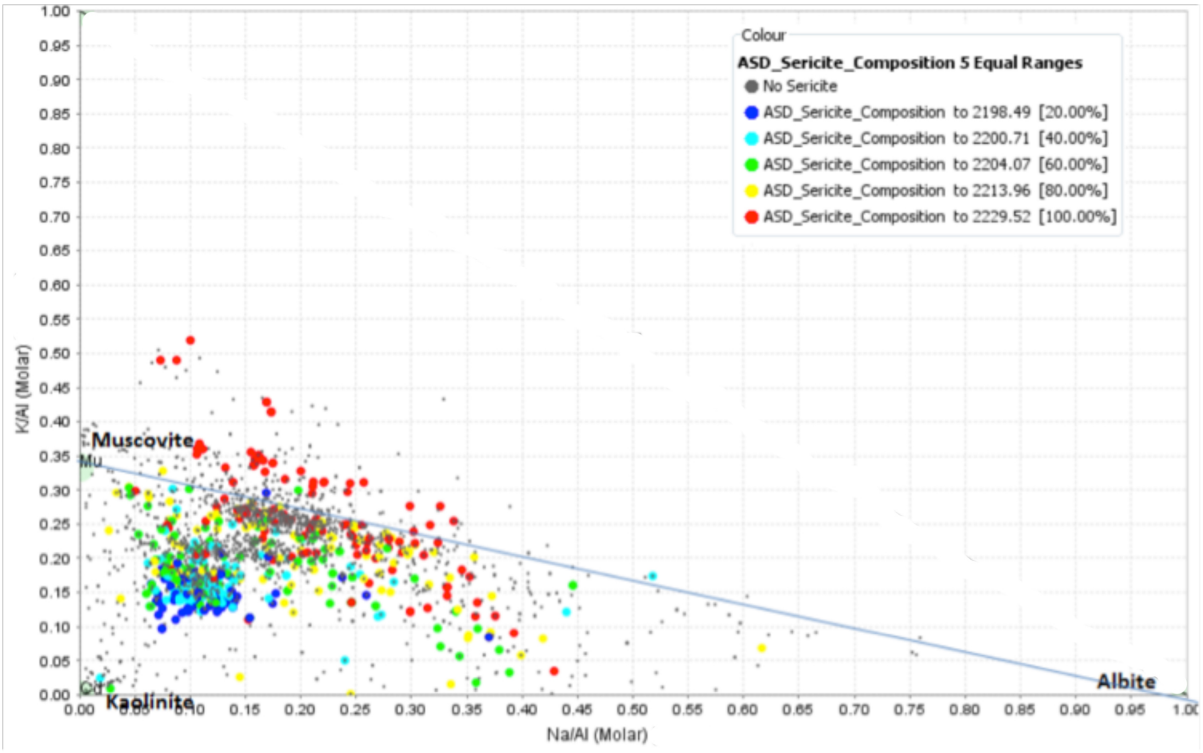


**Figure 2.7:** K/Al vs. Na/Al molar ratio plot, assay points have been coloured by the wavelength of the sericite from cold (short wavelength) to hot (long wavelengths) colours, modified from (Halley, 2012).

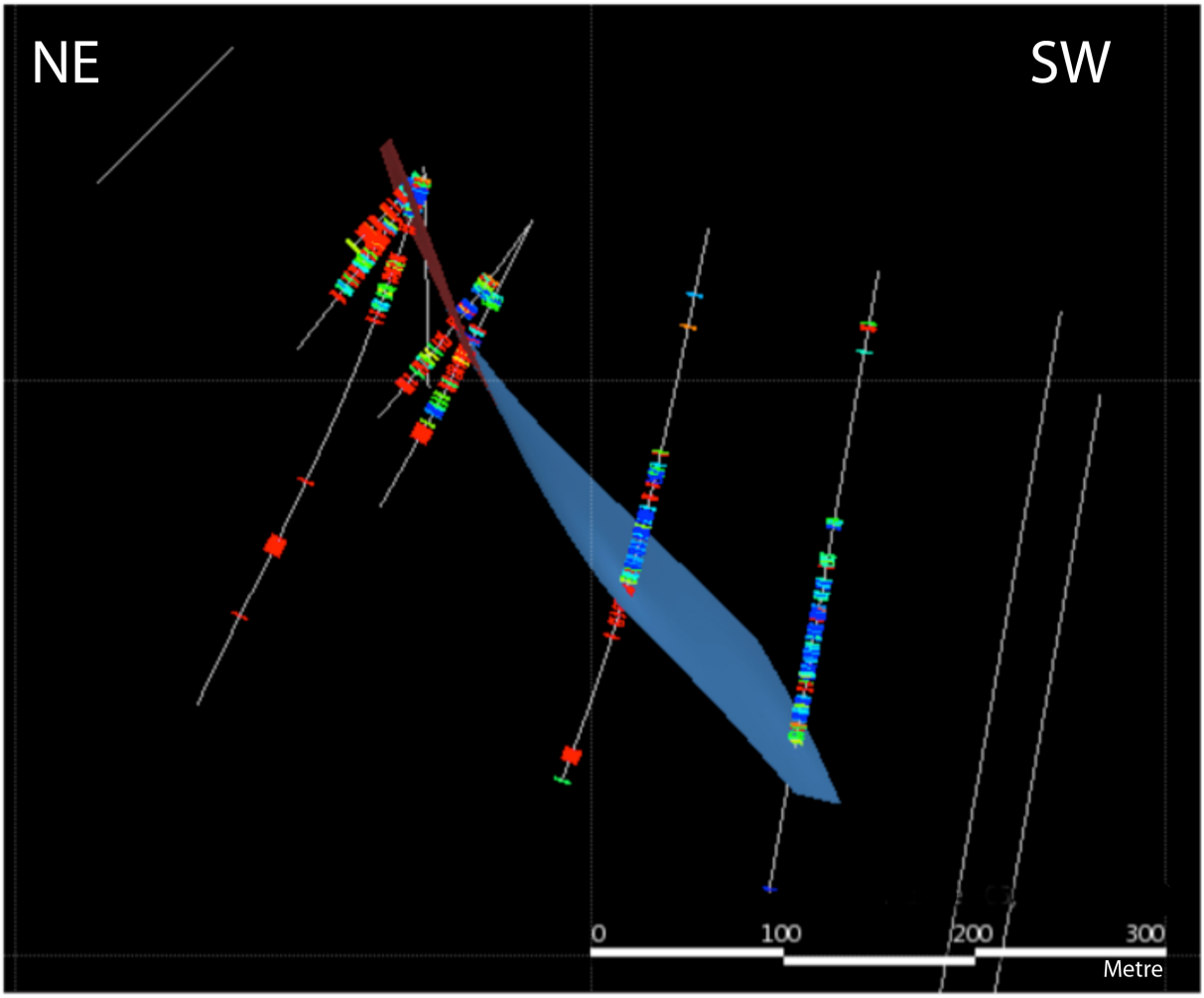


**Figure 2.8:** Cross-section of the Holmsletfjella drill holes (white lines) looking towards the southeast. With white mica wavelength ranges in 3D; red=phengite (>2215nm), blue=muscovite (<2200nm). The surface modelled shows the boundary between phengitic micas (below), and muscovite (above). Modified from (Halley, 2012).

Sc and V both are able to substitute Fe in Fe-silicate minerals such as pyroxene, amphibole, chlorite, biotite, etc. Due to this Sc and V generally plot with a very linear correlation. (Halley, 2012)

An arrow in figure 2.9 indicates the linear correlation of Sc and V. However, there is another trend, marked by a loop, that show samples strongly enriched in V relative to Sc. (Halley, 2012)

The V-enriched samples are shown in figure 2.10 to also contain anomalous amounts of Mo, Zn, U, Ag, As and Sb. In particular the association of V-Mo-U-Zn, is a diagnostic signature of an organometallic association. (Halley, 2012)

Most Carlin deposits are hosted in hydrocarbon trap sites. The host rocks prior to the Carlin Au event carry the association of V-Mo-U-Zn. Organic material provides a very effective chemical trap for Au and other redox-sensitive elements. The anomalous pathfinder chemistry in this system appears to be mapping the footprint of an organic rich fluid that migrated through these rocks, rather than being indicative of an orogenic gold system. (Halley, 2012)

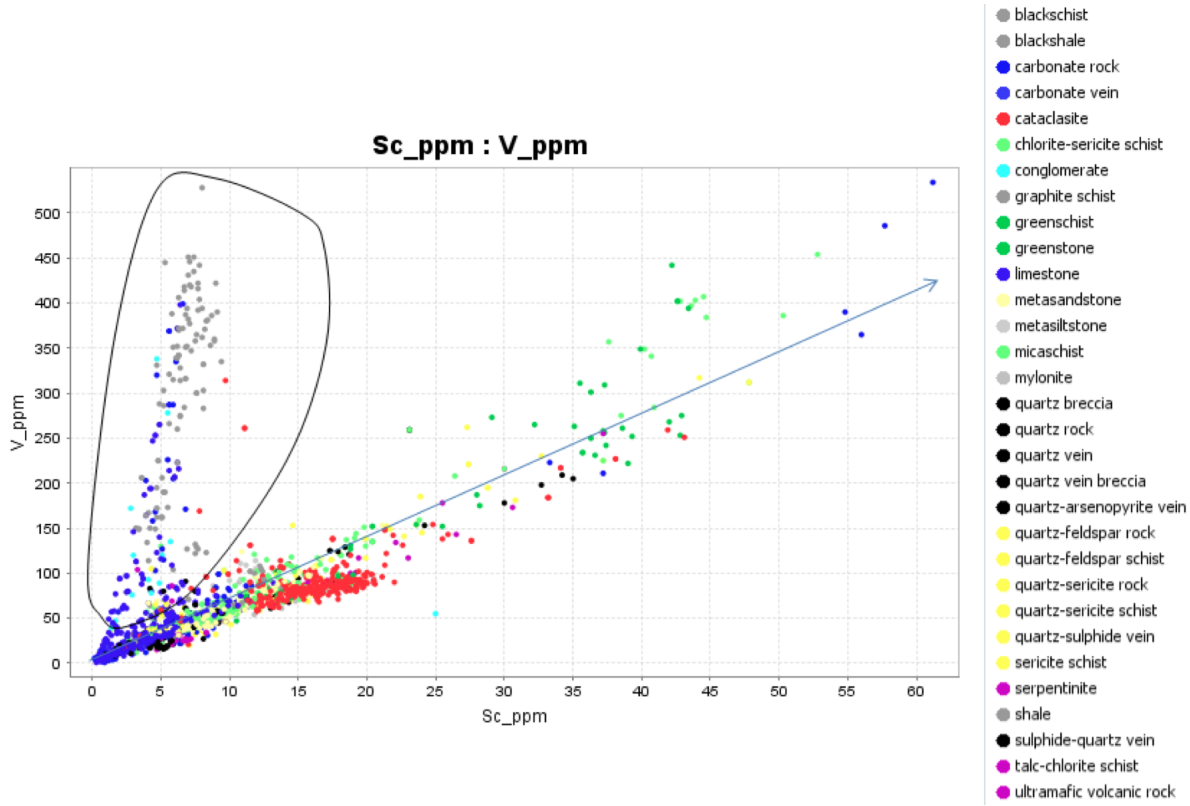


**Figure 2.9:** Sc vs. V, with an arrow and a loop marking two different trends, points have been coloured by the logging codes, from (Halley, 2012).

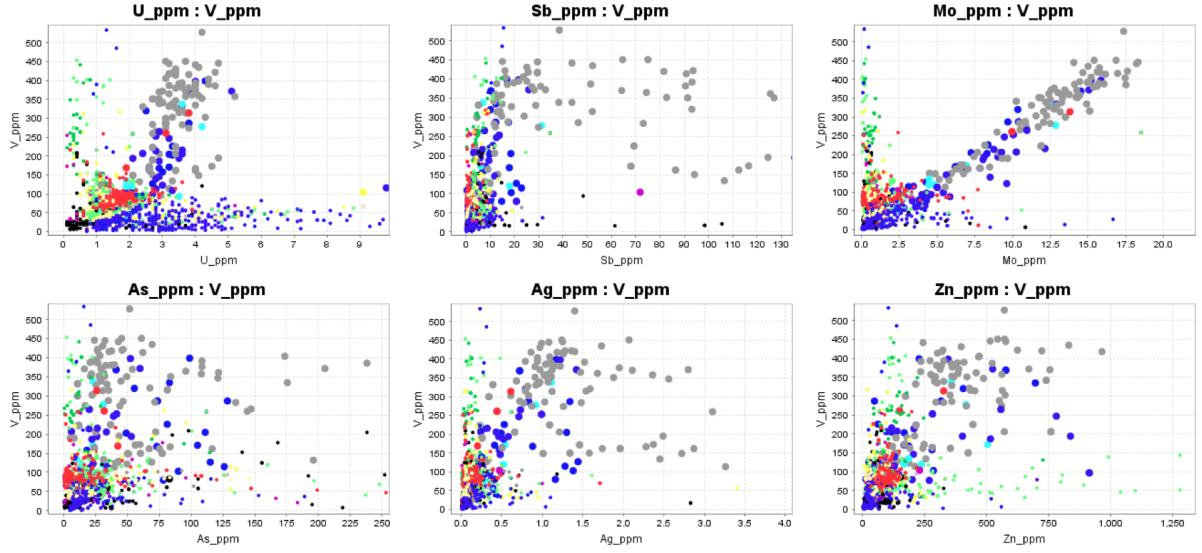


**Figure 2.10:** V vs. U, Sb, Mo, As, Ag, and Zn, points have been coloured by the logging codes. Refer to figure 2.9 for legend. From (Halley, 2012).

Figure 2.11 and 2.12 show the spatially distribution of the organometallic associated elements V and Mo. The blue surface model from figure 2.8 has been kept in figure 2.11 and 2.12 to show that the organometallic association are located above the muscovite-phengite boundary. (Halley, 2012)

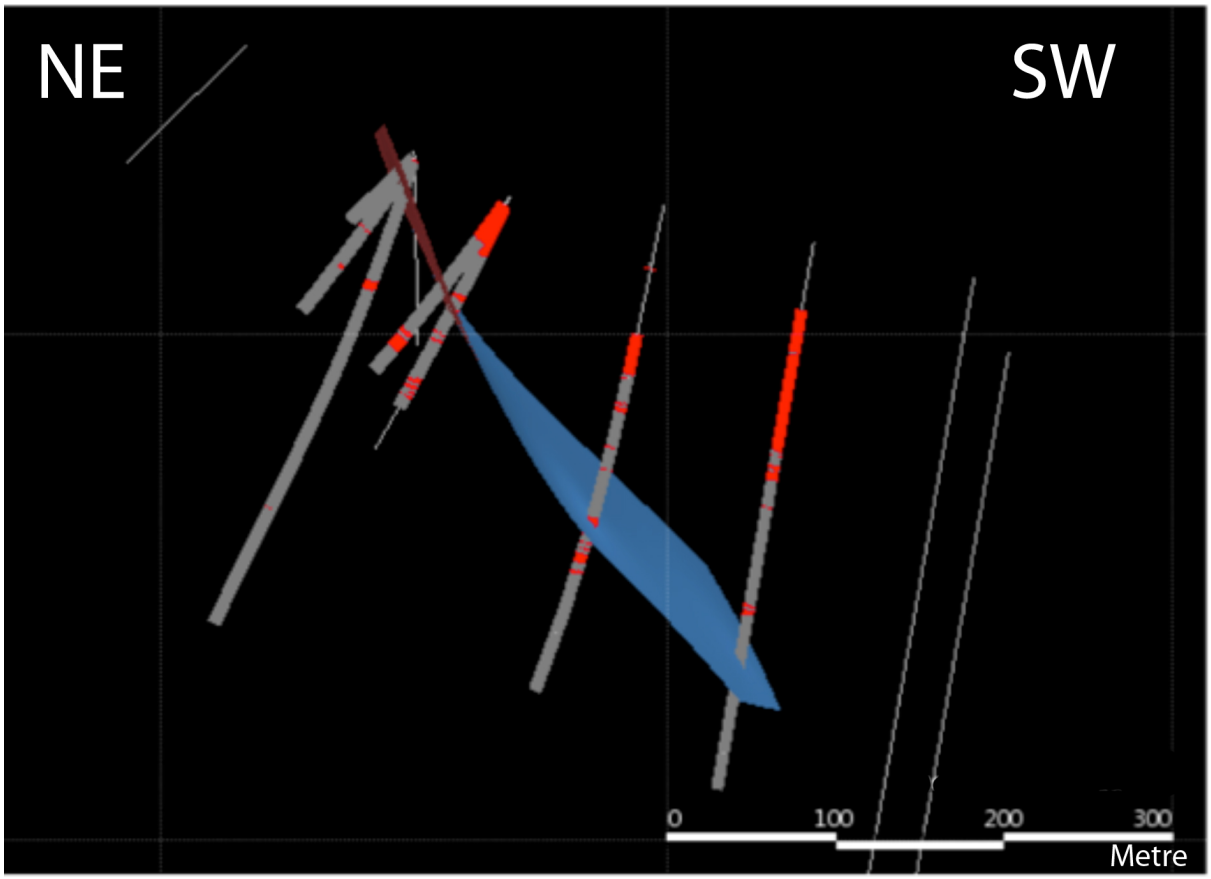


**Figure 2.11:** Cross-section of the Holmsletfjella drill holes (white lines) same view as figure 2.8 and 2.12; towards the southeast. Distribution of V-enriched samples (red) in relation to the surface model form figure 2.8, modified from (Halley, 2012).

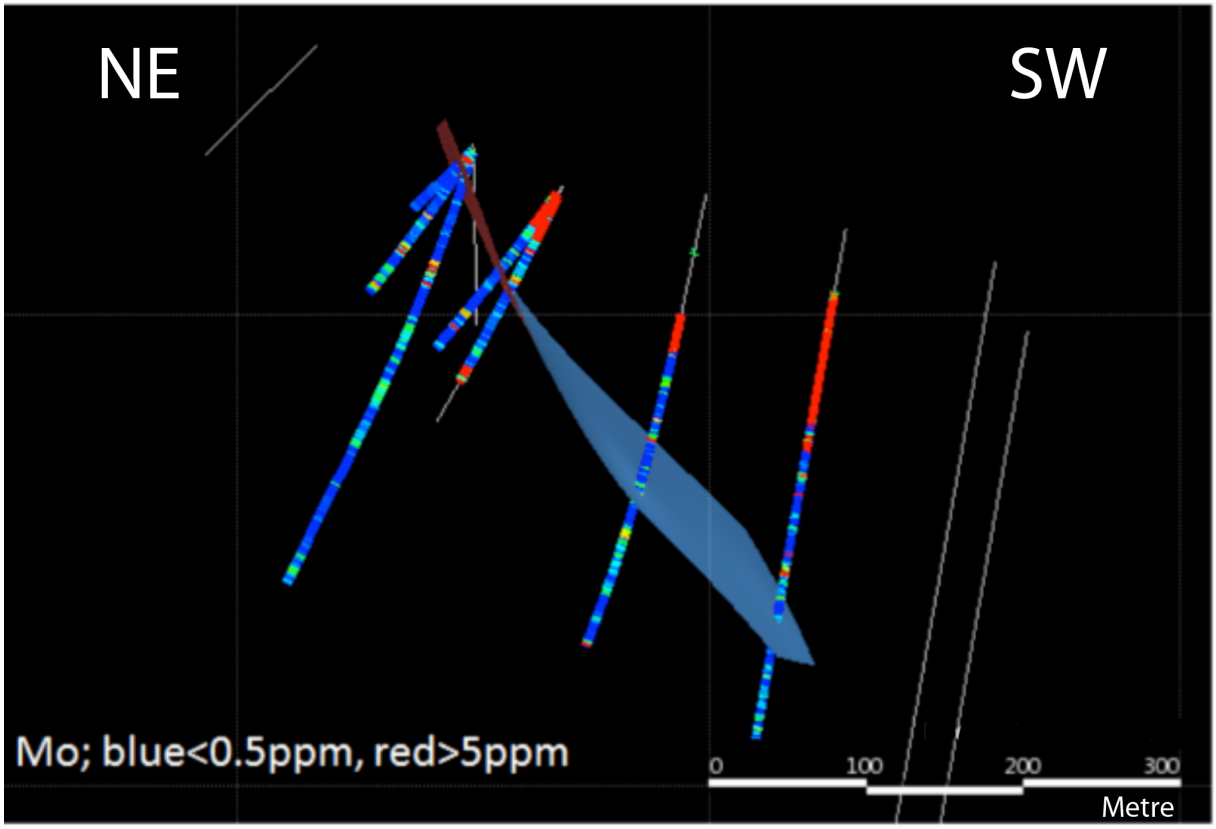


**Figure 2.12:** Cross-section of the Holmsletfjella drill holes (white lines) same view as figure 2.8 and 2.11; towards the southeast. Distribution of samples containing Mo in relation to the surface model form figure 2.8, modified from (Halley, 2012).

## 3 – Methods

Logging of the core from Holmsletfjella were done during the summer of 2010. This work consisted of measuring the core in order to determine core loss. Lithology and lithological boundaries were noted, when it comes to lithology the main focus is to be consistent so that one don't deviate and use two names for the same rock type, secondly comes assigning the correct name to the rock type. Determining the lithology also consists of noting the minerals that make up the rock and estimating the amount. When it came to mineralizations their type, extent and estimated amount were noted. Segments of the core were assembled like a jigsaw puzzle in order to orientate the core and measure orientation of structures. Based on lithology and mineralization, intervals for sampling were chosen. Intervals stretch up to a metre in length but will be cut short if there is a change in lithology or the occurrence of mineralizations; the aim is to have homogeneous samples no longer then one metre sent of for chemical analysis.

Main elements were analysed with X-Ray Fluorescence Spectroscopy (XRF) through the analytical method of:

"A calcined or ignited sample (0.9 g) is added to 9.0g of Lithium Borate Flux (50 % - 50 % $Li_2B_4O_7$ –$LiBO_2$), mixed well and fused in an auto fluxer between 1050 - 1100°C. A flat molten glass disc is prepared from the resulting melt. This disc is then analysed by X-ray fluorescence spectrometry" (ALS-Group, 2006b).

Samples were analysed for trace elements in two ways.

1 – "A prepared sample (0.25 g) is digested with perchloric, nitric, hydrofluoric and hydrochloric acids. The residue is topped up with dilute hydrochloric acid and analyzed by inductively coupled plasmaatomic emission spectrometry. Following this analysis, the results are reviewed for high concentrations of bismuth, mercury, molybdenum, silver and tungsten and diluted accordingly. Samples meeting this criterion are then analyzed by inductively coupled plasma-mass spectrometry. Results are corrected for spectral interelement interferences" (ALS-Group, 2006a).

2 – “A prepared sample (30 – 50 g) is fused with a mixture of lead oxide, sodium carbonate, borax and silica, inquarted with 6 mg of gold-free silver and then cupelled to yield a precious metal bead. The bead is digested for 2 minutes at high power by microwave in dilute nitric acid. The solution is cooled and hydrochloric acid is added. The solution is digested for an additional 2 minutes at half power by microwave. The digested solution is then cooled, diluted to 4 mL with 2 % hydrochloric acid, homogenized and then analyzed for gold, platinum and palladium by inductively coupled plasma – atomic emission spectrometry” (ALS-Group, 2005).

By the summer of 2011 the chemical analysis of the samples from last year was back and with this at hand it was possible to do a re-logging of the core. With the chemical data presented as graphs (see fig 5.6, 5.7, 5.8, 5.9 and App. 1) one was able to determine lithology and mineralizations with grater accuracy, and separate the core into different groups/formations. Combining what was visible in the core with the chemical data, intervals were chosen for thin section preparation. The result of the re-logging is what has been used in this thesis.

## 4 – Field Description

The Bulltinden Conglomerate Member contains clasts of graphite, quarts, marble, dolomite and limestone; the matrix is fine grained consisting of carbonate and quartz. The section contained within the drill core of the Bulltinden Conglomerate Member is coarseing upwards.

Holmsletfjella Formation is made up of graphite with varying degree of schistosity. A network of quartz-carbonate veins in the graphite makes it impossible to say whether the pyrite originates from the fluids or the host rock.

The ultramafic Vestgötabreen Complex is composed of serpentinites, which in some areas have been altered by listwanitization. Hand held XRF analysis, shown later to be supported by appendix 1, have yielded results between ~1000 - 2000ppm Cr and Ni.

Vestgötabreen Complex is dominated by greenstones and cataclasite. The term "cataclasite" were first used due to that the rock in the drill core was intensely fractured. Later one came upon more solid parts of the same rock, but in order to be consistent the term was kept. Both the cataclasite and the greenstone are fine-grained containing carbonate, mica and quartz.

Sandstones composed of quartz and carbonate make up the St. Jonsfjorden Group. In comparison to the other groups/formations the St. Jonsfjorden Group is narrow.

Alkhornet Formation of St. Jonsfjorden Group is the bottom formation of the drill holes and is composed of limestone. Variations within the unit are due to the amount of graphite in the limestone.


**Figure 4.1:** Colour codes for the different groups/formations are shown on the left side. On the right side are pictures of how the rocks in the different groups/formations look from the studied drill core.

# 5 – Maps, Cross-Sections and photos of the Holmsletfjella area

Through the use of the geological map of St. Jonsfjorden, (Bergh et al., 2003), and the re-logged core (Fig. 5.6, 5.7, 5.8, 5.9 and App. 1) a map (Fig. 5.1) and a schematic cross-section (Fig. 5.2) has been drawn. Modifications from the map and cross-section by (Bergh et al., 2003) to the map (Fig. 5.1) and cross-section (Fig 5.2) are based on fieldwork and drill cores from Holmsletfjella and the surrounding areas. Figure 5.3 show the location of the drill holes on an aerial orthophoto and where the cross-section in figure 5.5 is from. The relation between the map (Fig 5.1) and the aerial orthophoto with its drill hole locations (Fig 5.3) is illustrated by figure 5.4.

Figure 5.6, 5.7, 5,8 and 5,9 show the different elements and their abundance in relation to depth of the drill hole. In addition to this there is also the logged lithology and the position of where thin sections has been prepared from. Short descriptions of all the thin sections can be found in appendix 2. Formations and groups have been marked off on figure 5.6 to 5.9 corresponding to those used in figure 4.1, 5.1 and 5.2.

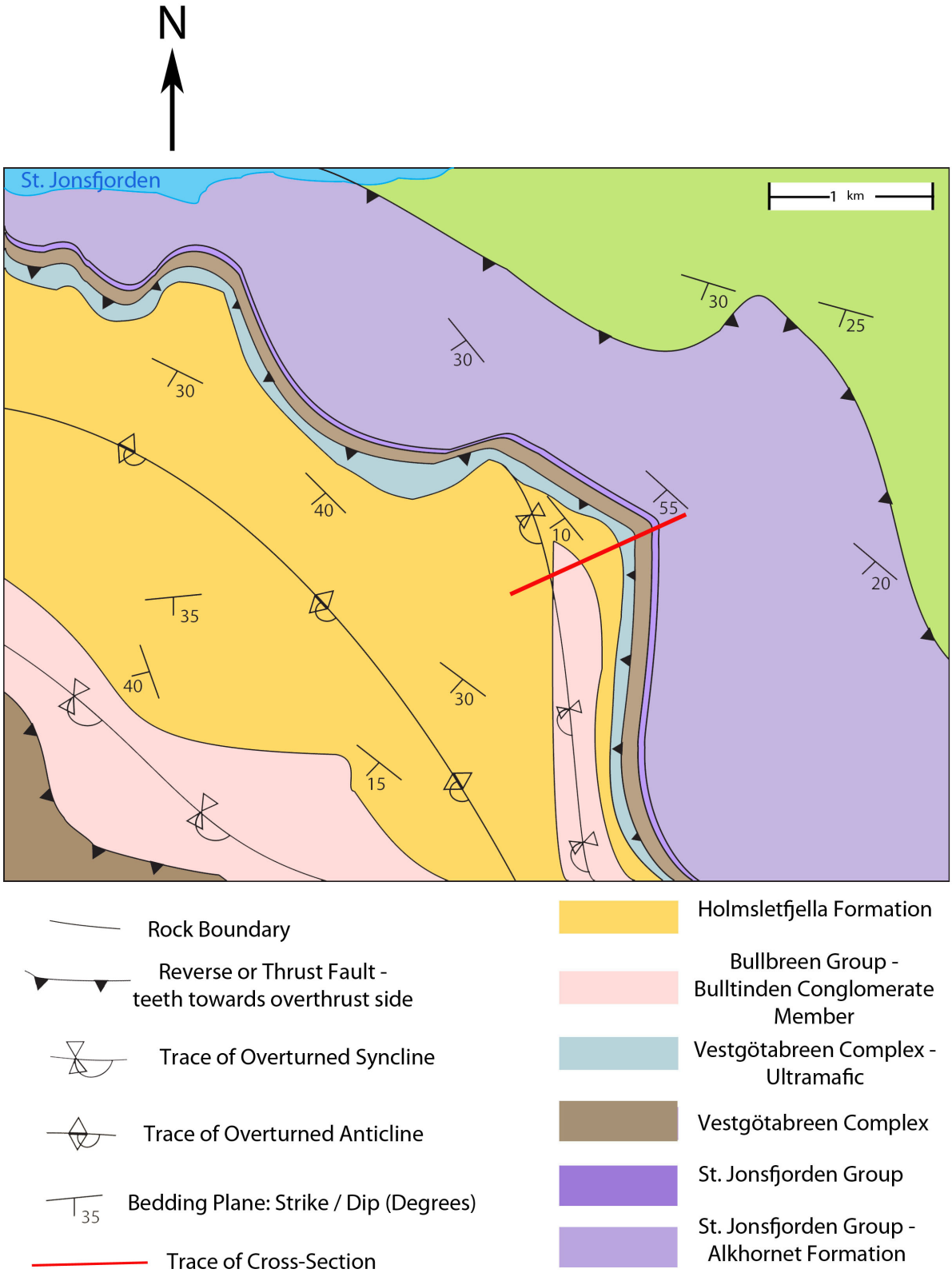


**Figure 5.1:** Geological map of the Holmsletfjella area, the red line mark the trace for the cross-section in figure 5.2. The map and the legend is from (Bergh et al., 2003), with modifications to the extent of the formations/groups based on fieldwork and drill cores.

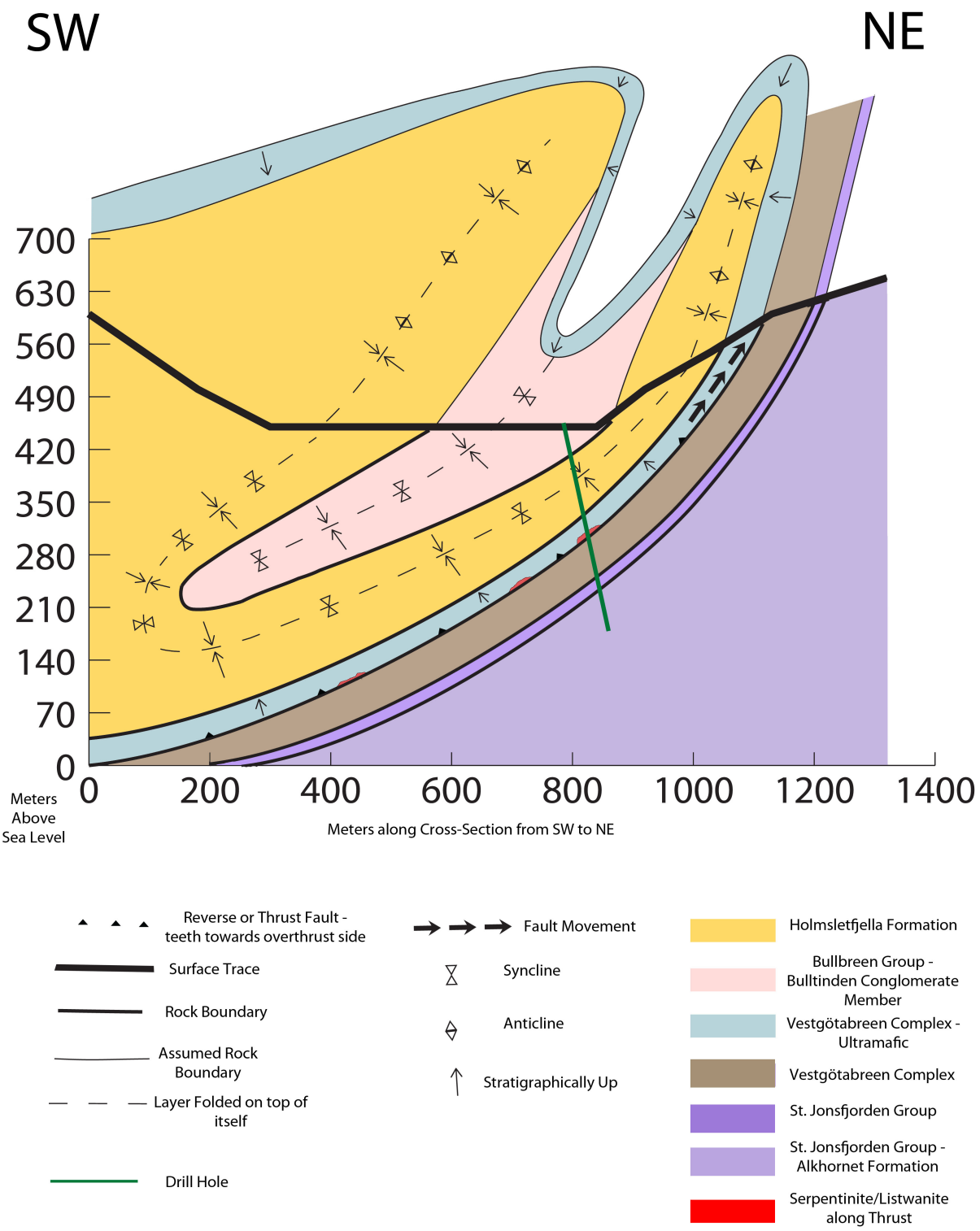


**Figure 5.2:** Cross-section of the drill area at Holmsletfjella, the cross-section has been marked in figure 5.1.

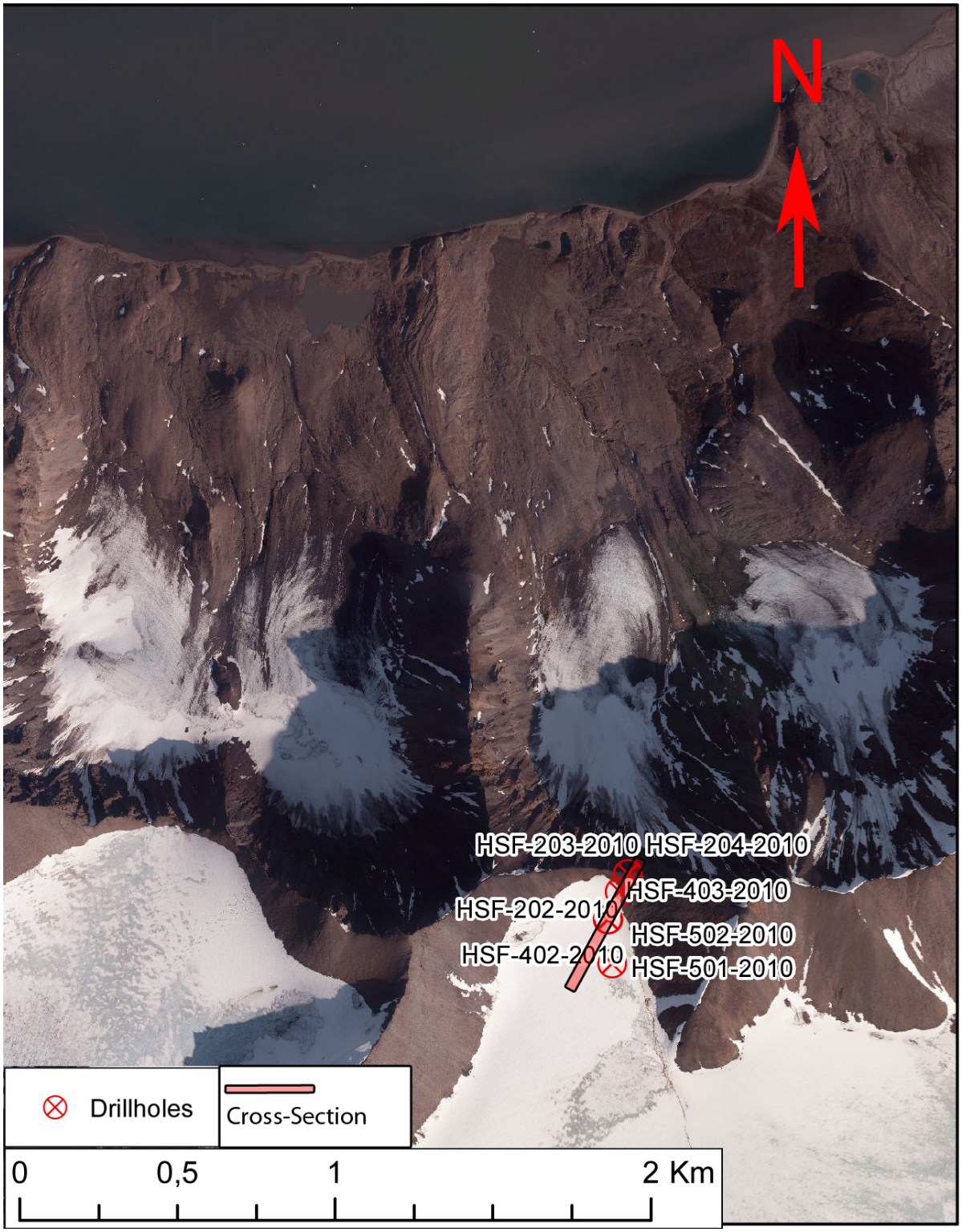


**Figure 5.3:** Location of the drill holes, the red line marks where figure 5.4 is from.

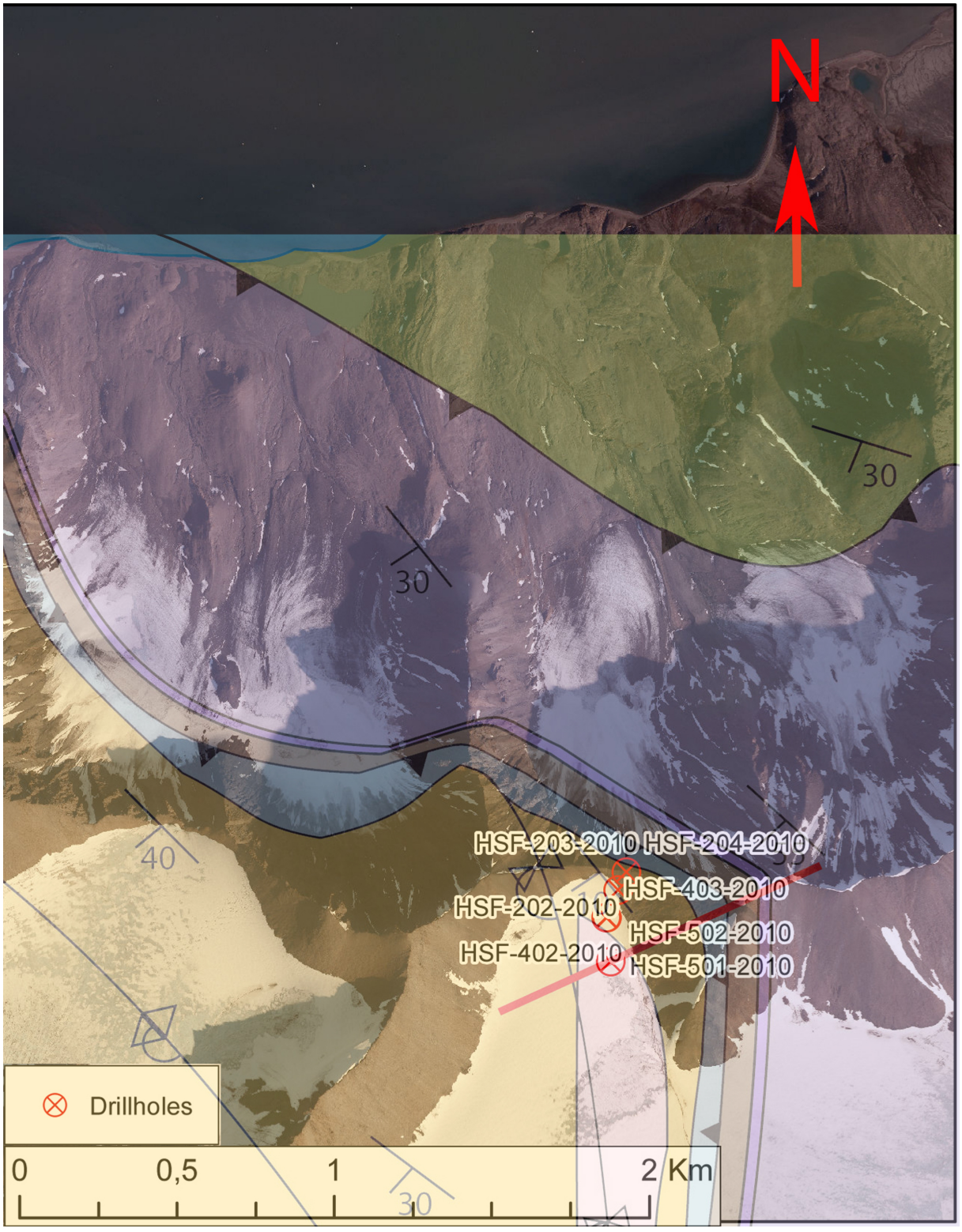


**Figure 5.4**: The map from figure 5.1 has been projected on top of the aerial photograph from figure 5.3, showing the relation between formations/groups, drill holes and topography.

The cross-section in figure 5.5 has some uncertainties concerning the HSF-200 holes in the northeastern corner of the section. This may in part be due to the 3D orientation of the different holes projected onto a 2D surface. There may also be some structural affects such as folding and thrusting that has not been accounted for in this cross-section.

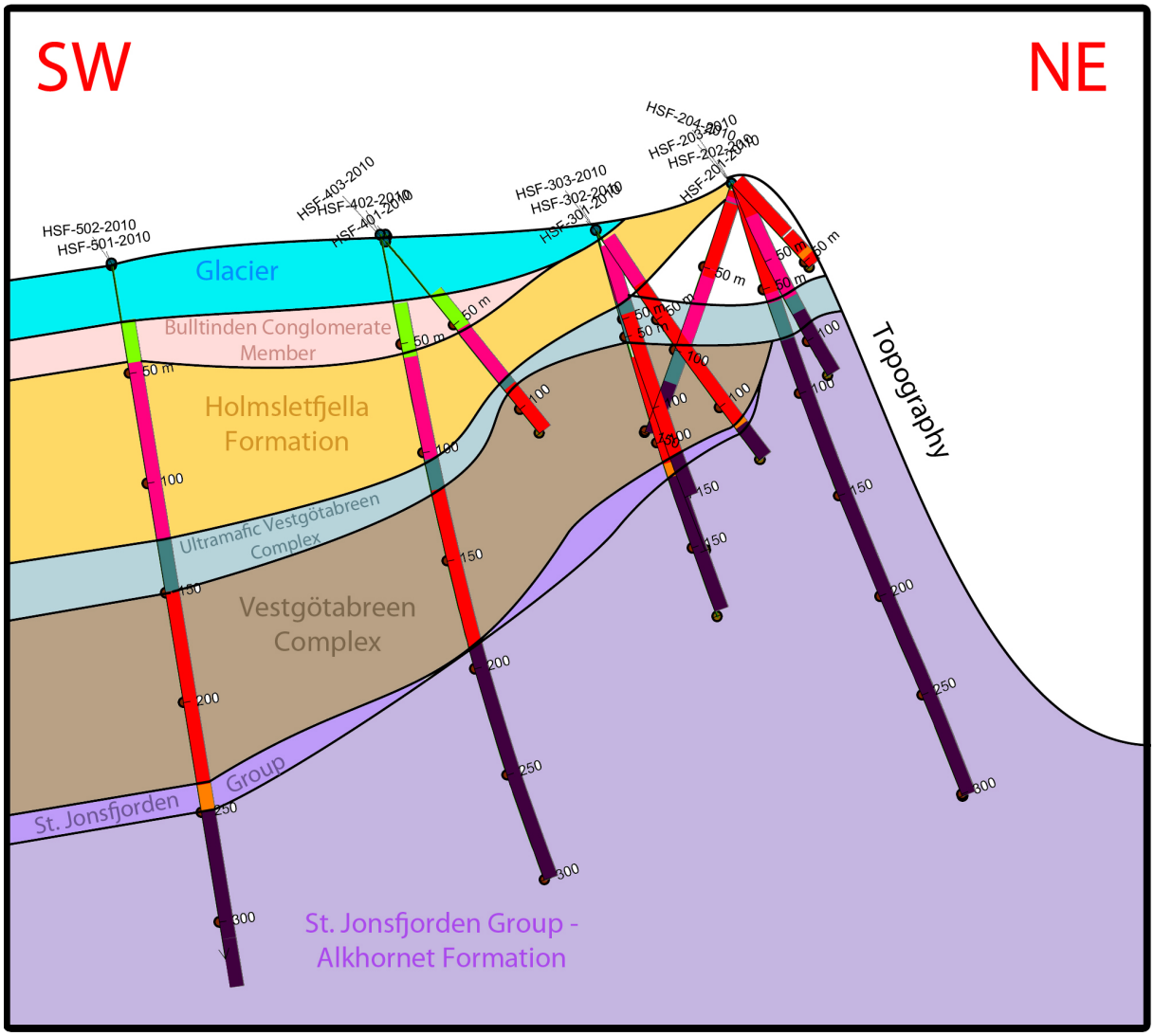


**Figure 5.5:** Cross-section of the drill holes from Holmsletfjella. The colour coding along the drill holes is not the same as that which has been used previously but in between the holes the colour coding matches that of figure 4.1, 5.1 and 5.2. Numbers along the drill holes indicate the length of the holes in metres. The topography is not to scale but is there to give some perspective as to the positioning of the drill holes.

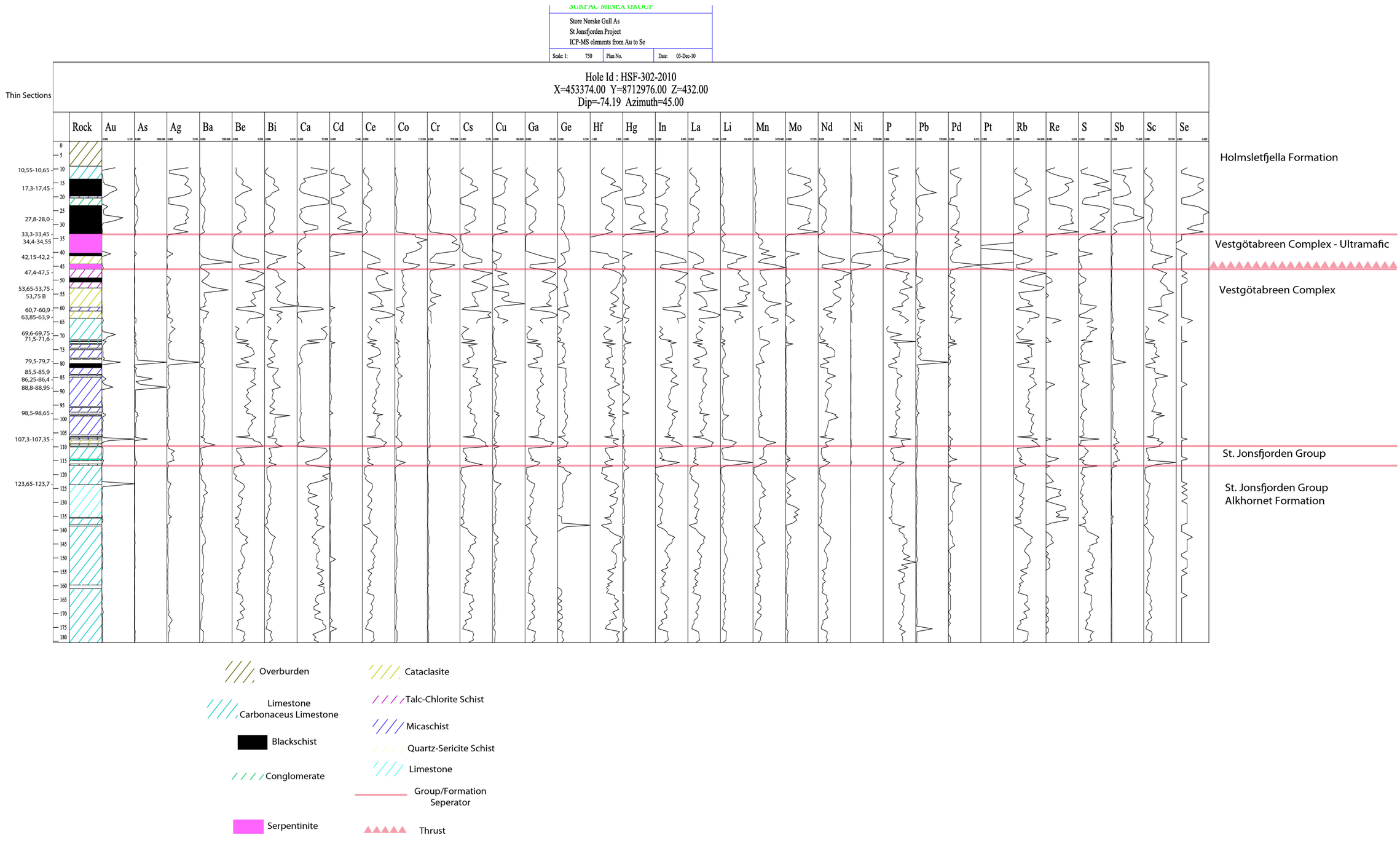


**Figure 5.6:** Plot of drill hole HSF-302-2010 with depth along the y-axis and different elements along the x-axis. The amount of the different elements is plotted as graphs in relation to depth.

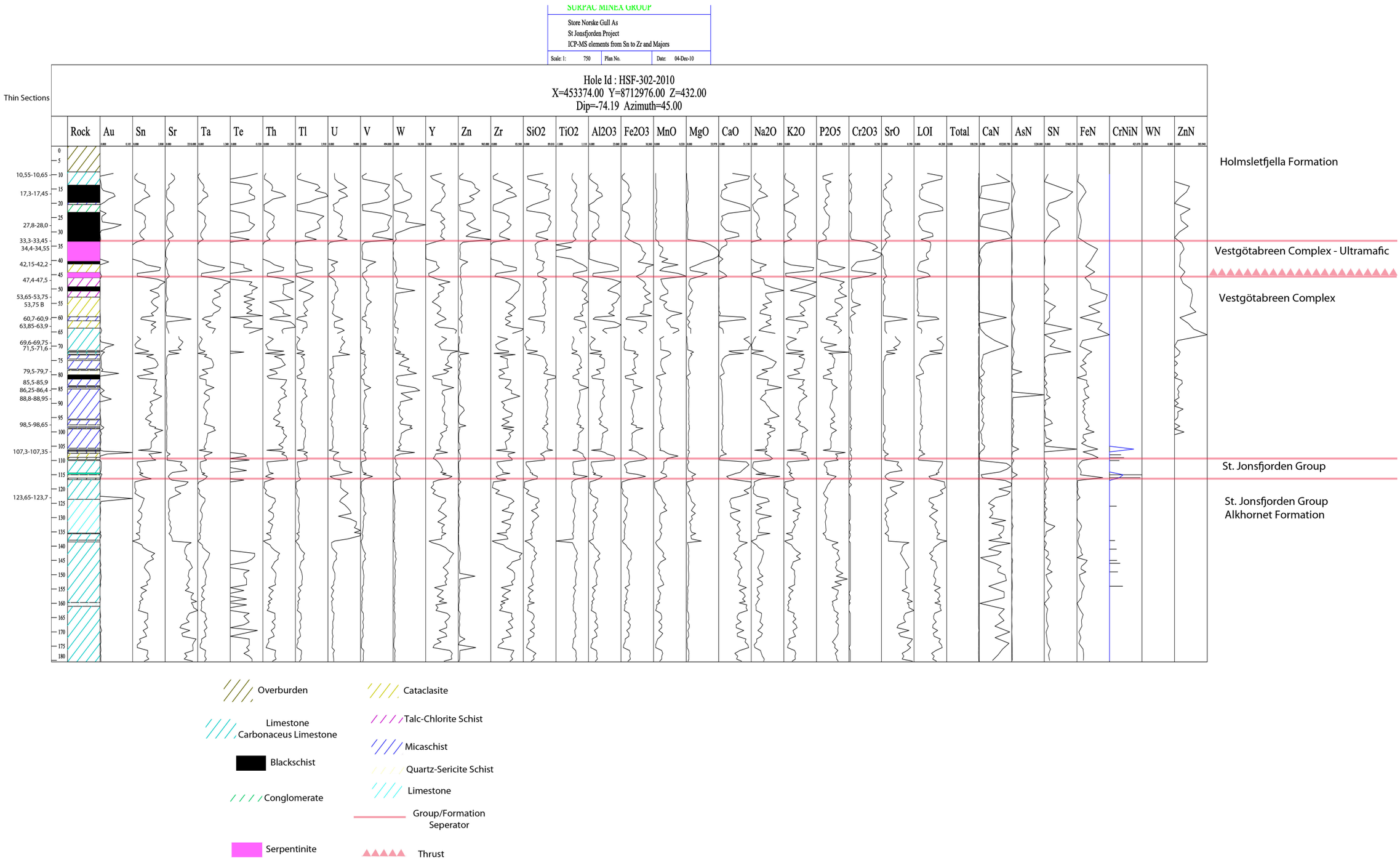


**Figure 5.7:** Plot of drill hole HSF-302-2010 with depth along the y-axis and different elements along the x-axis. The amount of the different elements is plotted as graphs in relation to depth.

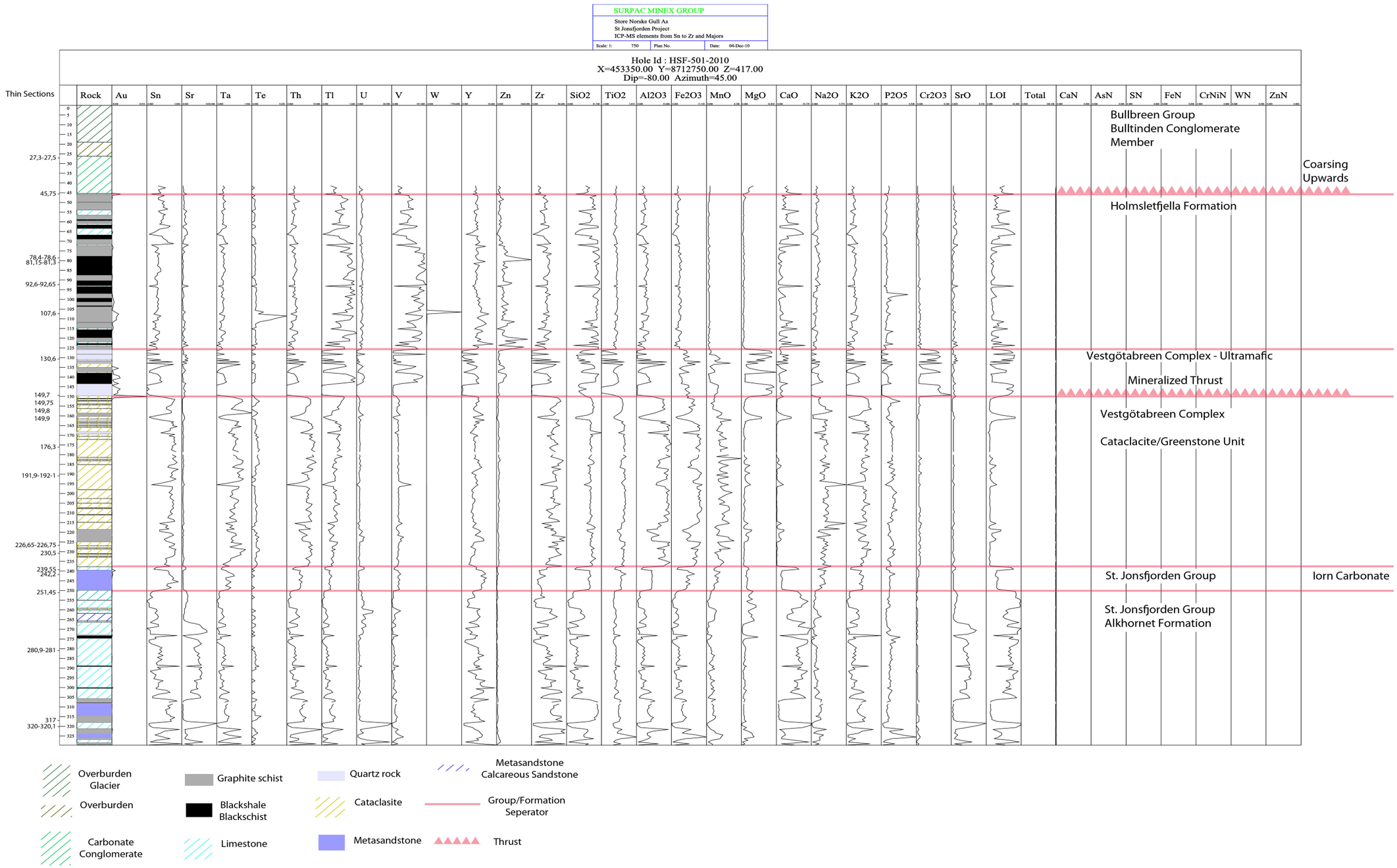


**Figure 5.8:** Plot of drill hole HSF-501-2010 with depth along the y-axis and different elements along the x-axis. The amount of the different elements is plotted as graphs in relation to depth.

SURPAC MINEX GROUP

Store Norske Gull As
St Jonsfjorden Project
ICP-MS elements from Au to Se

Scale: 1: 750 | Plan No. | Date: 03-Dec-10

Hole Id : HSF-501-2010
X=453350.00 Y=8712750.00 Z=417.00
Dip=-80.00 Azimuth=45.00

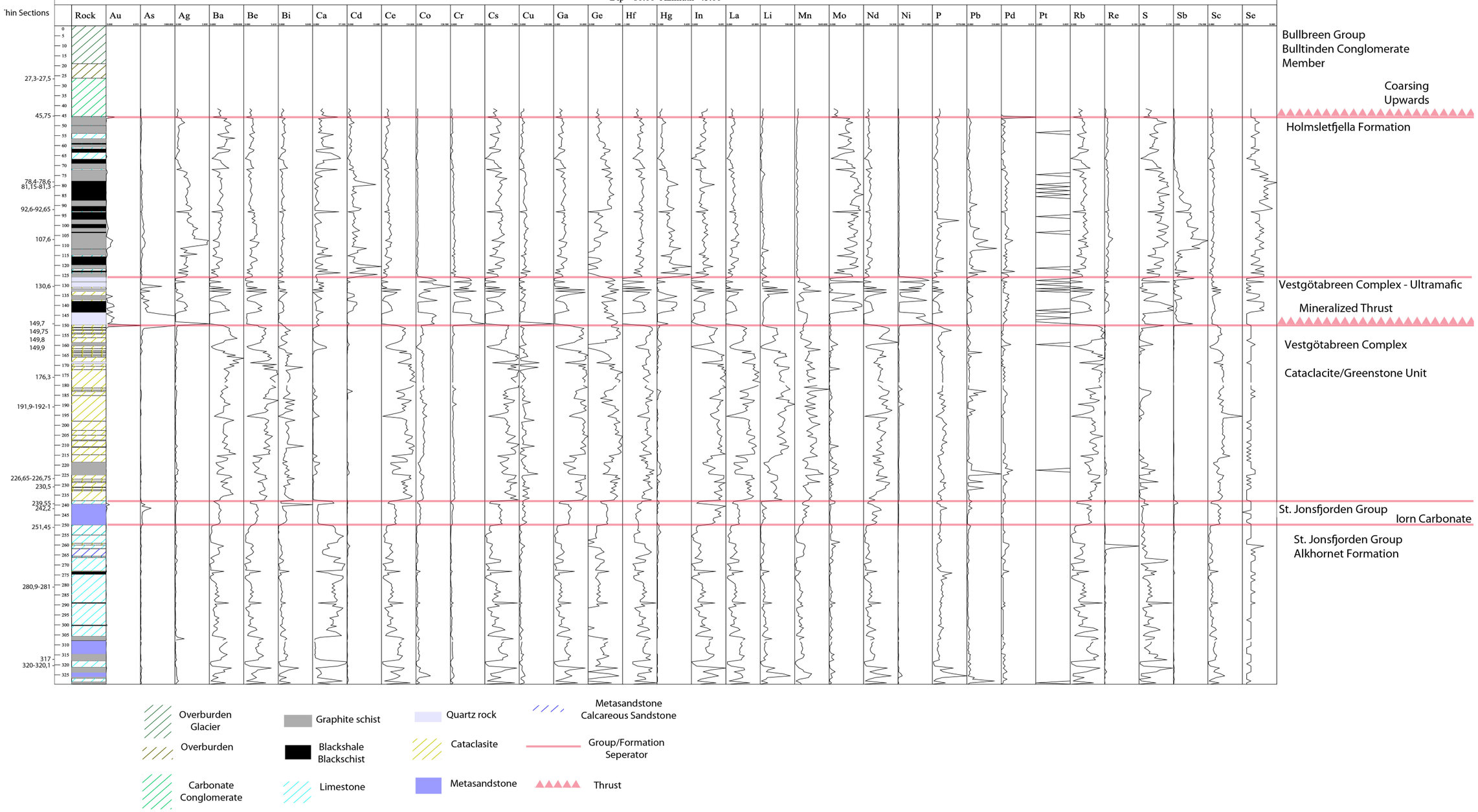


**Figure 5.9:** Plot of drill hole HSF-501-2010 with depth along the y-axis and different elements along the x-axis. The amount of the different elements is plotted as graphs in relation to depth.

# 6 – Petrography

## 6.1 – Bullbreen Group – Bulltinden Conglomerate Member

The Bulltinden Conglomerate Member as marked in drill hole HSF-402-2010, HSF-403-2010 and HSF-501-2010 (Appendix 1, Fig. 5.8 and 5.9) has not been chemically analysed, with the exception a few metres in the lowest part of the member and for two intervals in drill hole HSF-402-2010.

The Bulltinden Conglomerate Member of drill hole HSF-403-2010 contains a section with fossils (Fig. 6.1). Figure 6.1 show a horseshoe shaped fossil; this is a crinozoa and the size of makes it Silurian. There did exist crinozoas in Ordovician but not of this size. Rugose corals were also observed within this section of the core and they have a time span of Mid-Ordovician to Perm. Together with crinozoa this gives a lower and upper time limit to deposition of the conglomerate; respectively Silurian to Perm. High density of snails within this section was observed and is indicative of shallow water levels. Snails does not give any further limitations as to when the conglomerate could have formed since they have been around form Cambrian up till today. Geopetal infills show up in the Bulltinden Conglomerate Member to be up in the drill core as well. (Hanken, 2011)

**Figure 6.1:** Picture of fossils in drill hole HSF-403-2010, diameter of core is 5 cm.

In the top left part of figure 6.2 B a piece of the unaltered conglomerate is visible. By comparing the unaltered and the altered part of the conglomerate one clearly can make out the clasts in the altered part of the conglomerate.

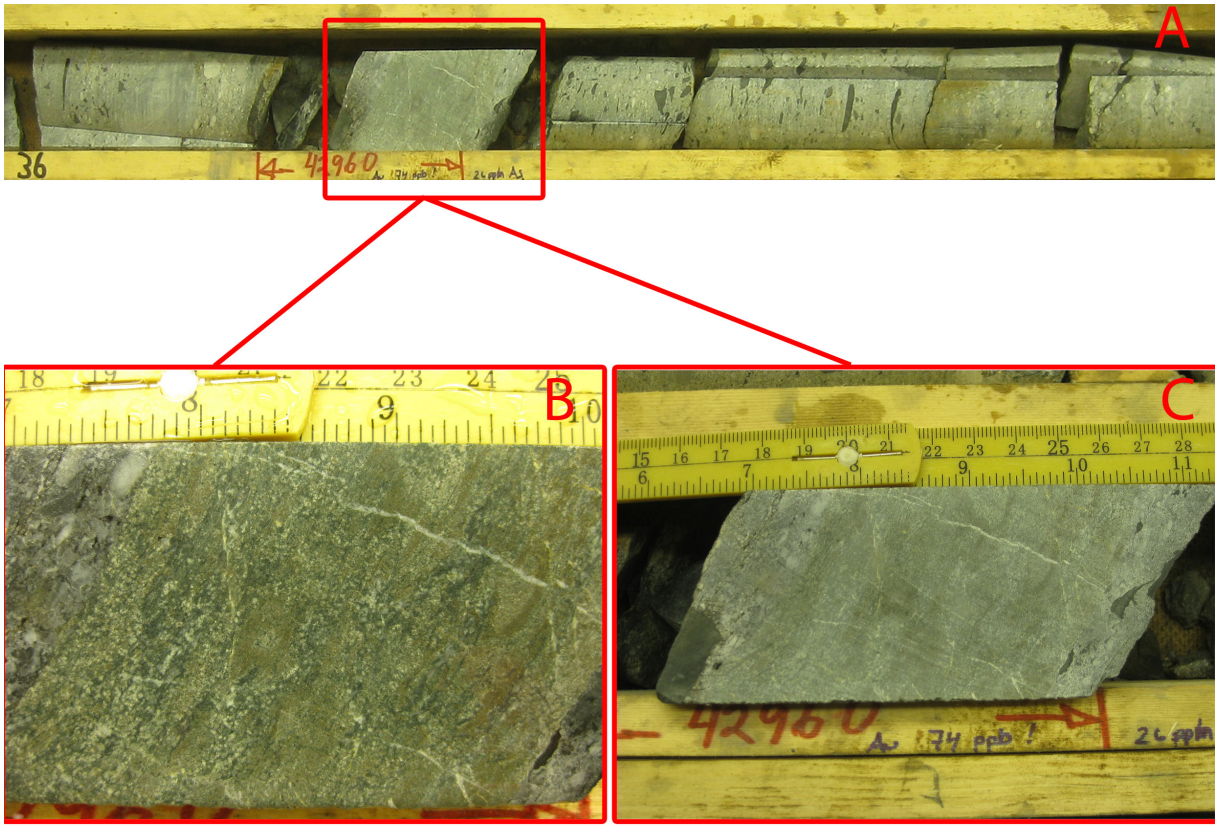


**Figure 6.2:** Picture A shows the altered conglomerate, between 36,2 metres and 36,3 metres, in relation to the unaltered conglomerate. Picture B is a close-up on the alteration and some of the conglomerate with a wet surface, whereas picture C is of the same piece as B only dry. From drill hole HSF-402-2010

Figure 6.3 shows the following minerals:
Quartz (Qtz) – appear colourless under PPL with subhedral grains up to 1 mm in size. Under XPL the quartz show gray to white undulating extinctions of the first order interference.

Carbonate (Cb) – show anomalous interference colours of upper-order creamy white with twin lamellae as pastel bands of pink and green under XPL. As part of the matrix in the conglomerate the carbonate is very fine-grained with the odd euhedral crystal reaching up to 0,5 mm in size. Under PPL the carbonate is colourless.

Muscovite (Mica) – with PPL the muscovite is colourless but under XPL it has interference colours of the second to third order. Grain size varies from fine-grained in the matrix and up to 1 mm for the largest grains. The muscovite grains are euhedral.

Chloritoid (Cld) – appears as green under PPL with pleochroism. With XPL the chloritoid show anomalous interference colours of red to dark blue. Grains are subhedral with size varying between 0,1-1 mm.

Pyrite (Py) – with PPL and XPL pyrite is opaque but under RL it has a white to yellow metallic shine. Grains are subhedral and up to 0,2 mm in length.

Arsenopyrite (Apy) - with PPL and XPL arsenopyrite is opaque but under RL it is white with a faint tint of yellow. The arsenopyrite grains are less than 0,1 mm and have a distinct needle shape with euhedral grain boundaries.

Figure 6.3 show the arsenopyrite, pyrite and chloritoid to be contained within the altered part of the Bulltinden Conglomerate Member.

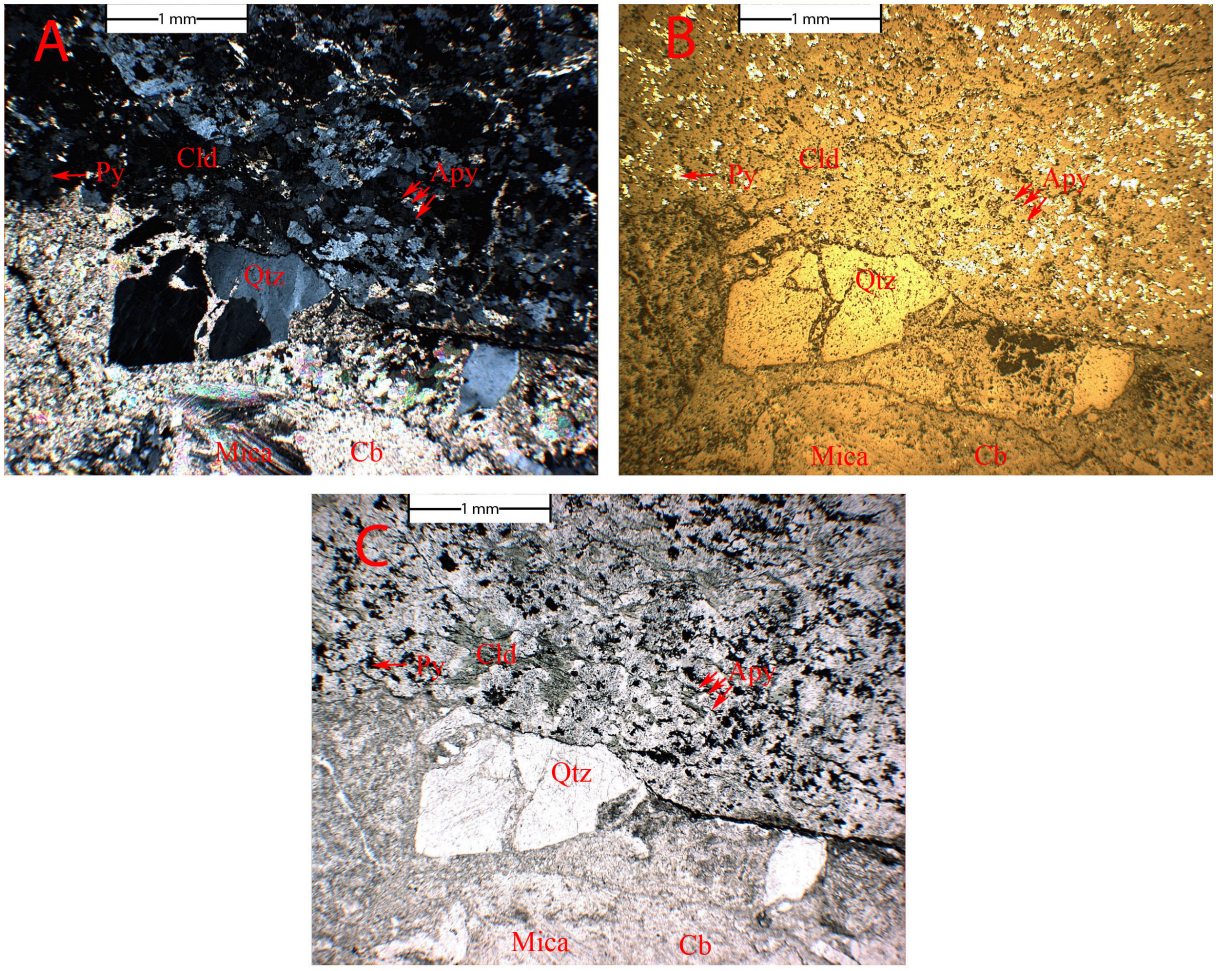


**Figure 6.3:** A – cross polarised light (XPL), B – reflected light (RL), C – plane polarised light (PPL). All are from the same section showing the conglomerate in the lower part and the alteration in the upper part. Thin section HSF-402-2010 36,2-36,3.

Of the two previously mentioned intervals chemically analysed in the Bulltinden Conglomerate Member of HSF-402-2010, figure 6.2 is one of them stretching from 36,2 metres to 36,3 metres, and the other one is between 39,1 metres and 39,7 metres.

Table 6.1 gives an enrichment factor of about 21 for Au and about 9 for As. V-score averages 200,98 for the unaltered conglomerate and 248,33 for the altered conglomerate (Table 6.1).

| Hole ID | From (m) | To (m) | As (ppm) | Au (ppm) | V-score |
|---|---|---|---|---|---|
| HSF-403-2010 | 45 | 46 | 5 | 0,002 | 233,22 |
| HSF-403-2010 | 46 | 47 | 5 | 0,007 | 191,47 |
| HSF-403-2010 | 47 | 48 | | | 158,76 |
| HSF-403-2010 | 48 | 49 | 5 | 0,005 | 122,2 |
| HSF-403-2010 | 49 | 50 | 9 | 0,001 | 212,12 |
| HSF-403-2010 | 50 | 51 | 11 | 0,007 | 204,26 |
| HSF-403-2010 | 51 | 52 | 6,8 | 0,001 | 284,8 |
| HSF-402-2010 | 36,2 | 36,3 | 26,1 | 0,074 | 227,4 |
| HSF-402-2010 | 39,1 | 39,7 | 83 | 0,065 | 269,26 |

**Table 6.1:** Au and As content in addition to V-score from unaltered conglomerate (HSF-403-2010) and altered conglomerate (HSF-402-2010).

## 6.2 – Holmsletfjella Formation

Figure 6.4 and 6.5 show the graphite schist of Holmsletfjella Formation. Graphite, quartz-carbonate veins and pyrites are all discernable in both figure 6.4 and 6.5. Graphitic- schists and shales with slight variation in vein density dominate Holmsletfjella Formation.

Figure 6.5 shows the following minerals:
Graphite (Gr) – with PPL and XPL graphite is opaque, it has inclusions of carbonate, quartz and pyrite and due to the amount of graphite it is not possible to estimate the shape or size of the crystals.

Quartz (Qtz) – appear colourless under PPL with subhedral grains up to 0,2 mm in size. Under XPL the quartz show gray to white undulating extinctions of the first order interference.

Carbonate (Cb) – show anomalous interference colours of upper-order creamy white with twin lamellae as pastel bands of pink and green under XPL. The carbonate crystals are subhedral reaching up to 0,2 mm in size. Under PPL the carbonate is colourless.

Pyrite (Py) – with PPL and XPL pyrite is opaque but under RL it has a white to yellow metallic shine. Grains are subhedral and up to 0,2 mm in length.

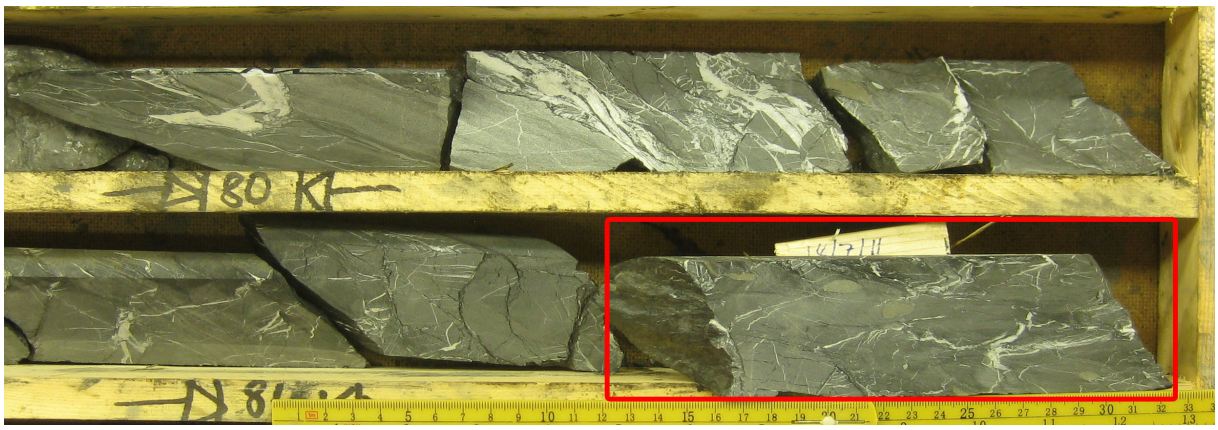

**Figure 6.4:** Blackschist from HSF-501-2010, thin section (Fig 6.5) has been made from the piece marked by the red square.

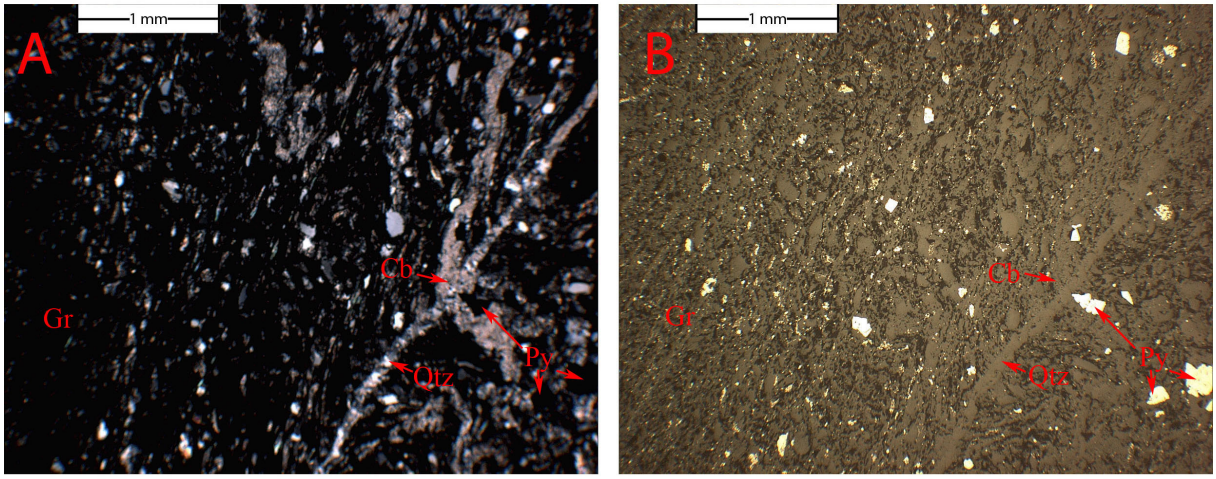


**Figure 6.5:** Figure A is XPL while figure B of the same section is with RL, PPL has not been included as it does not add much information to the relations of the minerals. Pictures are from thin section HSF-501-2010 81,15-81,3.

### 6.3 – Vestgötabreen Complex – Ultramafic

Carbonate, serpentinite, talc and pyrite, as seen in figure 6.6 B, C and D, make up the metamorphic ultramafic rock. From figure 6.6 A the dense network of veins stretching through the formation may be observed. The rock has been logged as serpentinite (Fig. 5.6 or 5.7)

Figure 6.6 shows the following minerals:
Talc (Tlc) – is colourless under PPL and show third order interference colours with XPL. Flakes of talc are up to 1 mm in length with anhedral grain boundaries.

Serpentine (Srp) – show first order gray and white interference colours under XPL. Under PPL the serpentine is colourless. The serpentine has formed fine-grained masses with somewhat diffuse and irregular grain boundaries. Serpentine masses may extend 1 mm in length.

Carbonate (Cb) – show anomalous interference colours of upper-order creamy white with twin lamellae as pastel bands of pink and green under XPL. The carbonate crystals are subhedral and about 1 mm in size. Under PPL the carbonate is colourless.

Pyrite (Py) – with PPL and XPL pyrite is opaque but under RL it has a white to yellow metallic shine. Grains are subhedral and up to 0,2 mm in length.

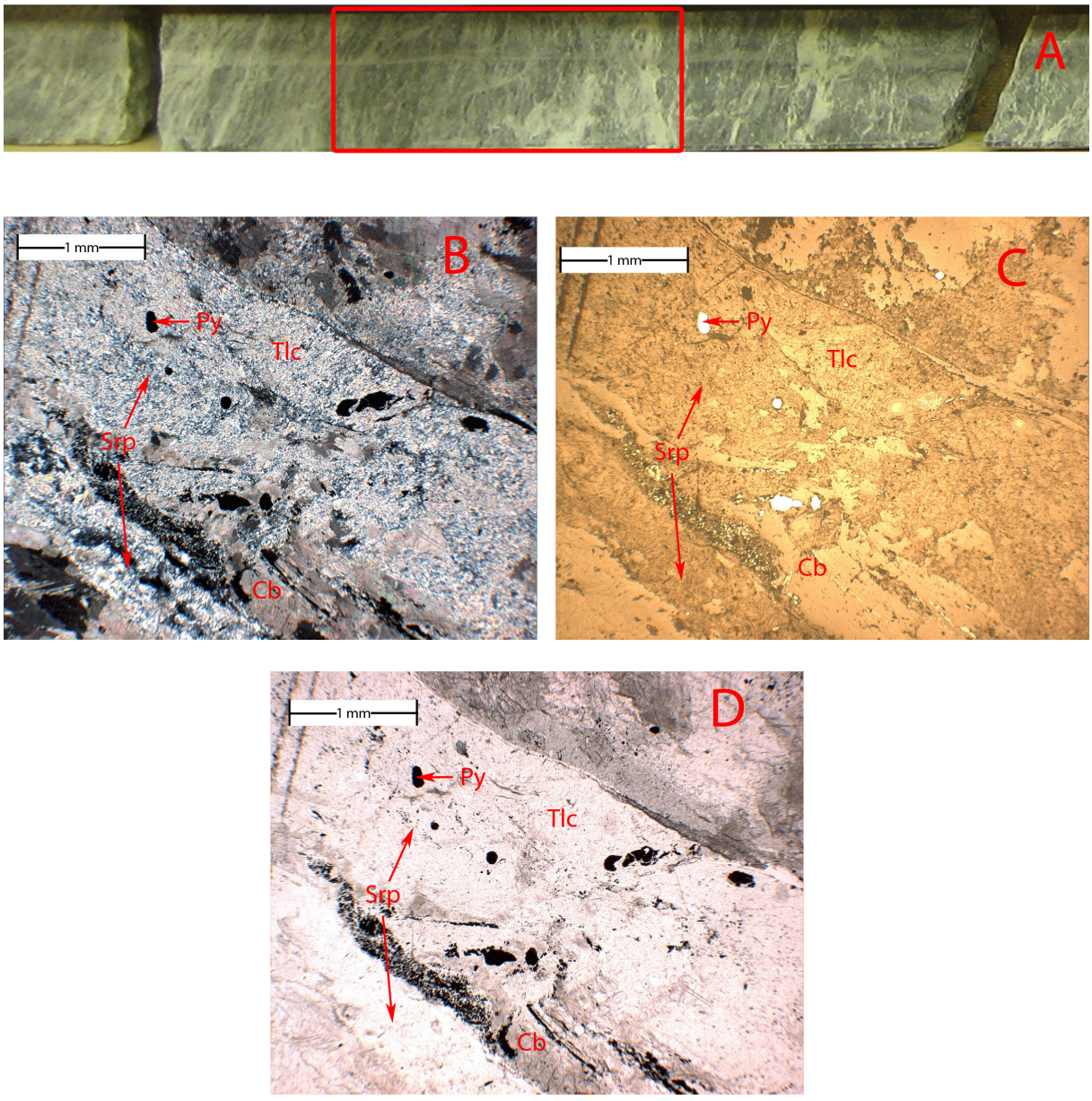


**Figure 6.6:** Picture A is of the ultramafic rock in HSF-302-2010 with a diameter of 5 cm. The red square marks where the thin section (HSF-302-2010 34,4-34,55) in figure B, C and D has been prepared from. B – XPL, C – RL and D – PPL.

Figure 6.7 is of a unit within the ultramafic Vestgötabreen Complex that has been logged as quartzite. In addition to containing quartz there is also carbonate, talc, serpentine, pyrite and arsenopyrite. The amount of serpentine form figure 6.6 to 6.7 is reduced and arsenopyrite and quartz has been introduced in the latter case.

Figure 6.7 shows the following minerals:
Quartz (Qtz) – appear colourless under PPL with subhedral grains up to 2 mm in size. Under XPL the quartz show gray to white undulating extinctions of the first order interference.

Carbonate (Cb) – show anomalous interference colours of upper-order creamy white with twin lamellae as pastel bands of pink and green under XPL. The carbonate crystals are subhedral and about 1,5 mm in size. Under PPL the carbonate is colourless.

Talc (Tlc) – is colourless under PPL and show third order interference colours with XPL. Flakes of talc are up to 0,7 mm in length with subhedral grain boundaries.

Serpentine (Srp) – show first order gray and white interference colours under XPL. Under PPL the serpentine is colourless. The serpentine has formed fine-grained masses with somewhat diffuse and irregular grain boundaries. Serpentine masses may extend 0,6 mm in length.

Pyrite (Py) – with PPL and XPL pyrite is opaque but under RL it has a white to yellow metallic shine. Grains are subhedral and up to 0,3 mm in length.

Arsenopyrite (Apy) - with PPL and XPL arsenopyrite is opaque but under RL it is white with a faint tint of yellow. The arsenopyrite grains are 0,2 mm in length and have a distinct needle shape with euhedral grain boundaries.

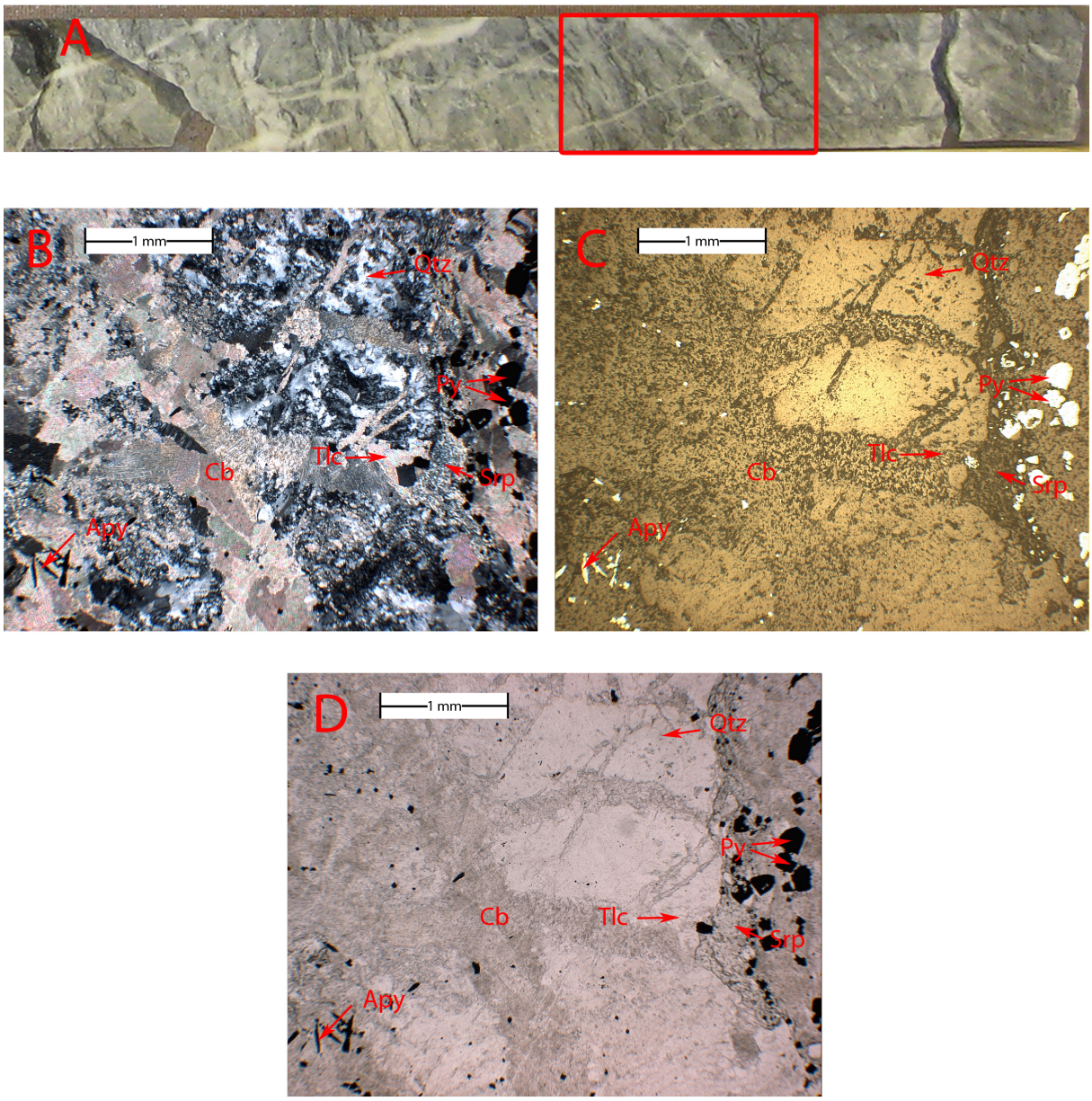


**Figure 6.7:** Picture A is of the ultramafic rock in HSF-501-2010 with a diameter of 5 cm. The red square marks where the thin section (HSF-501-2010 149,9) in figure B, C and D has been prepared from. B – XPL, C – RL and D – PPL.

### 6.4 – Vestgötabreen Complex

The Vestgötabreen Complex is composed of what has been logged as cataclasite and greenstone. Figure 6.8 shows the minerals quartz, mica and chlorite making up the rock. Fine-grained pyrite has been observed in thin section (Fig. 6.8 C) but not in the hand specimen. Compared to the two previous thin sections (Fig. 6.5 and 6.6) and the altered part of the Bulltinden Conglomerate Member thin section (Fig. 6.3) the grain size and abundance of pyrite in Vestgötabreen Complex has dropped.

Figure 6.8 show the following minerals:
Quartz (Qtz) – appear colourless under PPL with subhedral grains. Grain varies in size between less than 0,1 mm and up to over 2 mm. Under XPL the quartz show gray to white undulating extinctions of the first order interference. The strained quartz has been subjected to deformation via dislocation glide.

Muscovite (Mica) – with PPL the muscovite is colourless but under XPL it has interference colours of the second to third order. Grain size is fine-grained and less than 0,1 mm.

Chlorite (Chl) – show pleochroism between pale yellowish to pale green under PPL and first order white and yellow interference colours under XPL. The chlorite is fine-grained less than 0,1 mm.

Pyrite (Py) – with PPL and XPL pyrite is opaque but under RL it has a white to yellow metallic shine. The pyrite is very fine-grained and less than 0,1 mm.

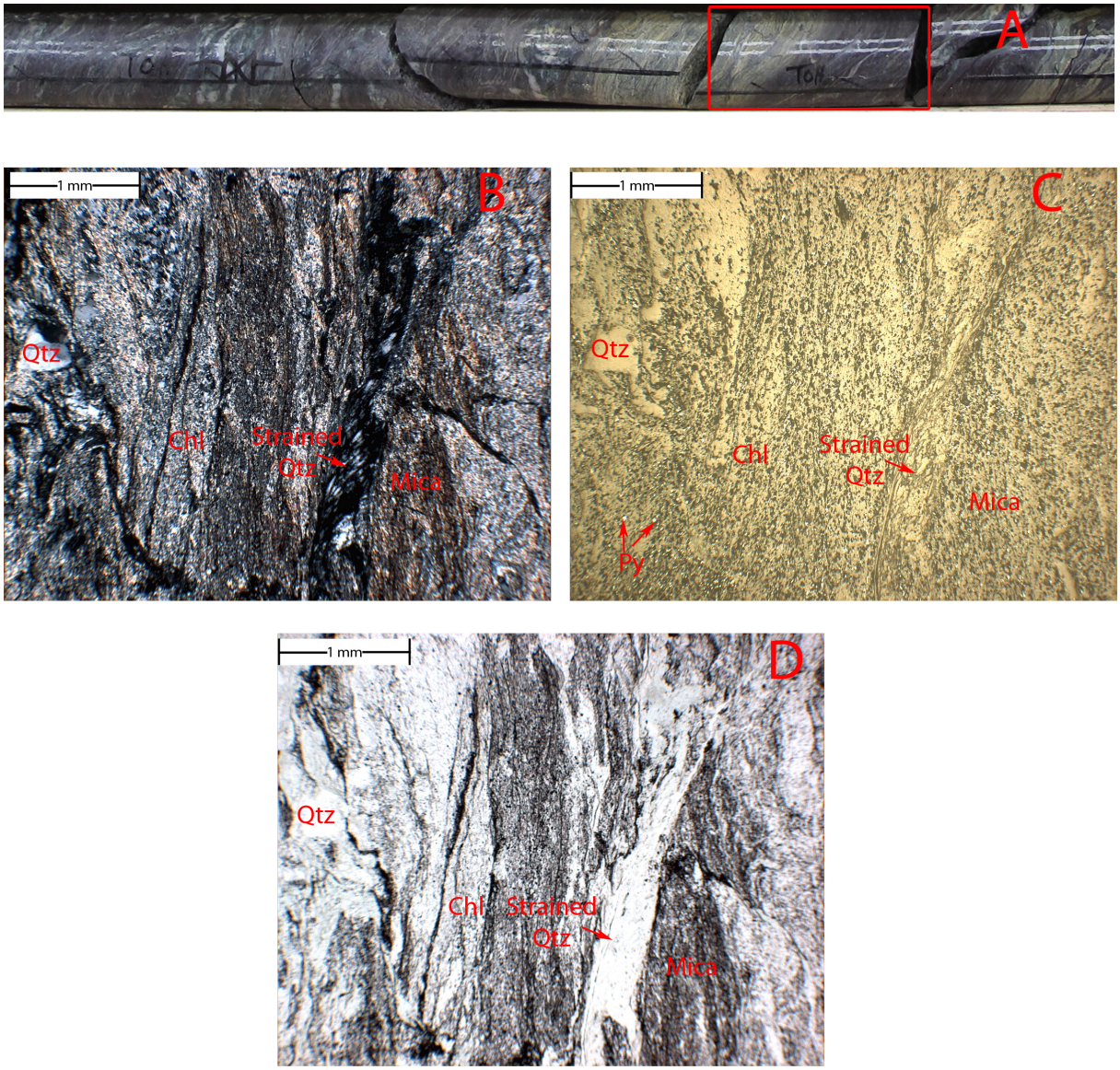


**Figure 6.8:** Picture A is of the cataclasite in HSF-501-2010 with a diameter of 5 cm. The red square marks where the thin section (HSF-501-2010 176,3) in figure B, C and D has been prepared from. B – XPL, C – RL and D – PPL.

## 6.5 – St. Jonsfjorden Group

The St. Jonsfjorden Group is composed of sandstone containing quartz, carbonate, mica and pyrite. Based on the circular pattern in the red square of figure 6.9 A one can tell that there is a fold hinge.

Figure 6.9 show the following minerals:
Carbonate (Cb) – show anomalous interference colours of upper-order creamy white with twin lamellae as pastel bands of pink and green under XPL. The carbonate crystals are subhedral and about 0,1mm to 1 mm in size. Under PPL the carbonate is colourless.

Quartz (Qtz) – appear colourless under PPL with subhedral grains. Grains varies between less than 0,1 mm and up to over 2 mm in size. Under XPL the quartz show gray to white undulating extinctions of the first order interference.

Muscovite (Mica) – with PPL the muscovite is colourless but under XPL it has interference colours of the second to third order. Grain size varies from less than 0,1 mm to 1 mm.

Pyrite (Py) – with PPL and XPL pyrite is opaque but under RL it has a white to yellow metallic shine. The pyrite is about 0,2 mm in length and subhedral.

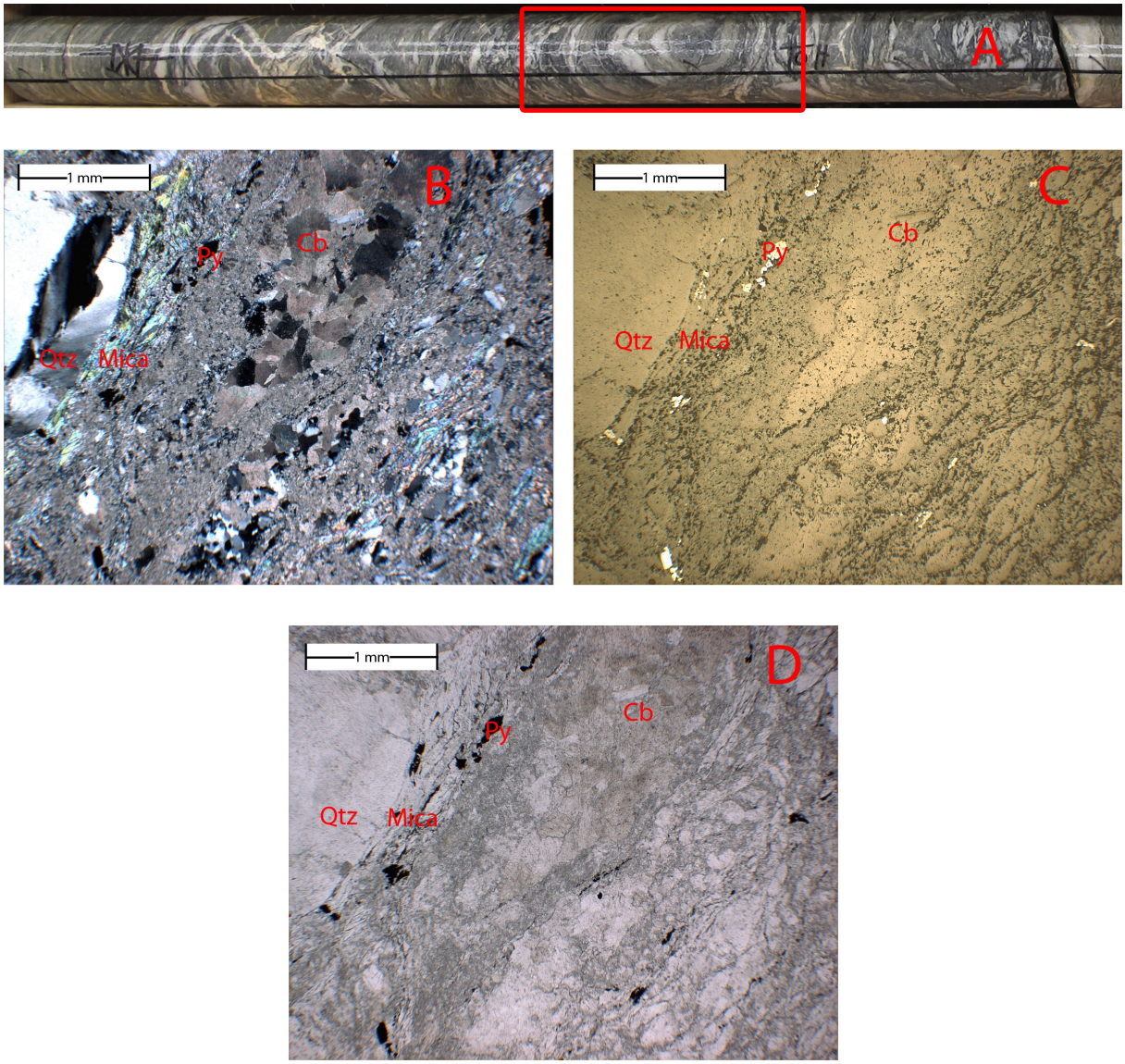


**Figure 6.9:** Picture A is of the sandstone in HSF-501-2010 with a diameter of 5 cm. The red square marks where the thin section (HSF-501-2010 242,2) in figure B, C and D has been prepared from. B – XPL, C – RL and D – PPL.

### 6.6 – St. Jonsfjorden Group – Alkhornet Formation

The Alkhornet Formation of St. Jonsfjorden Group is a limestone formation; the limestone varies slightly in how carbonaceous it is. The limestone is composed of carbonate and the carbonaceous limestone is in addition composed of graphite and some pyrite. White bands in figure 6.10 A and in the left part of 6.10 B, C and D is quartz-carbonate veins. Graphite rich parts of the limestone appear as dark bands (Fig. 6.10 A); one such band is included in the right part of the thin section photos (Fig. 6.10 B, C and D) and this where the pyrite resides.

Figure 6.10 show the following minerals:
Carbonate (Cb) – show anomalous interference colours of upper-order creamy white with twin lamellae as pastel bands of pink and green under XPL. The carbonate crystals are subhedral varying from less than 0,1 mm in central part of the thin section to about 1 mm in size in the lower left corner. Under PPL the carbonate is colourless.

Quartz (Qtz) – appear colourless under PPL with subhedral grains. Size of the quartz crystals varies between 0,1 mm and up to 1 mm. Under XPL the quartz show gray to white undulating extinctions of the first order interference.

Graphite (Gr) – with PPL and XPL graphite is opaque. The grain size cannot be estimated due to the opaque nature of graphite. The graphite has anhedral boundaries and inclusions of pyrite.

Pyrite (Py) – with PPL and XPL pyrite is opaque but under RL it has a white to yellow metallic shine. The pyrite is about 0,2 mm in length and subhedral.

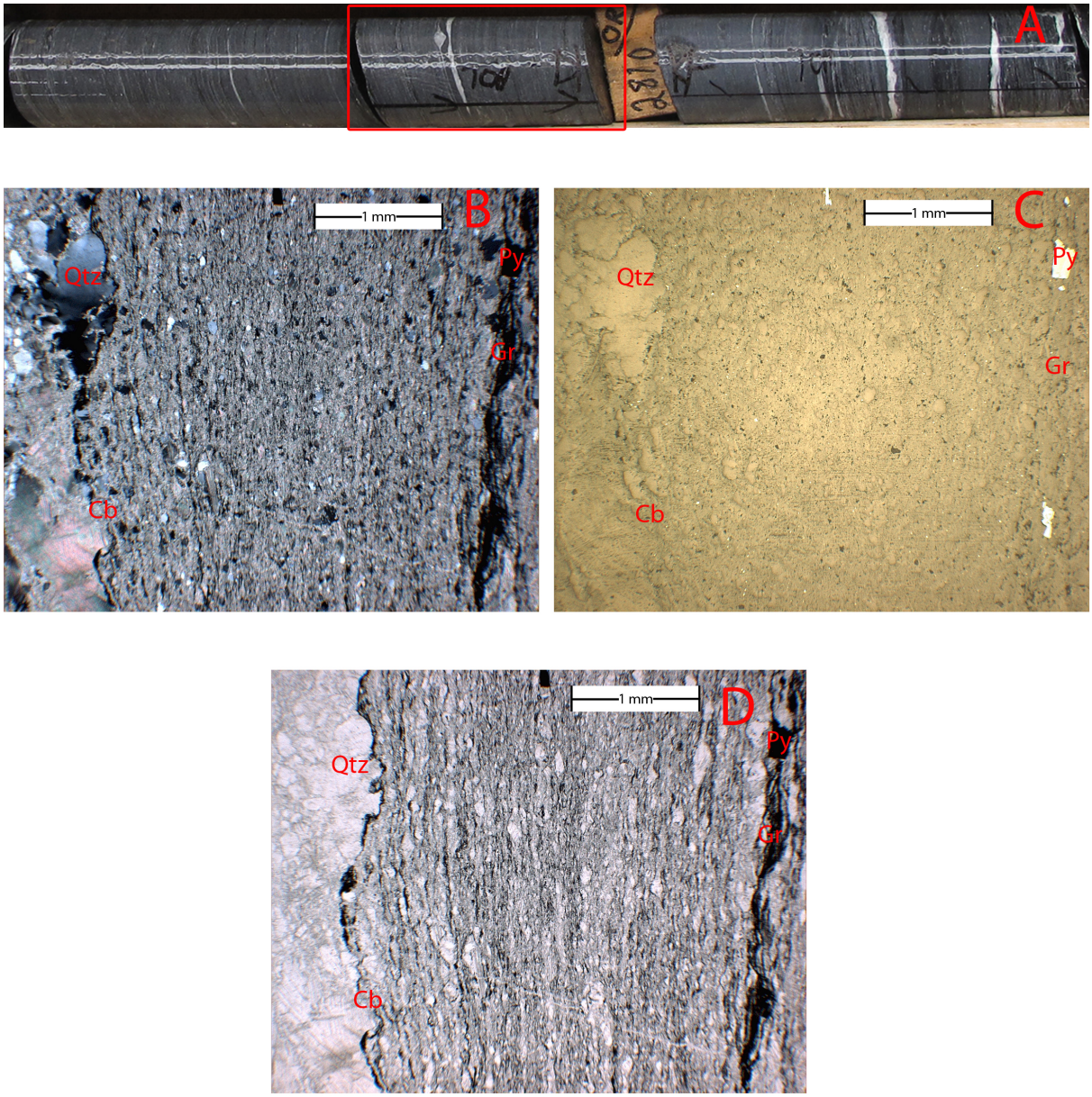


**Figure 6.10:** Picture A is of the limestone in HSF-501-2010 with a diameter of 5 cm. The red square marks where the thin section (HSF-501-2010 280,9-281) in figure B, C and D has been prepared from. B – XPL, C – RL and D – PPL.

## 7 – Geochemistry

In order to obtain patterns within and between groups/formations concerning difference in element concentrations a separation of groups/formations by colour coding helps discerning patterns. By plotting elements against one another relations between different elements can also be discerned.

Both figure 7.1 and 7.2 show a linear trend between Al and Sc with the different formations/groups clustered together. The ultramafic part of the Vestgötabreen Complex is clustered together in the lower left corner slightly above the linear trend, with the exception of a few samples in both figure 7.1 and 7.2. These samples have not been logged as ultramafic but rather as cataclasite (see fig. 5.6 or 5.7 and 5.8 or 5.9).

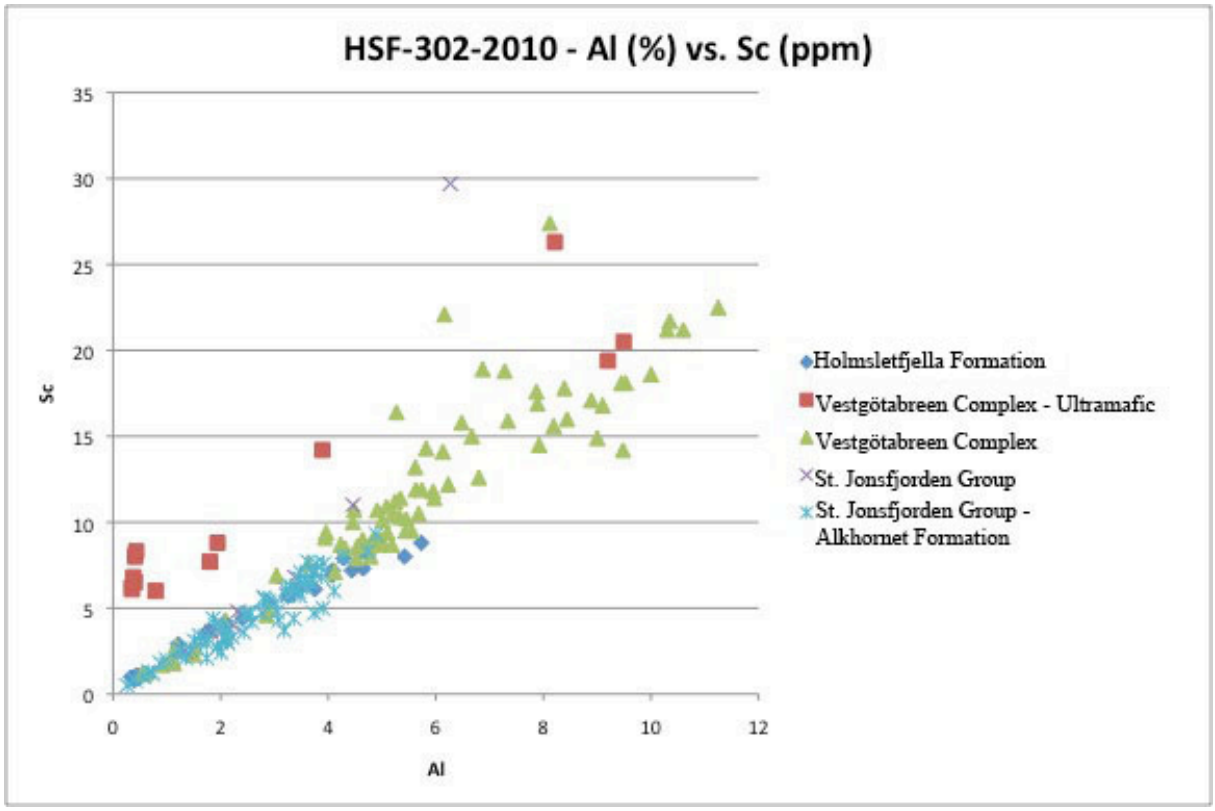


**Figure 7.1:** Immobile trace elements plot from HSF-302-2010.

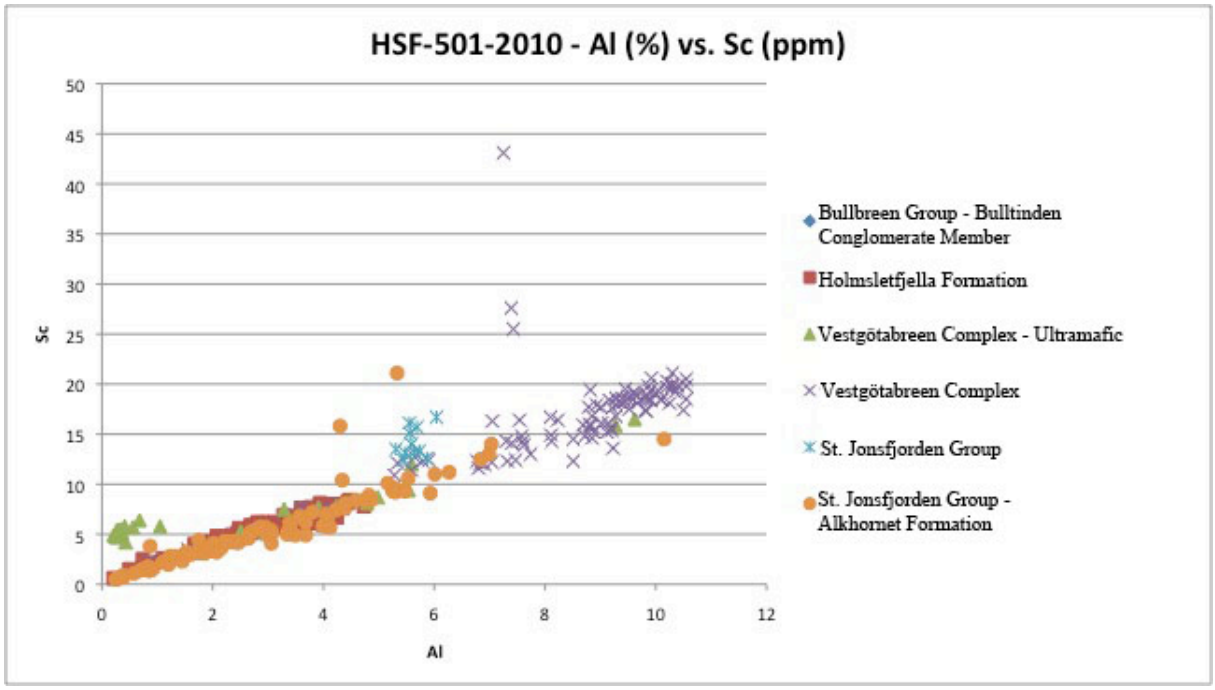


**Figure 7.2:** Immobile trace elements plot from HSF-501-2010.

The ultramafic Motalafjella Formation plots with high values for both Ni and Cr in figure 7.3 and 7.4. Similar as to figure 7.1 and 7.2, not all the points in the ultramafic Vestgötabreen Complex plot together. Some of them plot with the remaining formations/groups in the lower left corner.

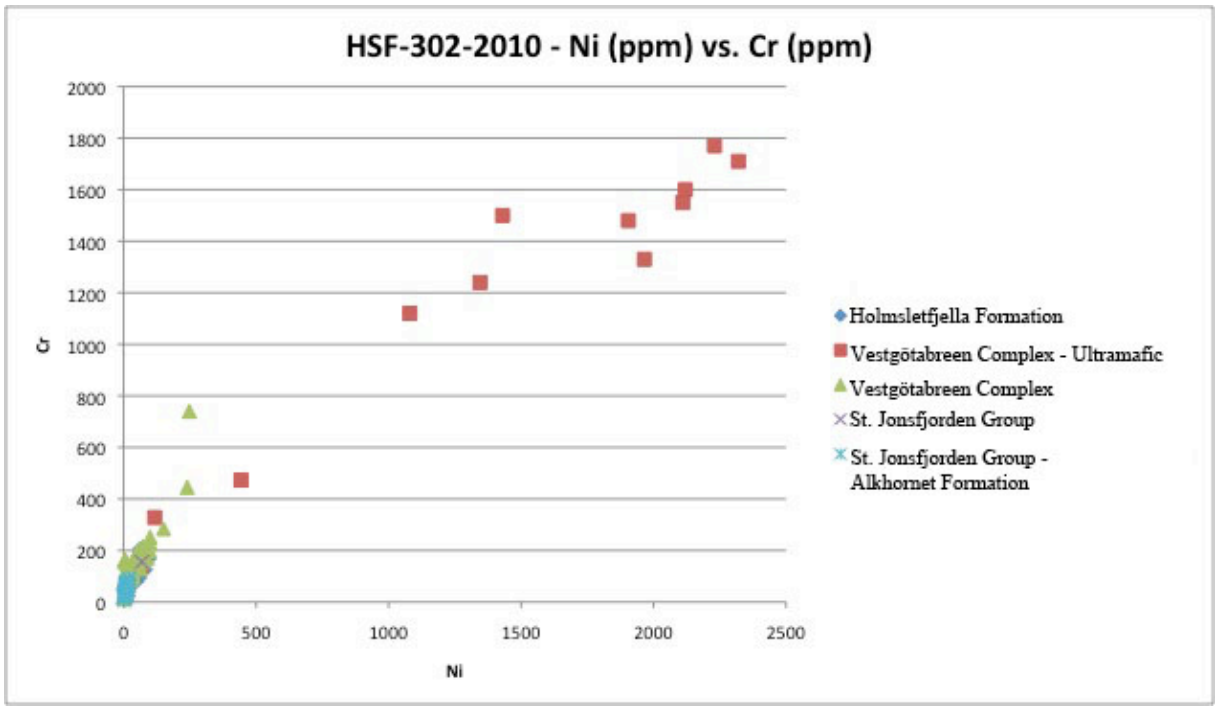


**Figure 7.3:** Plot of associated elements to ultramafic rocks.

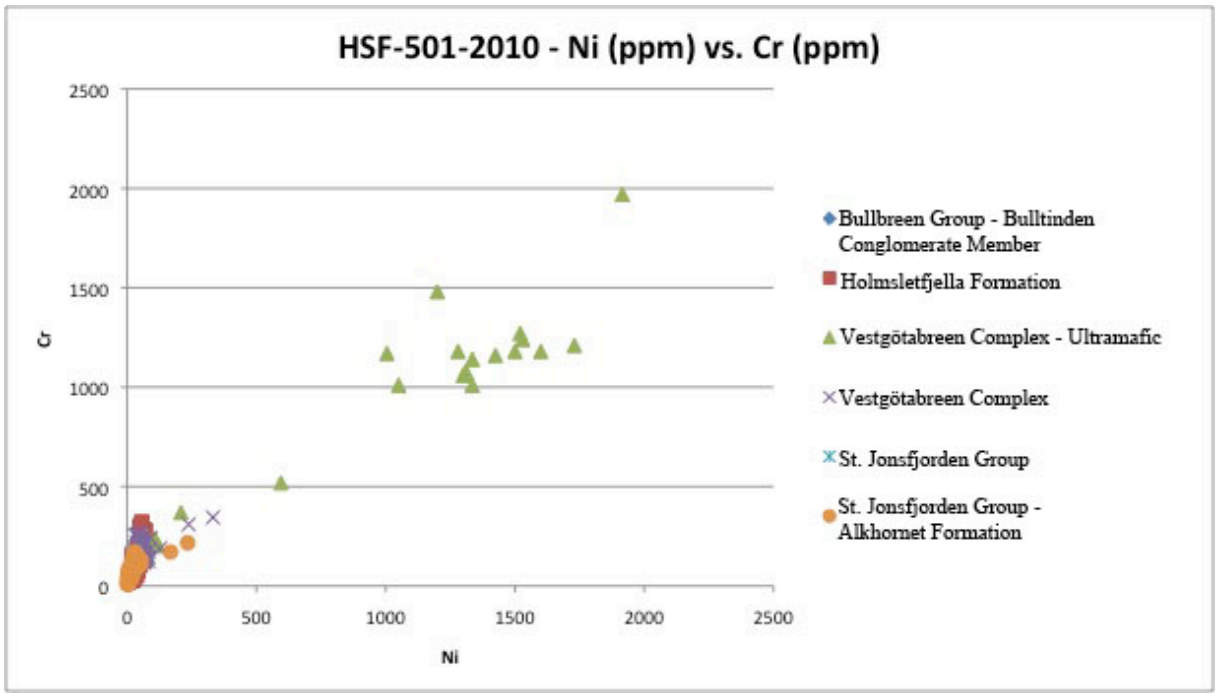


**Figure 7.4:** Plot of associated elements to ultramafic rocks.

St. Jonsfjorden Group and Alkhornet Formation both plot above the muscovite-albite tie line in figure 7.5 and 7.6. The Holmsletfjella Formation plots along the muscovite-albite tie line whereas the ultramafic part of the Vestgötabreen Complex plots in the lower left corner of kaolinite. The Vestgötabreen Complex in figure 7.5 is much wider spread then the Vestgötabreen Complex of figure 7.6, and in figure 7.5 it stretches out on both sides of the muscovite-albite tie line whereas in figure 7.6 it is located in a tight cluster just beneath the muscovite-albite tie line. In both figure 7.5 and 7.6 all the formations plot relatively clustered together.

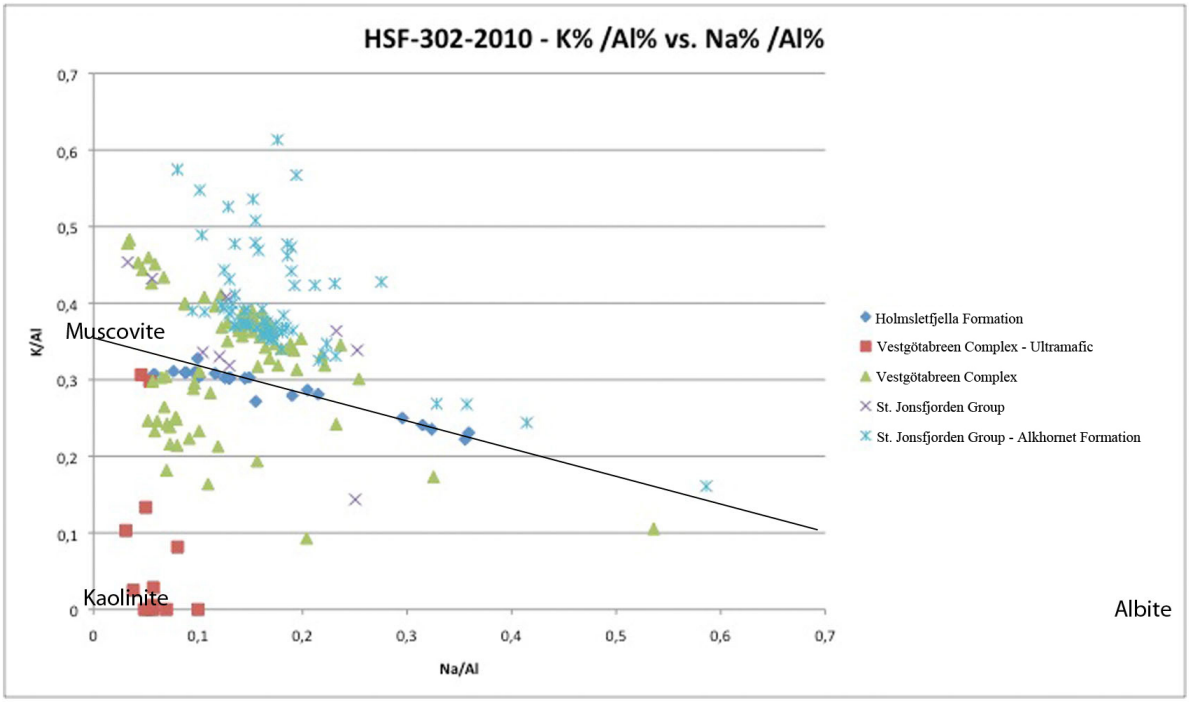


**Figure 7.5:** K/Al vs. Na/Al ratio plot from HSF-302-2010. The muscovite, kaolinite and albite composition has been marked off in order to obtain the muscovite-albite tie line, which is the descending black line.

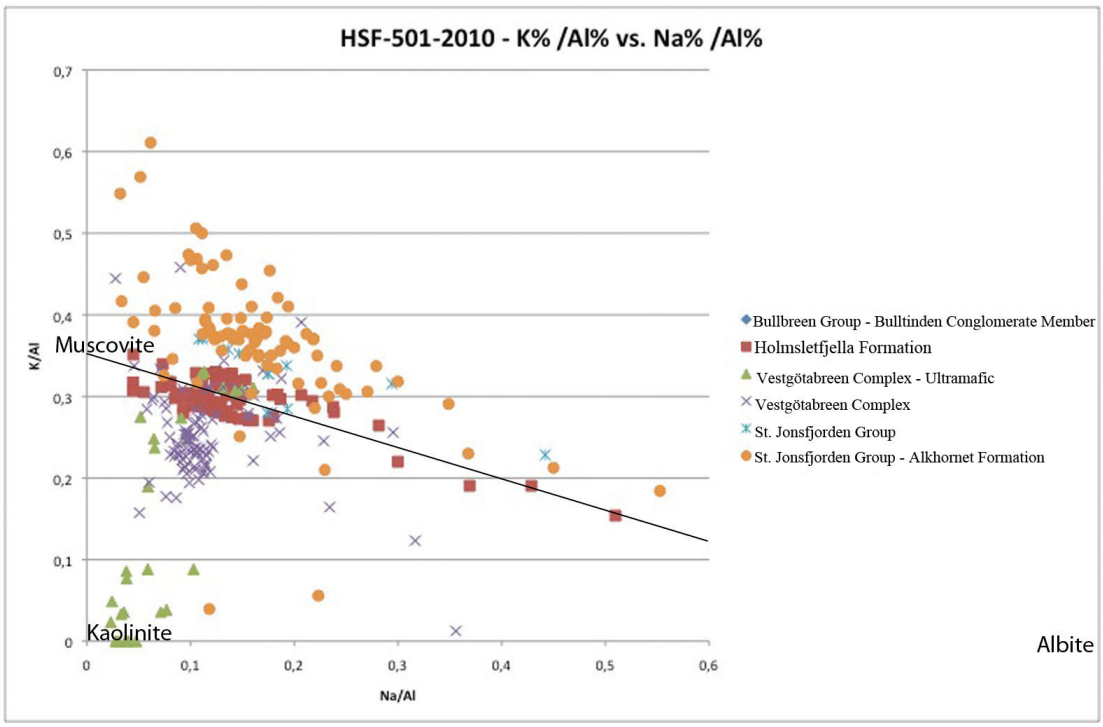


**Figure 7.6:** K/Al vs. Na/Al ratio plot from HSF-501-2010. The muscovite, kaolinite and albite composition has been marked off in order to obtain the muscovite-albite tie line, which is the descending black line.

Figure 7.7 and 7.9 both show linear trends between Sc and V in two directions. Holmsletfjella Formation makes up one of the linear trend whit the greatest slope in figure 7.7 while the rest of the groups/formations makes up the other one. The same is true for figure 7.9 only that the ultramafic Vestgötabreen Complex has shifted from the linear trend with the smallest slope into the linear trend with the greatest slope.

Figure 7.8 and 7.10 show that the same samples that were high in V in figure 7.7 and 7.9 also have elevated content of Ag, As, Mo, Sb, U and Zn. As do not show as strong a correlation as the other element toward the V-rich samples, but they do have a small correlation with an almost vertical trend.

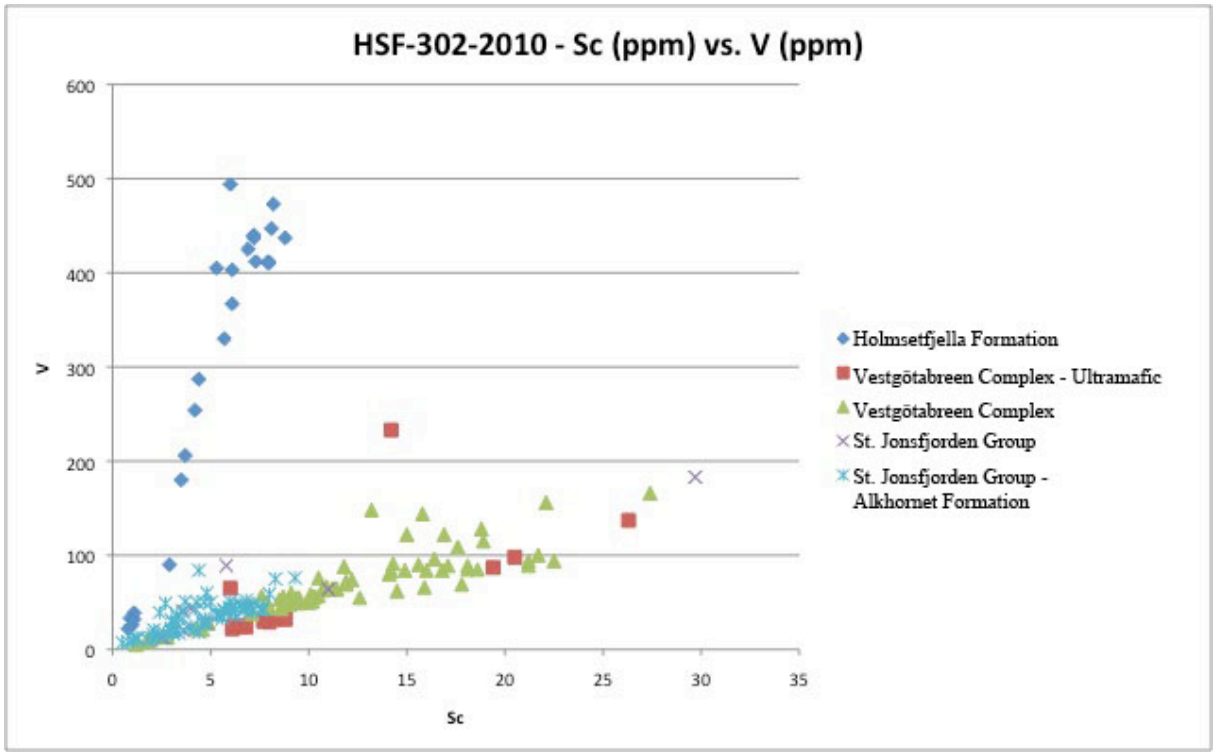


**Figure 7.7:** Sc vs. V plot HSF-302-2010

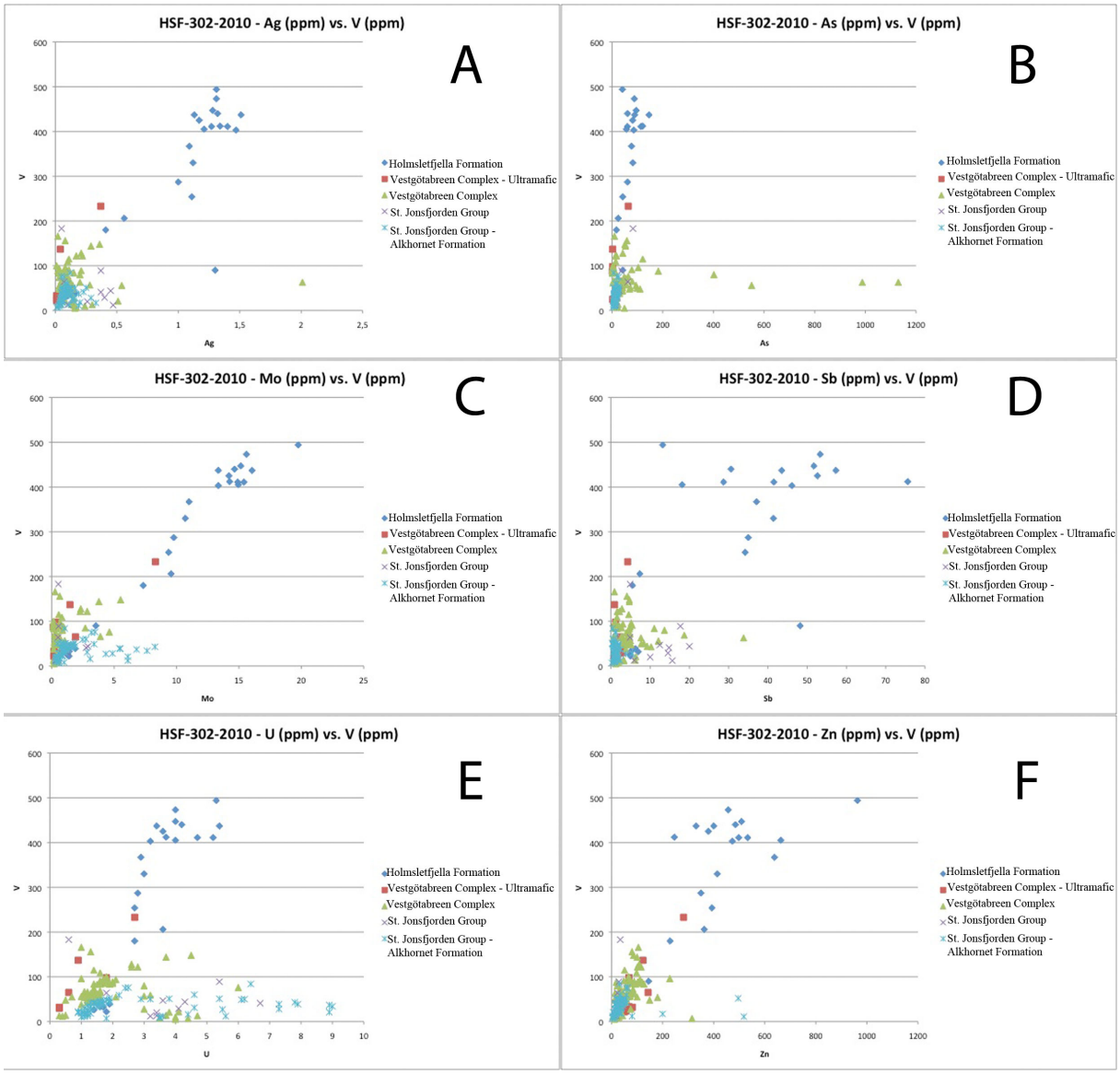


**Figure 7.8:** V plotted against different elements. All plots are from HSF-302-2010.

A: Ag vs. V

B: As vs. V

C: Mo vs. V

D: Sb vs. V

E: U vs. V

F: Zn vs. V

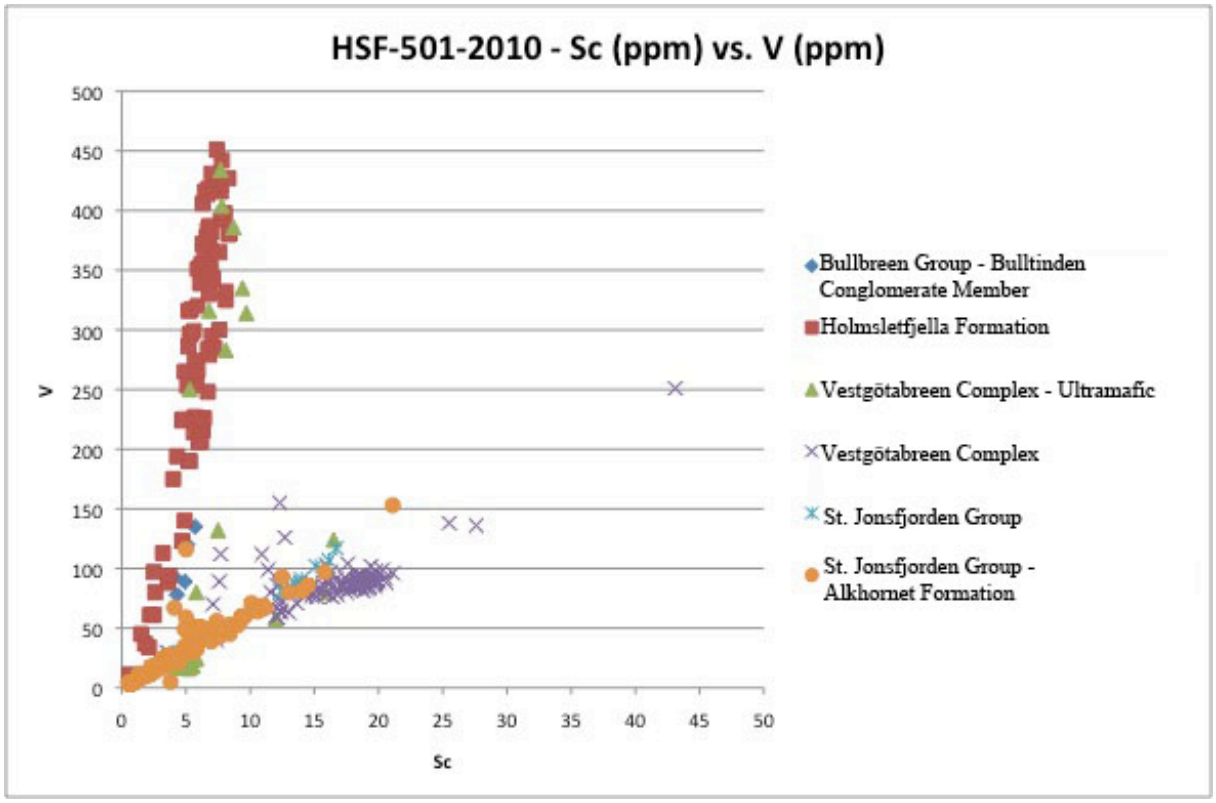


**Figure 7.9:** Sc vs. V plot from HSF-501-2010.

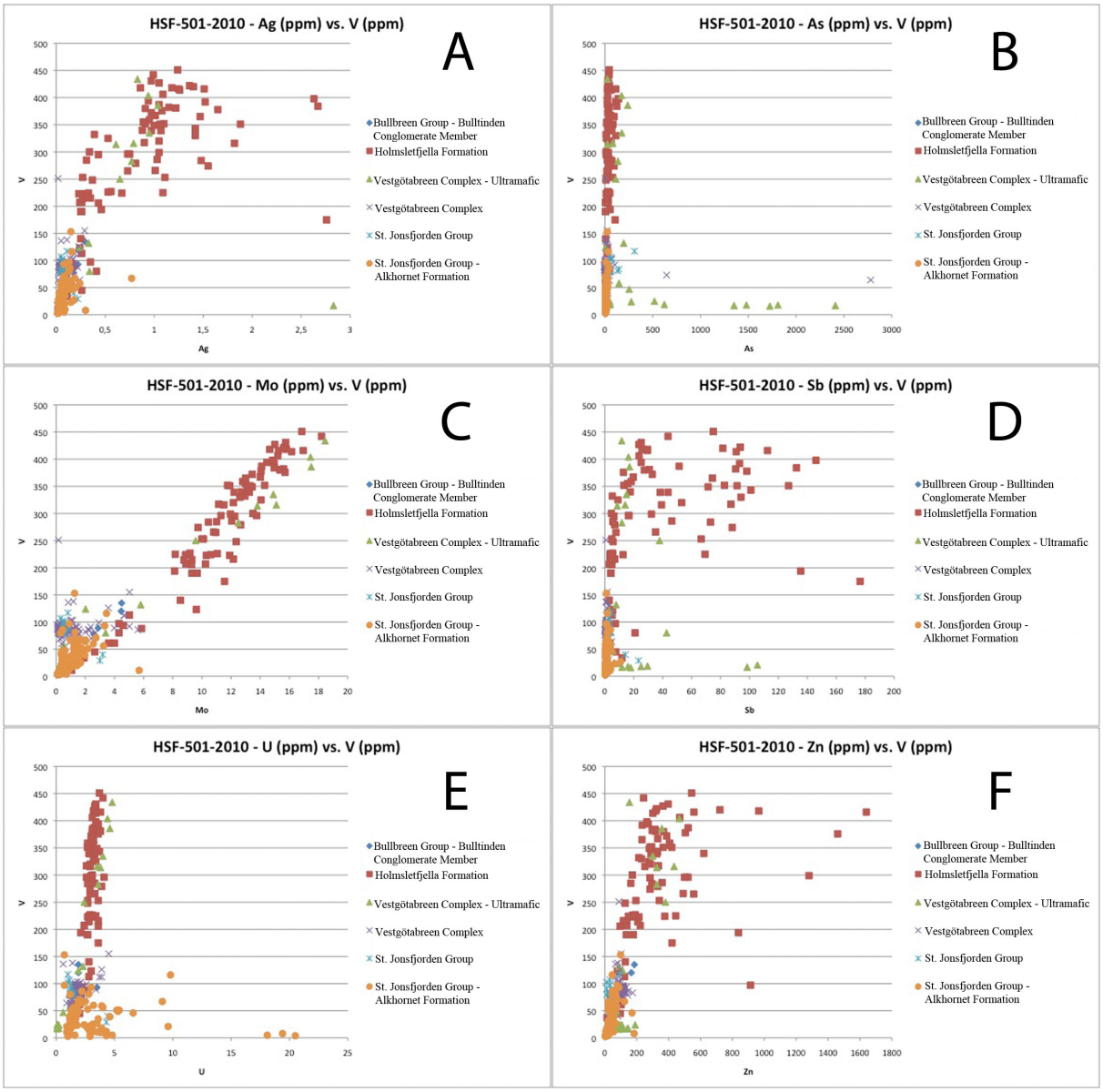


**Figure 7.10:** V plotted against different elements. All plots are from HSF-501-2010.

A: Ag vs. V

B: As vs. V

C: Mo vs. V

D: Sb vs. V

E: U vs. V

F: Zn vs. V

V-score (V+Mo+Ni+Zn) through the drill core show elevated results for Holmsletfjella Formation and the ultramafic Vestgötabreen Complex in both figure 7.11 and 7.12. Both these units have V-scores around 1000 whereas the remaining formations/groups have V-scores closer to 100 with some above and some below.

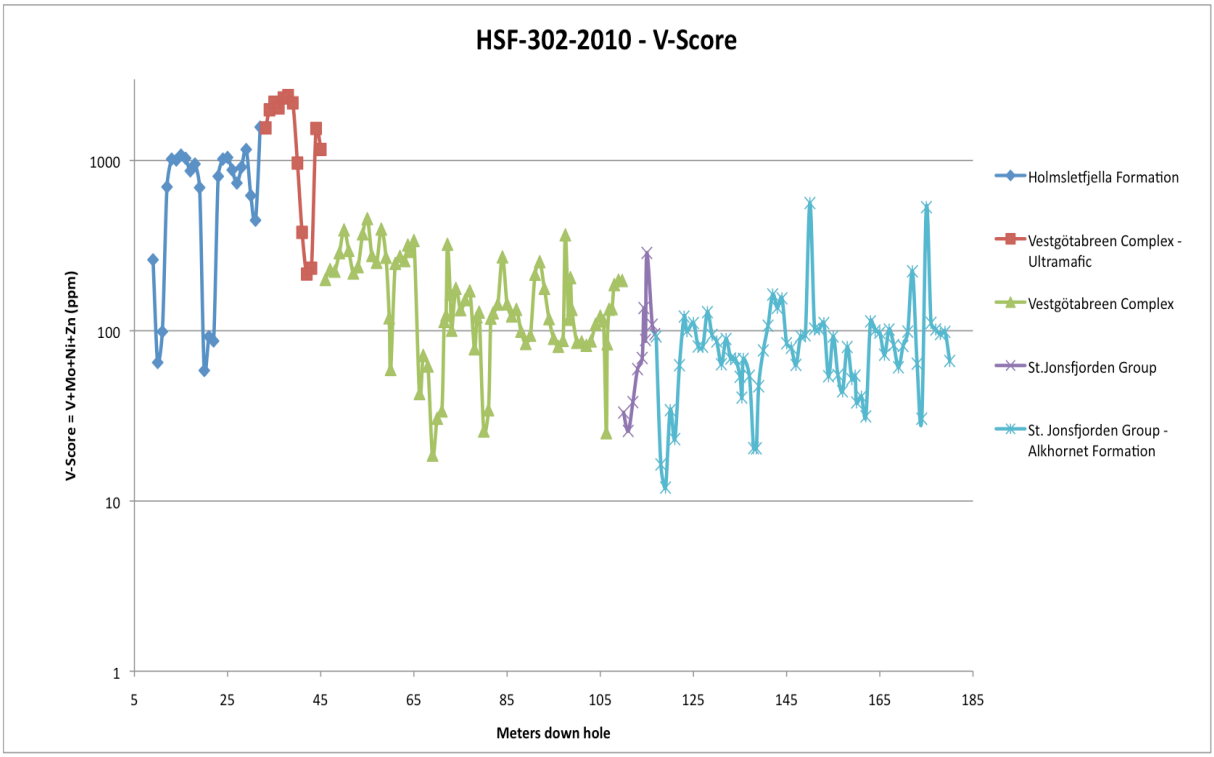


**Figure 7.11:** Tracking the V-score (V+Mo+Ni+Zn) through the drill hole HSF-302-2010 with different colours assigned to the different formations/groups. Note the y-axis is logarithmic.

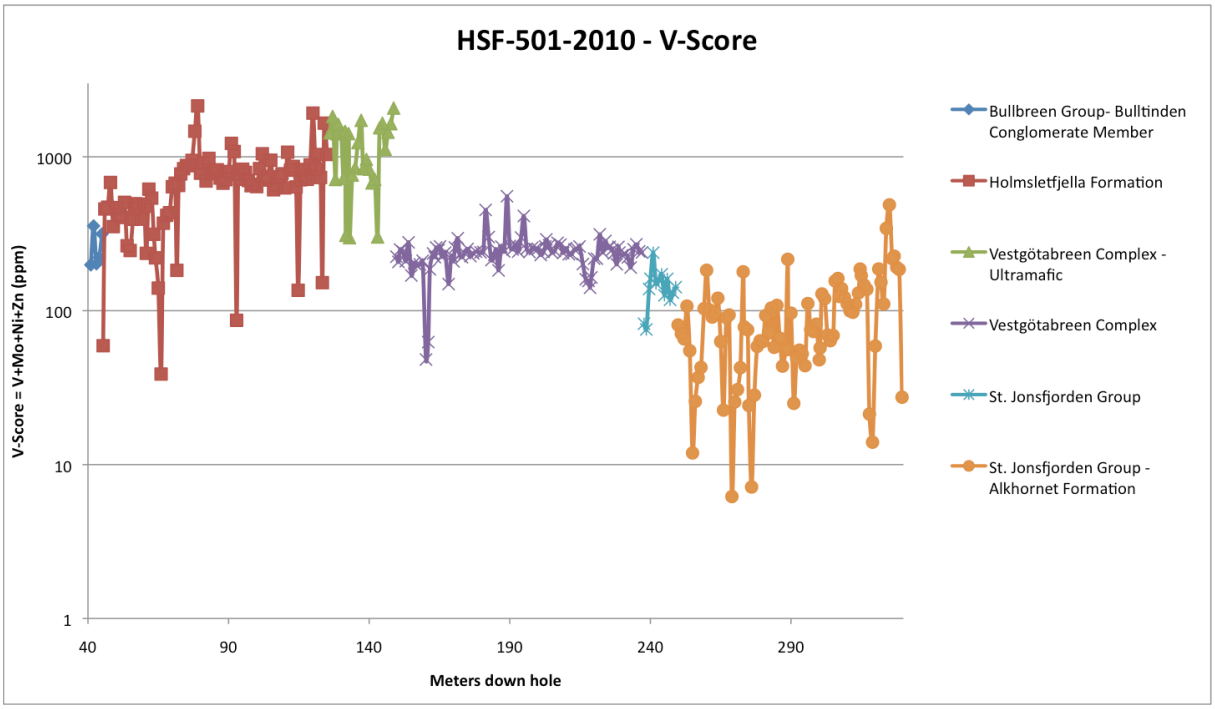


**Figure 7.12:** Tracking the V-score (V+Mo+Ni+Zn) through the drill hole HSF-501-2010 with different colours assigned to the different formations/groups. Note the y-scale is logarithmic.

The Au content shown in figure 7.13 and 7.14 is the same as that of figure 5.6 or 5.7 and 5.8 or 5.9 respectively, only here it is colour coded according to formation/group.

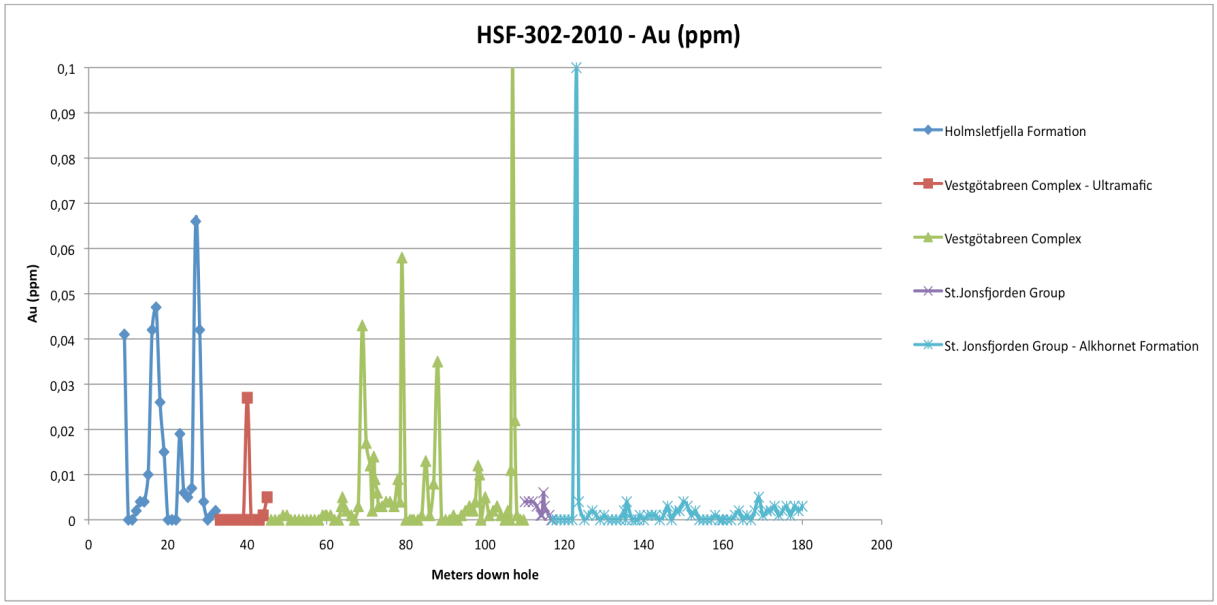


**Figure 7.13:** Show Au content through the drill hole HSF-302-2010 with different colours assigned to the different formations/groups.

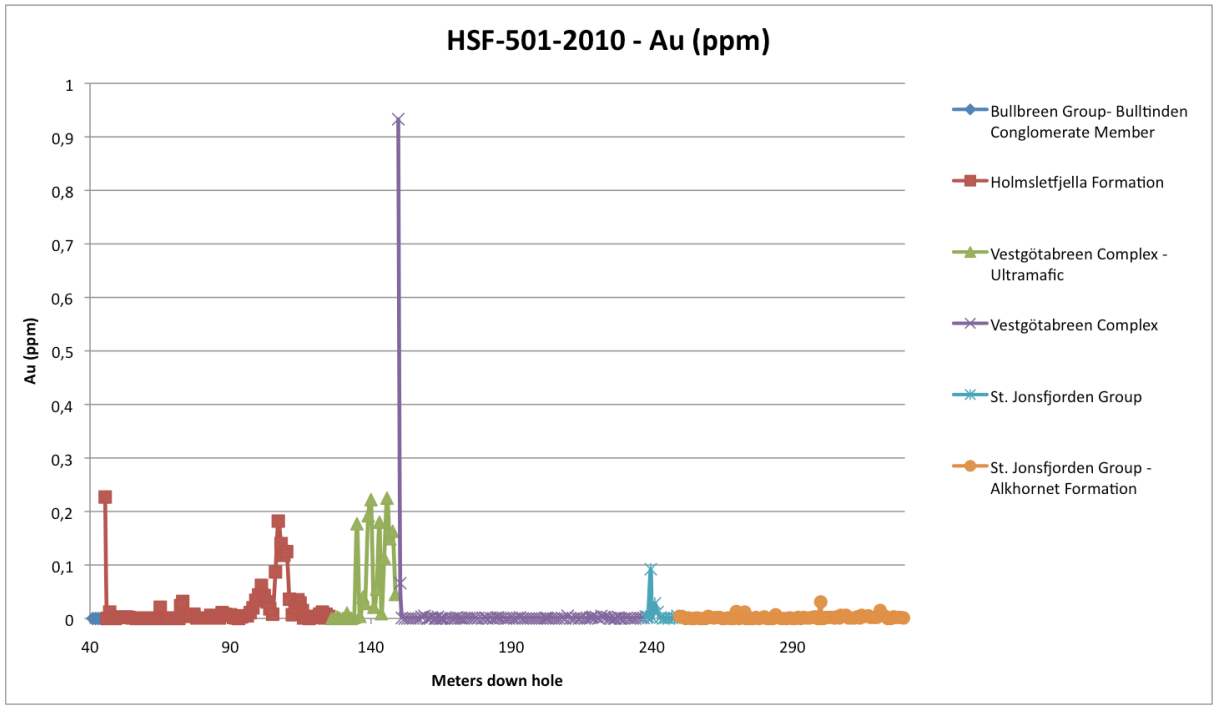


**Figure 7.14:** Show Au content through the drill hole HSF-501-2010 with different colours assigned to the different formations/groups.

# 8 – Discussion

## 8.1 – Bullbreen Group – Bulltinden Conglomerate Member

Fossils collected from the Bulltinden Conglomerate Member at Motalafjella first yielded an age of Late Ordovician to Early Silurian, upon further sampling the two collections of samples have yielded an age Silurian most likely of either Wenlock or Ludlow age (Harland et al., 1979). The fossils found in the drill core at Holmsletfjella match this age, although with a much wider time frame of Silurian to Permian, as concluded by (Hanken, 2011). The formation of the conglomerates has been considered to be in a shallow marine environment during a phase of Silurian faulting (Harland et al., 1979). This put into context with the alteration cutting the conglomerate and enriching it in Au and As (Table 5.1) gives a lower limit of either Wenlock or Ludlow for when the mineralization has occurred.

Due to the preservation of the conglomerate texture within the alteration zone (Fig 5.2 B) it is clear hydrothermal processes drive the mineralization. Further support of a hydrothermal alteration and not a metamorphic or igneous mineralization is that the alteration does not extend more then a metre. Granted that metamorphic or igneous processes may drive the hydrothermal activity it is not what deposited the mineralization. Driving the hydrothermal processes would then likely be the granitic intrusions (Fig 1.9 and 1.10) associated with the second phase of Caledonian folding, which resulted in the folding of Late Ordovician to Mid-Silurian flyschoid sediments into E-vergent overturned structures (Ohta et al., 1997).

## 8.2 – Holmsletfjella Formation

The Holmsletfjella Formation as described by (Harland et al., 1979) does not match the description given in chapter 6.2. (Harland et al., 1979) described it as a unit of calcareous siltstone, argillites and polymict conglomerates. Whereas graphitic- schists and shales dominate the section marked as Holmsletfjella Formation in the drill cores. The reason for marking it as Holmsletfjella Formation in the drill core is that it matches up with the stratigraphy drawn up by (Harland et al., 1979) and (Bergh et al., 2003).

There are two explanations as to how the graphitic- schists and shales may be a part of the Holmsletfjella Formation.

One is that the graphite derives from organic rich sediments that formed under anoxic conditions, later to be included in the Holmsletfjella Formation during thrusting and folding in Caledonian time. The reason for the graphitic- schists and shales not being described as a part of Holmsletfjella Formation may then be that it has been removed from parts of the formation by thrusting or that it is lens shaped restricting its spatial extent.

Two, the graphitic- schists and shales of Holmsletfjella Formation is a result of alteration by hydrothermal processes. Figure 7.7, 7.8, 7.9 and 7.10 plus the SWIR Mineralogical Survey (Halley, 2012) (Chapter 2.1.1), support this interpretation by the generation of the anomalous pathfinder chemistry association of V-Mo-U-Zn, contained within the Holmsletfjella Formation, which appears to be mapping the footprint of an organic rich fluid migrating through the rocks. In which case the fluids may have migrated through the Holmsletfjella Formation and altering a local part of it, this would then explain why graphitic rocks is not listed as a major part of the formation.

### 8.3 – Vestgötabreen Complex – Ultramafic

Figure 7.3 and 7.4 both show the Ultramafic Vestgötabreen Complex to be elevated in levels of Cr and Ni with Cr varying between 1000-2000 ppm and Ni between 1000-2500 ppm. Figure 7.1, 7.2, 7.3 and 7.4 all show that some of the samples within the ultramafic Vestgötabreen Complex don't plot together with the rest of the ultramafic samples. The contact between the ultramafic Vestgötabreen Complex and the underlying Vestgötabreen Complex has been logged as a thrust contact. This thrusting may have resulted in the incorporation of adjacent lithologies into the ultramafic Vestgötabreen Complex, thereby accounting for samples deviating from the main bulk.

This may account for there being some lithologies that are not ultramafic within the ultramafic Vestgötabreen Complex in figure 5.6 and 5.7 (HSF-302-2010) but not the absence of ultramafic rocks in figure 5.8 and 5.9 (HSF-501-2010). The reason for there

not being logged any ultramafic rocks within the HSF-501-2010 drill hole may be explained by taking a look at figure 6.6 and 6.7 in conjunction with table 1.1. Mineralogically the thin section in figure 6.6 falls within the left part of table 1.1, with its serpentine, talc and carbonate. Figure 6.7 on the other hand falls within the right part of table 1.1, with quartz being introduced and mere minor amounts of serpentine remain. Quartz in the ultramafic rock of HSF-501-2010 may have lead to a faulty assignment of the name; quartz rock. Based on the interpretation above he quartz rock in figure 5.8 and 5.9 is listwanites. The non-typical mineralogy of thin section HSF-501-2010 149,9 (Fig. 6.7) is due to that ultramafic rocks has been metamorphosed into serpentinite and succeeded by listwanite alteration. The lack of listwanite in HSF-302-2010 and the appearance in HSF-501-2010 gives support to that the listwanite bodies are lenticular as shown in figure 5.2. The lenticular shape would most likely be a result of shearing along the thrust fault between the ultramafic and the non-ultramafic Vestgötabreen Complex (Fig 5.1 and 5.2).

From the description given by (Harland et al., 1979) there is no mention of ultramafic rocks in conjunction with any of the formations or groups. Vestgötabreen Formation is a suit of metamorphic rocks of blue schist facies, this matches well with metamorphic facies of serpentinite which is of blue- or green schist facies (Evans, 1977). In addition some of the lithologies are derived from basic igneous rocks (Harland and Wright, 1979), and serpentinites have been marked as a lithology within the Vestgötabreen Complex by (Bergh et al., 2003). Figure 5.1 and 5.2 supports the ultramafic Vestgötabreen Complex as the best fit from a structural point of view.

### 8.4 – Vestgötabreen Complex

Figure 6.8 show the cataclasite to be fine-grained in thin section; this makes it hard to determine the ratio between minerals and assigning a specific rock type. The figure also shows the quartz to be strained and the thin section to be densely fractured. Brecciation associated with the Vestgötabreen Complex (Harland and Wright, 1979) and its structural interpretation (Bergh et al., 2003) (Fig. 5.1 and 5.2) support the assigning of the cataclasite to the Vestgötabreen Complex.

By comparing figure 7.5 and 7.6 it is clear that the Vestgötabreen Complex in figure 7.5 is much wider spread then the Vestgötabreen Complex of figure 7.6. Thus representing the diversified lithology within the Vestgötabreen Complex in drill hole HSF-302-2010, compared to the same unit in HSF-501-2010 (Fig 5.6 or 5.7 and 5.8 or 5.9).

### 8.5 – St. Jonsfjorden Group

The narrow unit of sandstone that makes up a part of the St. Jonsfjorden Group most likely fall under the Løvliebreen Formation. The upper member of the Løvliebreen Formation is described as massive dark quartzites (Harland et al., 1979), figure 6.9 has shown the sandstone to be dark with fractures of quartz and carbonate, making Løvliebreen Formation the best fit for the sandstones. To avoid confusion the unit will still be referred to as St. Jonsfjorden Group and not Løvliebreen Formation.

### 8.6 – St. Jonsfjorden Group – Alkhornet Formation

From the map by (Bergh et al., 2003) and (figure map and cross) the only possible formation for the limestone is the Alkhornet Formation. Due to varying amounts of carbonaceous material the limestone varies in darkness.

### 8.7 – Alteration

Note the similarity of the tight clusters of data in figure 7.5 and 7.6 to that of figure 2.5 and 2.6. Tightly clustered rocks on an alteration plot indicates that the majority of the samples have not had significant losses or gains of alkali elements (Halley, 2012). Associated with this is that the alteration not been widespread in addition to not being very intense (Halley, 2012). St. Jonsfjorden Group and Alkhornet Formation both plot above the muscovite-albite tie line in figure 7.5 and 7.6, this is due to that the micas have a phengitic composition where Fe or Mg have replaced Al resulting in a higher K/Al ratio. Mica composition is thereby zoned spatially with a phengitic composition in the lower part of the drill holes and a muscovitic composition in the upper part. These results correspond well with those of (Halley, 2012) and the subsequent interpretation of a rock buffered alteration. Carbonate in Alkhornet Formation and St. Jonsfjorden Group may have acted as a buffer and created a more alkaline environment in which

phengite has been stable (Eq. 2.1). Without the sufficient amount of carbonate in the other formations/groups an efficient buffer could not exist and the result is a muscovitic composition to the micas. From this the zonation shown by the mica reflects a host rock control rather than a zonation of the hydrothermal system.

Sc and V both have the capability of substituting Fe in Fe-silicates, thus they generally plot with a very linear correlation. Figure 7.7 and 7.9 both show two such linear correlations. Holmsletfjella Formation is the one formation in figure 7.7 that does not conform to the others and has a greater slope. This shows the Holmsletfjella Formation of drill hole HSF-302-2010 to have elevated levels of V. The same is true for figure 7.9 only that in addition to Holmsletfjella Formation the ultramafic Vestgötabreen Complex also has elevated levels of V. From this one can assume that the increased levels of V resulted from hydrothermal fluids precipitating V. By plotting V against Ag, As, Mo, Sb, U and Zn (Fig 7.8 and 7.10) it is possible to discern whether the samples that are rich in V also have elevated levels of the above mentioned elements. Most of the elements show a strong correlation to elevated levels V with the exception of As and U. As and U would have shown similar patterns as the other elements towards V but there are some samples with much higher levels of As and U that obscures the trend by increasing the values on the x-axis. Both the As and U (Fig. 7.8 and 7.10) in relation to the samples with elevated levels of V generates a slope. This slope is almost vertical but the fact that it is not entirely vertical means there is a correlation between increasing V and, As and U. This supports the findings of (Halley, 2012) in generating the same diagnostic signature of an organometallic association; V-Mo-U-Zn.

In addition to the above-mentioned organometallic association; the V-score (V+Mo+Ni+Zn) is tracking the redox-sensitive trace elements, in particular, Mo, V, U, Zn, Ni, Cr, As, Cu and Pb. As shown by (Large, 2010, Large et al., 2011) these elements are enriched in carbonaceous black shales and show a relation to gold in ores thereby giving strong evidence that Au and As were initially pre-concentrated by normal diagenetic processes involving adsorption onto organic matter and incorporation into diagenetic pyrite. Au and As show very strong correlation (Fig. 5.6, 5.9 and App. 1.1, 1.3), even at small concentrations, this supports that the Au and As enrichments originated from the same source. Through figure 7.11 and 7.12 it is possible to track the V-score in the drill

core, the levels for the V-score is substantially higher for the Holmsletfjella Formation and the ultramafic Vestgötabreen Complex.

By comparing figure 7.11 to 7.13 and 7.12 to 7.14 it becomes clear that they do not match very well in the aspect of elevated V-score and elevated Au. In fact the Au is not elevated much at all with almost 1 ppm at the most. Rather than being indicative of a gold system, orogenic, Carlin or otherwise, the anomalous pathfinder chemistry of the V-score seems to be mapping the footprint of an organic rich fluid migrating through the rocks. The chemistry indicates that the fluids might have originated from a source that could have held Au at a pre-enriched concentration. Whether the fluids migrating through these rocks had precipitated the Au at an earlier stage or retained the Au to be deposited at a later stage is not to be said. There is also the possibility that the rock here in studied is at the periphery of an Au bearing system. One thing is to be said and that is that the system carries the hallmarks of a source-rock model for Carlin-type and orogenic gold deposits as described by (Large, 2010, Large et al., 2011) (Chapter 1.6.4).

V-score from table 6.1 does not show nearly as significant differences between results as figure 7.11 and 7.12 does. Average V-score for the altered conglomerate is 248,33 and 200,98 for the unaltered conglomerate; both fall in the same range with a low V-score, when regarding figure 7.11 and 7.12. If the alteration in the conglomerate is not the same as the one elevating the V-score; then it most likely is in relation with the listwanite alteration. This makes the listwanite alteration no older than Wenlock or Ludlow.

## 8.8 – Geological history in relation to mineralizations

Two Caledonian tectonothermal events are recorded through $^{40}Ar/^{39}Ar$ studies of the metamorphic rocks at Motalafjella. Combining these with petrologic characteristics gives first a subduction of oceanic crust in Early to Middle Ordovician, with high-pressure and medium temperature. Secondly, deposition and uplift of flysch took place from Caradocian to Early Wenlockian. Following this Late Wenlockian folding, thrusting and low-grade metamorphism of flysch and older sequences came about. (Ohta et al., 1989)

If the listwanite alteration is no older than Wenlock or Ludlow age it would most likely be associated with the Late Wenlockian low-grade metamorphism if not Tertiary. (Ohta et al., 1989) talks about a Tertiary thermal overprint and not metamorphism, this indicates lower temperatures and the driving force for an alteration would be lower compared to that of Caledonian. Granitic intrusions would be absent during Tertiary since there is no subduction related to the generation of the West Spitsbergen Fold Belt. Granitic intuitions (Ohta et al., 1997) are on the other hand associated with the Late Wenlockian phase of folding and would generate heat and contribute with fluids.

Orogenic gold deposits typically develop in terrains that have experienced moderate to high temperatures and low to moderate pressure during metamorphism. As a consequence granitic melts are generated at large volumes. Distal spatial relationships are to be expected between certain intrusions and deposits. (Groves et al., 2003)

The high pressure during the Early to Middle Ordovician metamorphism does not match the typical orogenic gold deposit. Late Wenlockian low-grade metamorphism and granitic intrusions point towards the same timeframe as the listwanite alteration. In addition to Late Wenlockian being the best fit in the aspects of metamorphic grade and intrusion wise, orogenic gold deposits generally form in the latter part of the deformational-metamorphic-magmatic history of the orogen (Groves et al., 2000).

Granitic intrusions raise the question: do the fluids involved in such a mineralization derive from deep metamorphic processes, crustal granites or some other source? Following the V-score in (Fig 7.11 and 7.12) in combination with (Large, 2010, Large et al., 2011) the source would most likely be the carbonaceous black shales termed VAMSNAZ (V, As, Mo, Se, Ni, Ag and Zn) shales. For the VAMSNAZ shales to form, there would have to be a period of deposition, one such period took place from Caradocian to Early Wenlockian (Ohta et al., 1989), just in time for an Au and As mobilisation in Late Wenlockian. Granitic intrusions may have played a part in mobilising the Au as far as heat is concerned but it is not where the Au-rich fluids were derived from.

If the correlation between glaucophane schist belts and compressive plate boundaries was valid during the Caledonian Orogeny, then a compressive plate boundary may have

existed in the Oscar II Land region at this time (Horsfield, 1972). By combining a compressive plate boundary location with figure 1.9, one ends up with one type of mineralization; namely orogenic. There is a weakness to this interpretation, as (Horsfield, 1972) has pointed out; that Tertiary faulting may have displaced the glaucophane schist from its original location.

If the Tertiary faulting has displaced the glaucophane schist the mineralization may be of Carlin-type. Carlin-type deposits are very similar to orogenic deposits, but where orogenic deposits are related to compression, Carlin-type form after the onset of extensional forces (Robb, 2005). The lack of observed normal faults is not enough to discard Carlin-type deposits but the observation of thrust faults does add support to an orogenic mineralization. Both the Caledonian Orogeny and the West Spitsbergen Fold Belt had folding and thrusting from the west to the east (Harland, 1985). This may have resulted in a reactivation of low-angle normal faults as thrust faults, and thus obscuring the normal faults.

Due to the collapse of the Caledonian mountain chain in Devonian time (Birkenmajer, 1981) and the erosion of the West Spitsbergen Fold Belt (Dallmann, 1999) it is unlikely that the mineralization is porphyry, epithermal or volcanic-hosted massive sulphide. This is due to that they all are situated high in the crust (Fig 1.9) and are therefore commonly eroded (Groves et al., 2003).

Both the listwanite alteration and what is most likely an orogenic gold mineralization may have been displaced during the evolution of the West Spitsbergen Fold Belt or the Au may have been remobilised. These are both things that complicate the history and obscure the pattern.

# 9 – Summary/Conclusion

Subduction of oceanic crust in Early to Middle Ordovician resulted I high-pressure metamorphism in Oscar II Land. From Caradocian to Early Wenlockian deposition of the Bulltinden Conglomerate Member and the VAMSNAZ shales took place. After this low-grade metamorphism, folding and thrusting followed in Late Wenlockian. It is at this time that alteration of serpentinite to listwanite occured, and that organic-rich fluids are sourced from the VAMSNAZ shales carrying the V-score signature. The organic-rich fluids are rock buffered with a low water-to-rock ratio resulting in that the Holmsletfjella Formation and the Ultramafic Vestgötabreen Complex are the two units affected. Thrust faults are the most likely pathways for the fluids. This makes the organic-rich fluids related to orogenic gold deposits rather than Carlin-type. The Au-As correlation in the drill core is related to the VAMSNAZ shales where Au and As were initially pre-concentrated by normal diagenetic processes involving adsorption onto organic matter and incorporation into diagenetic pyrite.

Low concentrations of Au in the Holmsletfjella drill cores combined with weak a correlation between the V-score and the Au, results in that the drill cores from Holmsletfjella is tracking the periphery rim of an orogenic gold deposit soured from VAMSNAZ shales.

Erosion of the Caledonian mountain chain in Devonian time was followed by the generation of the West Spitsbergen Fold Belt in Tertiary time. The West Spitsbergen Fold Belt may have reactivated pre-existing faults, which could have relocated a possible deposit. In addition it might also have remobilised the Au from a deposit thereby obscuring a pre-existing mineralization pattern. Erosion of the West Spitsbergen Fold Belt may have removed deposits leaving only the periphery of the deposits. Faulting may have prevented erosion through relocation of possible deposits to greater depths.

More work is needed on a regional scale in order to determine the extent of the system and its relations to the structural history. Accompanying this with more detailed studies of the alteration could give valuable information as to the origin of the system. From this one could contribute to whether a carbonaceous source-rock model is to be considered part of an ore-forming process or considered as a separate ore-forming process.

## 10 – References


ALGEO, T. J. & MAYNARD, J. B. 2004. Trace-element behavior and redox facies in core shales of Upper Pennsylvanian Kansas-type cyclothems. *Chemical Geology,* 206**,** 289-318.

ALS-GROUP. 2005. *RE: Fire Assay Procedure.* Type to SIMONSEN, H. K.

ALS-GROUP. 2006a. *Geochemical Procedure* [Online]. Available: http://www.alsglobal.com/upload/minerals/downloads/method-descriptions/Method%20Descriptions-ME-MS61.pdf [Accessed 26. April 2012].

ALS-GROUP. 2006b. *Whole Rock Geochemistry* [Online]. Available: http://www.alsglobal.com/upload/minerals/downloads/method-descriptions/Method%20Descriptions-ME-XRF06.pdf [Accessed 26. April 2012].

AREHART, G. B. 1996. Characteristics and origin of sediment-hosted disseminated gold deposits: A review. *Ore geology reviews,* 11**,** 383-403.

AREHART, G. B., CHRYSSOULIS, S. L. & KESLER, S. E. 1993. Gold and arsenic in iron sulfides from sediment-hosted disseminated gold deposits; implications for depositional processes. *Economic Geology,* 88**,** 171-185.

ASH, C. & ARKSEY, R. 1990. The listwanite-lode gold association in British Columbia. *Ministry of Energy, Mines & petroleum Resources***,** 359-364.

ASH, C. H., MACDONALD, R. W. & REYNOLDS, P. 2001. *Relationship Between Ophiolites and Gold-Quartz Veins in the North American Cordillera*, British Columbia, Ministry of Energy and Mines.

BERGH, S., OHTA, Y., ANDRESEN, A., MAHER, H. D., BRAATHEN, A. & DALLMANN, W. 2003. *Geological map of Svalbard, sheet B8G St. Jonsfjorden*, 1:100000. Norsk Polarinstitutt.

BERNARD-GRIFFITHS, J., PEUCAT, J. & OHTA, Y. 1993. Age and nature of protoliths in the Caledonian blueschist-eclogite complex of western Spitsbergen: a combined approach using U-Pb, Sm-Nd and REE whole-rock systems. *Lithos,* 30**,** 81-90.

BIRKENMAJER, K. 1981. The geology of Svalbard, the western part of the Barents Sea, and the continental margin of Scandinavia. *The Ocean Basins and Margins: The Arctic Ocean***,** 265.

BLAKE, M. 1969. Blueschist-facies metamorphism related to regional thrust faulting. *Tectonophysics,* 8**,** 237-246.

BOHLKE, J. 1982. Orogenic (metamorphic-hosted) gold-quartz veins. *US Geological Survey Open File Report,* 795**,** 70-76.

BOYLE, R. & JONASSON, I. 1973. The geochemistry of arsenic and its use as an indicator element in geochemical prospecting. *Journal of Geochemical Exploration,* 2**,** 251-296.

BOYLE, R. W. & CANADA, G. S. O. 1979. *The geochemistry of gold and its deposits (together with a chapter on geochemical prospecting for the element)*, Geological Survey of Canada.

BUCHER, K. & FREY, M. 2002. *Petrogenesis of metamorphic rocks*, Springer Verlag.

CALVERT, S. E. & PEDERSEN, T. 1993. Geochemistry of recent oxic and anoxic marine sediments: Implications for the geological record. *Marine geology,* 113**,** 67-88.

CHALLINOR, A. 1967. The structure of Brøggerhalvøya, Spitsbergen. *Geological Magazine,* 104**,** 322-326.

CLINE, J. S., HOFSTRA, A. H., MUNTEAN, J. L., TOSDAL, R. M. & HICKEY, K. A. 2005. Carlin-type gold deposits in Nevada: Critical geologic characteristics and viable models. *Economic Geology 100th anniversary volume***,** 451-484.

COLEMAN, R. 1971. Plate tectonic emplacement of upper mantle peridotites along continental edges. *Journal of Geophysical Research,* 76**,** 1212-1222.

DALLMANN, W. & OHTA, Y. Pre-tertiary stratigraphy and principal geological units of Svalbard. *Norwegian Polar Institute***,** 1-24.

DALLMANN, W. K. 1999. *Lithostratigraphic lexicon of Svalbard: review and recommendations for nomenclature use : Upper Palaeozoic to Quaternary bedrock,* Tromsø, Norsk polarinstitutt.

DALLMEYER, R., PEUCAT, J., HIRAJIMA, T. & OHTA, Y. 1989. Tectonothermal chronology within a blueschist-eclogite complex, west-central Spitsbergen, Svalbard: Evidence from and Rb-Sr mineral ages. *Lithos,* 24**,** 291-304.

EILU, P. & GROVES, D. 2001. Primary alteration and geochemical dispersion haloes of Archaean orogenic gold deposits in the Yilgarn Craton: the pre-weathering scenario. *Geochemistry: Exploration, Environment, Analysis,* 1**,** 183-200.

ERNST, W. 1970. Tectonic contact between the Franciscan mÈlange and the Great Valley sequenceóCrustal expression of a late Mesozoic Benioff zone. *Journal of Geophysical Research,* 75**,** 886-901.

EVANS, B. W. 1977. Metamorphism of alpine peridotite and serpentinite. *Annual Review of Earth and Planetary Sciences,* 5**,** 397.

FERRY, J. M. 1981. Petrology of graphitic sulfide-rich schists from south-central Maine: an example of desulfidation during prograde regional metamorphism. *American Mineralogist,* 66**,** 908.

FOSSEN, H., PEDERSEN, R., BERGH, S. & ANDRESEN, A. 2007. En fjellkjede blir til. *In:* RAMBERG, I. B., BRYHNI, I. & NØTTVEDT, A. (eds.) *Landet blir til: Norges geologi.* Norsk geologisk forening.

GEOPOOL. 2008. *Spectral Mapping of Alteration Minerals* [Online]. Available: http://www.geopool.fi/data/GeoPool_SMAM_2008.pdf [Accessed 5. May 2012].

GOLDFARB, R., GROVES, D. & GARDOLL, S. 2001. Orogenic gold and geologic time: a global synthesis. *Ore geology reviews,* 18**,** 1-75.

GROVES, D. I., GOLDFARB, R. J., GEBRE-MARIAM, M., HAGEMANN, S. & ROBERT, F. 1998. Orogenic gold deposits: A proposed classification in the context of their crustal distribution and relationship to other gold deposit types. *Ore geology reviews,* 13**,** 7-27.

GROVES, D. I., GOLDFARB, R. J., KNOX-ROBINSON, C. M., OJALA, J., GARDOLL, S., YUN, G. Y. & HOLYLAND, P. 2000. Late-kinematic timing of orogenic gold deposits and significance for computer-based exploration techniques with emphasis on the Yilgarn Block, Western Australia. *Ore geology reviews,* 17**,** 1-38.

GROVES, D. I., GOLDFARB, R. J., ROBERT, F. & HART, C. J. R. 2003. Gold deposits in metamorphic belts: Overview of current understanding, outstanding problems, future research, and exploration significance. *Economic Geology,* 98**,** 1-29.

HALLEY, S. 2012. Results of a SWIR mineralogical survey of the Rautavaara and Svalbard prospects. Mineral Mapping.

HANKEN, N. M. 2011. Type to SIMONSEN, H. K.

HARLAND, W. 1985. Caledonide Svalbard. *The Caledonide orogenóScandinavia and related areas***,** 999-1016.

HARLAND, W., HORSFIELD, W., MANBY, G. & MORRIS, A. 1979. An outline pre-Carboniferous stratigraphy of central western Spitsbergen. *Norsk Polarinstitutt Skrifter,* 167**,** 119-144.

HARLAND, W., WALLIS, R. & GAYER, R. 1966. A revision of the Lower Hecla Hoek succession in central north Spitsbergen and correlation elsewhere. *Geol. Mag,* 103**,** 70-97.

HARLAND, W. & WRIGHT, N. 1979. Alternative hypothesis for the pre-Carboniferous evolution of Svalbard. *Norsk Polarinstitutt Skrifter,* 167**,** 89-117.

HARLAND, W. B., ANDERSON, L. M., MANASRAH, D. & BUTTERFIELD, N. J. 1997. *The geology of Svalbard*, Geological Society.

HARLAND, W. B., CUTBILL, J., FRIEND, P. F., GOBBETT, D., HOLLIDAY, D., MATON, P., PARKER, J. & WALLIS, R. 1974. *The Billefjorden Fault Zone, Spitsbergen: the long history of a major tectonic lineament*, Norsk Polarinstitutt.

HIRAJIMA, T., BANNO, S., HIROI, Y. & OHTA, Y. 1988. Phase petrology of eclogites and related rocks from the Motalafjella high-pressure metamorphic complex in Spitsbergen (Arctic Ocean) and its significance. *Lithos,* 22**,** 75-97.

HODGSON, C. J. 1989. The structure of shear-related, vein-type gold deposits: A review. *Ore geology reviews,* 4**,** 231-273.

HOFSTRA, A., LEVENTHAL, J., NORTHROP, H., LANDIS, G., RYE, R., BIRAK, D. & DAHL, A. 1991. Genesis of sediment-hosted disseminated-gold deposits by fluid mixing and sulfidization: Chemical-reaction-path modeling of ore-depositional processes documented in the Jerritt Canyon district, Nevada. *Geology,* 19**,** 36.

HOLTEDAHL, O. 1913. Zur Kenntnis der Karbonablagerungen des Westlichen Spitzbergens: ll. Allgemelne stratigraphische und tektonische Beobachtungen; Skr. Vidensk. Selsk. Kristiania. *Math. Naturw. KL***,** 1-46.

HORSFIELD, W. 1972. Glaucophane schists of Caledonian age from Spitsbergen. *Geological Magazine,* 109**,** 29-36.

HU, K., ZHAI, J., LIU, Y., WANG, H., ZHANG, J. & JIA, R. 2000. Genesis and organic geochemical characteristics of the carbonaceous rock stratabound gold deposits, South China. *Science in China Series D: Earth Sciences,* 43**,** 507-520.

JOHNSTON, W. D. & THORPE, M. R. 1940. *The gold quartz veins of Grass Valley, California*, Gov. Print. Off.

KERRICH, R., GOLDFARB, R., GROVES, D. & GARWIN, S. 2000. The geodynamics of world-class gold deposits: characteristics, space-time distribution, and origins. *Society of Economic Geologists Reviews in Economic Geology,* 13.

KETRIS, M. & YUDOVICH, Y. E. 2009. Estimations of clarkes for carbonaceous biolithes: World averages for trace element contents in black shales and coals. *International Journal of Coal Geology,* 78**,** 135-148.

LARGE, R. 2010. Evidence for a Two-stage Process in the Genesis of Sediment-hosted Gold-Arsenic Deposits.

LARGE, R. R., BULL, S. W. & MASLENNIKOV, V. V. 2011. A Carbonaceous Sedimentary Source-Rock Model for Carlin-Type and Orogenic Gold Deposits. *Economic Geology,* 106**,** 331-358.

LINDGREN, W. 1896. *The gold-quartz veins of Nevada City and Grass Valley districts, California*, Govt. print. off.

LYBERIS, N. & MANBY, G. 1993. The origin of the West Spitsbergen Fold Belt from geological constraints and plate kinematics: implications for the Arctic. *Tectonophysics,* 224**,** 371-391.

MAHER, J. & WELBON, A. 1992. Influence of Carboniferous structures on Tertiary tectonism at St. Jonsfjorden and Bellsund, Western Svalbard. *Norsk Geologisk Tidsskrift,* 72**,** 1-9.

MCKEITH, T., SCHODDE, R. & BALTIS, E. 2010. Gold Discovery Trends. *SEG Newsletter,* 81**,** 1 and 20-26.

NØTTVEDT, A. & WORSLEY, D. 2007. Vidstrakte sletter, kull og salt. *In:* RAMBERG, I. B., BRYHNI, I. & NØTTVEDT, A. (eds.) *Landet blir til: Norges geologi.* Norsk geologisk forening.

OHTA, Y., DALLMEYER, R. & PEUCAT, J. 1989. Caledonian terranes in Svalbard. *Geological Society of America Special Paper,* 230**,** 1-15.

OHTA, Y., KRASILSCIKOV, A. A. & TCBCNKOV, A. M. Year. Precambrian and Caledonian events in Svalbard, northwestern edge of the Eurasian plate: A review in a regional context of the North Atlantic and Arctic Ocean. *In*, 1997. Vsp, 27.

ORVIN, A. K. 1934. *Geology of the Kings Bay Region, Spitsbergen: With Special Reference to the Coal Deposits*, I kommisjon hos J. Dybwad.

POLARINSTITUTT, N. 2011. Norsk Polarinstitutt. Available: http://eivind.npolar.no/Geocortex/Essentials/Web/viewer.aspx?Site=svbk_v01_no [Accessed 14/10 2011].

RIMMER, S. M. 2004. Geochemical paleoredox indicators in Devonian-Mississippian black shales, Central Appalachian basin (USA). *Chemical Geology,* 206**,** 373-391.

ROBB, L. J. 2005. *Introduction to ore-forming processes*, Wiley-Blackwell.

SIBSON, R. H., ROBERT, F. & POULSEN, K. H. 1988. High-angle reverse faults, fluid-pressure cycling, and mesothermal gold-quartz deposits. *Geology,* 16**,** 551.

SISSON, V. & ONSTOTT, T. 1986. Dating blueschist metamorphism: A combined 40Ar/39Ar and electron microprobe approach. *Geochimica et Cosmochimica Acta,* 50**,** 2111-2117.

TRIBOVILLARD, N., ALGEO, T. J., LYONS, T. & RIBOULLEAU, A. 2006. Trace metals as paleoredox and paleoproductivity proxies: An update. *Chemical Geology,* 232**,** 12-32.

WEDEPOHL, H. 1995. The composition of the continental crust. *Geochimica et Cosmochimica Acta,* 59**,** 1217-1232.

WEISS, L. 1953. Tectonic features of the Hecla Hoek Formation to the south of St. Jonsfjord, Vestspitsbergen. *Geol. Mag,* 90**,** 273-286.

WELBON, A. I. & MAHER JR, H. D. 1992. Tertiary tectonism and basin inversion of the St. Jonsfjorden region, Svalbard. *Journal of structural geology,* 14**,** 41-55.

WOOD, S. 1996. The role of humic substances in the transport and fixation of metals of economic interest (Au, Pt, Pd, U, V). *Ore geology reviews,* 11**,** 1-31.

# Appendix 1

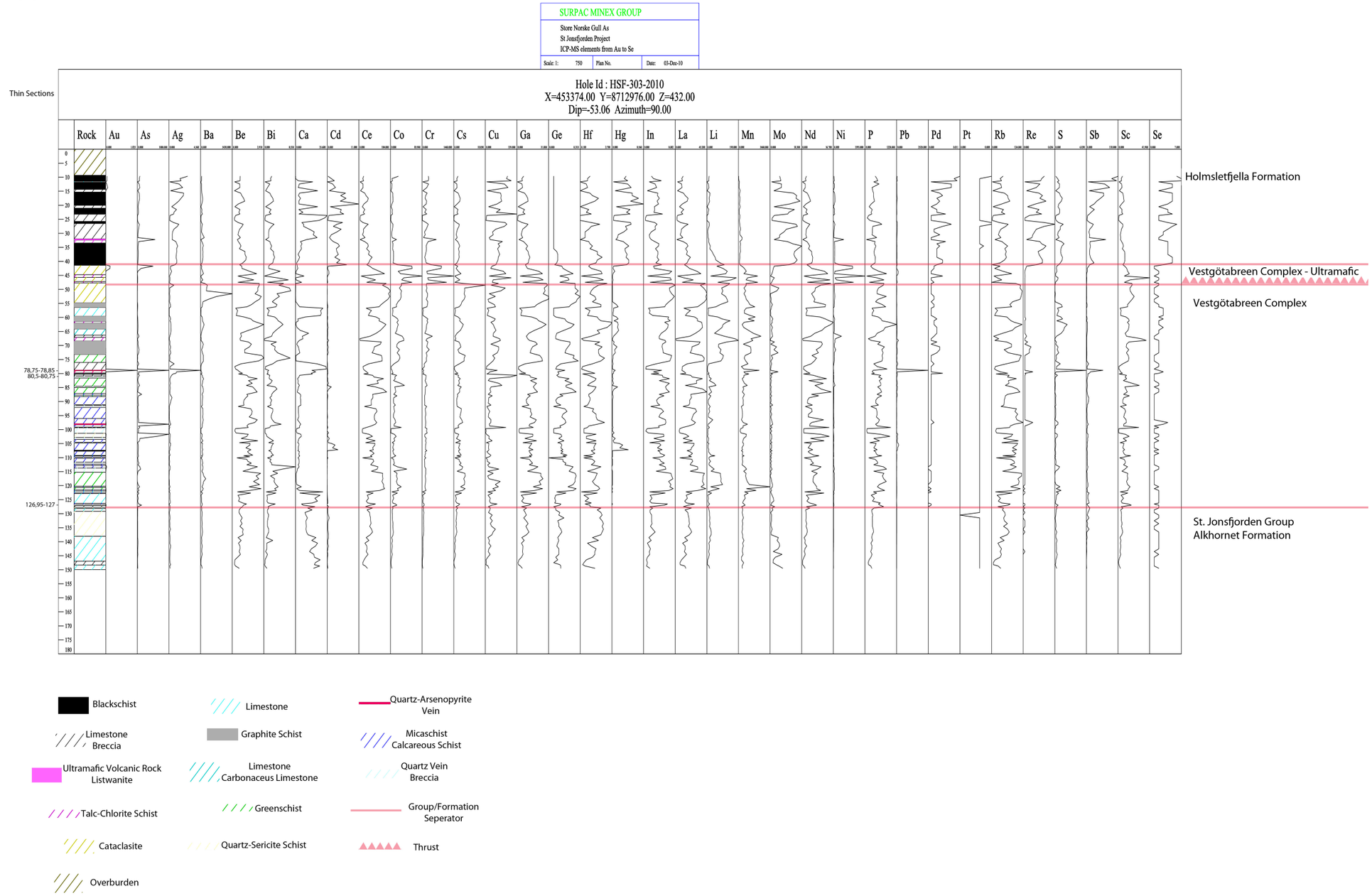


**Appendix 1.1:** Plot of drill hole HSF-303-2010 with depth along the y-axis and different elements along the x-axis. The amount of the different elements is plotted as graphs in relation to depth.

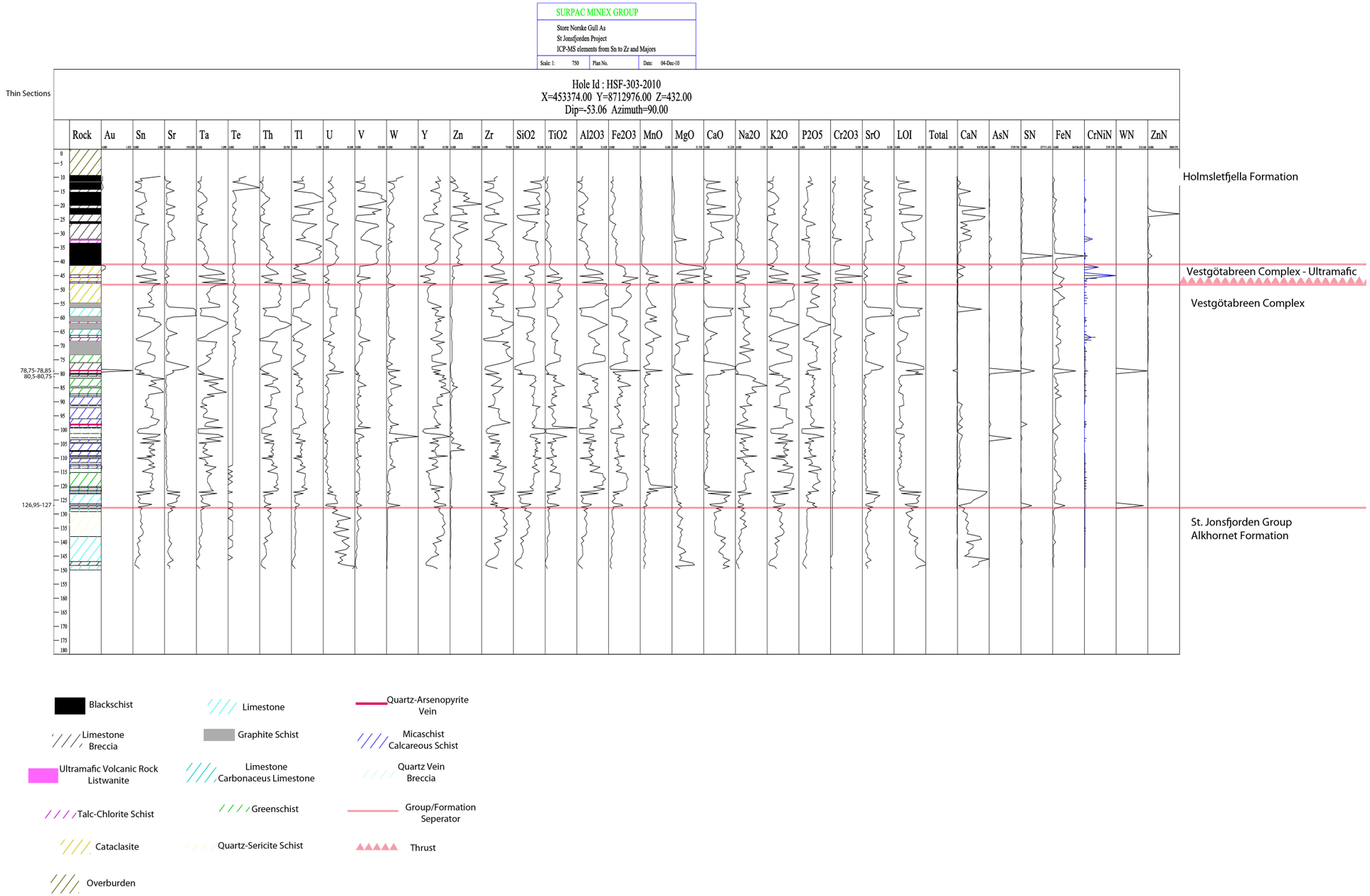


**Appendix 1.2:** Plot of drill hole HSF-303-2010 with depth along the y-axis and different elements along the x-axis. The amount of the different elements is plotted as graphs in relation to depth.

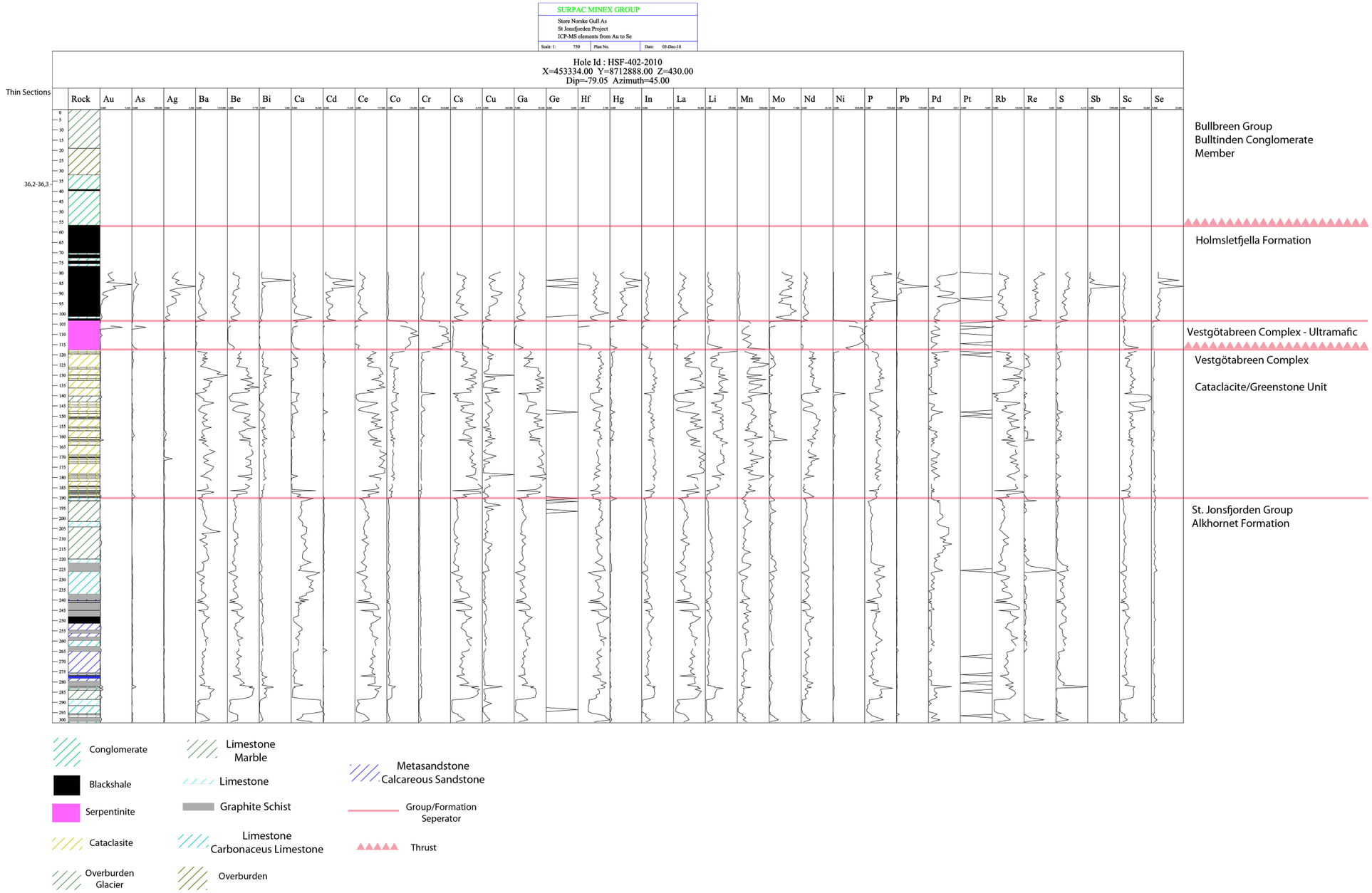


**Appendix 1.3:** Plot of drill hole HSF-402-2010 with depth along the y-axis and different elements along the x-axis. The amount of the different elements is plotted as graphs in relation to depth.

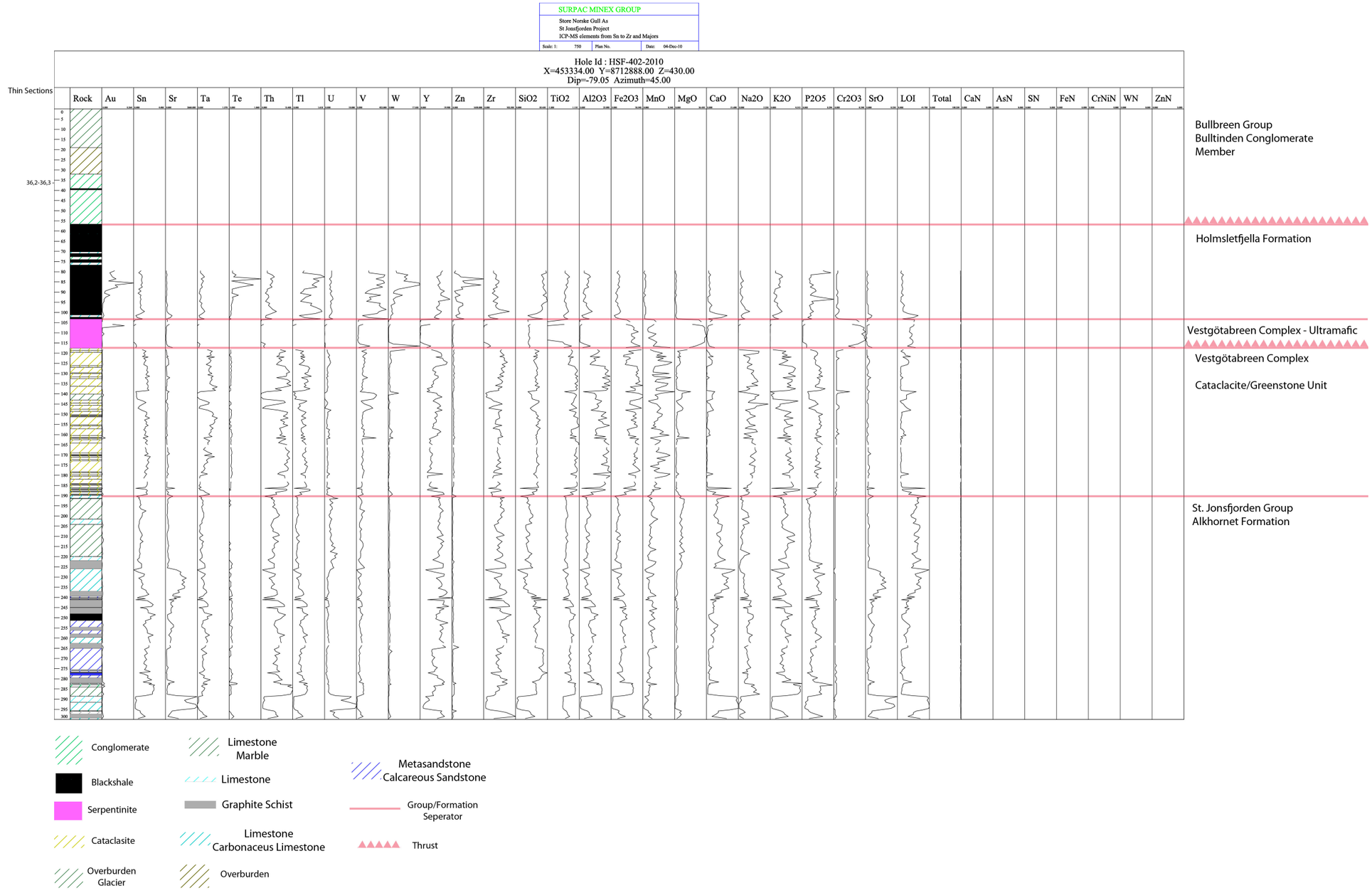


**Appendix 1.4:** Plot of drill hole HSF-402-2010 with depth along the y-axis and different elements along the x-axis. The amount of the different elements is plotted as graphs in relation to depth.

## Appendix 2

**Brief description of all the thin sections (TS):**

| Drill Hole | Meter | Group/Formation | Au Plot | As Plot | Remarks Plot | Rock Type TS | Mineral TS | Mineral TS | Mineral TS | Mineral TS | Mineral TS | Mineral TS |
|---|---|---|---|---|---|---|---|---|---|---|---|---|
| HSF-302 | 10.55-10.65 | Holmsletfjella Formation | Peak | | | Limestone | Carbonate | Graphite | Sulphides | Quartz | | |
| HSF-302 | 17.3-17.45 | Holmsletfjella Formation | Medium Peak | Very Small Peak | | Graphite schist | Graphite | Pyrite | Quartz | Carbonate | | |
| HSF-302 | 27.8-28.0 | Holmsletfjella Formation | Medium Peak | Very Small Peak | | Graphite schist | Graphite | Quartz | Carbonate | Muscovite | Pyrite | |
| HSF-302 | 33.3-33.45 | Border Holmsletfjella Fm. and Ultramafic Vestgötabreen complex | | | Cr spikes in the Ultamafic part | Graphite schist | Carbonate | Quartz | Graphite | Muscovite | | |
| HSF-302 | 34.4-34.55 | Ultramafic Vestgötabreen complex | | | Cr peak | Serpentinite | Carbonate | Muscovite | Serpentine | Pyrite | | |
| HSF-302 | 42.15-42.2 | Ultramafic Vestgötabreen complex | Small Peak | Very Small Peak | Cr peak | Serpentinite | Carbonate | Serpentine | Muscovite | Graphite | Chlorite | Chloritoid |
| HSF-302 | 47.4-47.5 | Vestgötabreen complex | | | High Al | Cataclasite | Muscovite | Quartz | Chloritoid | Chlorite | | |
| HSF-302 | 53.65-53.75 | Vestgötabreen complex | | | High Al | Cataclasite | Muscovite | Chlorite | Quartz | | | |
| HSF-302 | 53.75 B | Vestgötabreen complex | | | High Al | Cataclasite | chlorite | Quartz | Chloritoid | Hematite | | |
| HSF-302 | 60,7-60,9 | Vestgötabreen complex | | | | Quartz-Carbonate Rock | Carbonate | Quartz | Pyrite | | | |
| HSF-302 | 63,85-63,9 | Vestgötabreen complex | Small Peak | | | | Quartz | Muscovite | Chloritoid | Pyrite | | |
| HSF-302 | 69.6-69.75 | Vestgötabreen complex | peak | Very Small Peak | | Carbonate Rock | Carbonate | Muscovite | Pyrite | | | |
| HSF-302 | 71.5-71.6 | Vestgötabreen complex | Small Peak | Very Small Peak | | Carbonate Rock | Carbonate | Muscovite | Quartz | Pyrite | | |
| HSF-302 | 79.5-79.7 | Vestgötabreen complex | Peak | Peak | | Cataclasite | Carbonate | Muscovite | Quartz | Pyrite | Arsenopyrite | |
| HSF-302 | 85.5-85.9 | Vestgötabreen complex | Small Peak | Small Peak | Begining of medium Au and As peak | Carbonate Rock | Carbonate | Quartz | Muscovite | Pyrite | Arsenopyrite | |
| HSF-302 | 86.25-86.4 | Vestgötabreen complex | Small Peak | Small Peak | Mid way up the medium Au and As peak | | Carbonate | Quartz | Muscovite | Pyrite | | |
| HSF-302 | 88.8-88.95 | Vestgötabreen complex | Medium Peak | Medium Peak | Same peak as the two previous TS | | Quartz | Carbonate | Muscovite | Pyrite | Arsenopyrite | |
| HSF-302 | 98.5-98.65 | Vestgötabreen complex | Small Peak | Small Peak | | Quartz-Carbonate Rock | Quartz | Carbonate | Muscovite | sulphides | | |
| HSF-302 | 107.3-107.35 | Vestgötabreen complex | Just before peak | Just before peak | | | Quartz | Carbonate | Muscovite | Graphite | Pyrite | |
| HSF-302 | 123.65-123.7 | St. Jonsfjorden Group, Alkhornet Fm. | Peak | | | Carbonate Rock | Carbonate | Quartz | Muscovite | Pyrite | | |

| Drill Hole | Meter | Group/Formation from Plot | Au Plot | As Plot | Remarks Plot | Rock Type TS | Mineral TS | Mineral TS | Mineral TS | Mineral TS | Mineral TS | Mineral TS |
|---|---|---|---|---|---|---|---|---|---|---|---|---|
| HSF-501 | 27.3-27.5 | Bulltinden Conglomerate Member | | | Less shale upwards, Coarsing upwards | Conglomerate | Carbonate | Quartz | | | | |
| HSF-501 | 45,75 | Holmsletfjella Formation | Small peak | | | Graphite schist | Carbonate | Graphite | Pyrite | Quartz | | |
| HSF-501 | 78.4-78.6 | Holmsletfjella Formation | | | | Graphite schist | Graphite | Quartz | Carbonate | Muscovite | Pyrite | |
| HSF-501 | 81.15-81.3 | Holmsletfjella Formation | | | | Graphite schist | Graphite | Carbonate | Quartz | Pyrite | | |
| HSF-501 | 92.6-92.65 | Holmsletfjella Formation | | | | Graphite schist | Graphite | Quartz | Carbonate | Pyrite | | |
| HSF-501 | 107,6 | Holmsletfjella Formation | Peak | | | Black shale | Graphite | Carbonate | Quartz | Pyrite | | |
| HSF-501 | 130,6 | Holmsletfjella Formation | | | Just before Au peak | Carbonate Rock | Carbonate | Quartz | | | | |
| HSF-501 | 149,7 | Ultramafic Vestgötabreen Complex | Peak | | Quartzite | Listwanite | Quartz | Carbonate | Talc | Serpentine | Pyrite | |
| HSF-501 | 149,75 | Ultramafic Vestgötabreen Complex | Peak | | Quartzite | Listwanite | Quartz | Carbonate | Talc | Serpentine | Pyrite | |
| HSF-501 | 149,75 | Ultramafic Vestgötabreen Complex | Peak | | Quartzite | Listwanite | Quartz | Carbonate | Talc | Serpentine | Pyrite | |
| HSF-501 | 149,8 | Ultramafic Vestgötabreen Complex | Peak | | Quartzite | Listwanite | Quartz | Carbonate | Talc | Serpentine | Pyrite | |
| HSF-501 | 149,9 | Ultramafic Vestgötabreen Complex | Peak | | Quartzite | Listwanite | Quartz | Carbonate | Talc | Serpentine | Pyrite | Arsenopyrite |
| HSF-501 | 176,3 | Vestgötabreen complex | | | Cataclasite | Cataclasite | Quartz | Muscovite | Chlorite | | | |
| HSF-501 | 191,9-192,1 | Vestgötabreen complex | | | Cataclasite | Cataclasite | Muscovite | Chlorite | Carbonate | | | |
| HSF-501 | 226,65-226,75 | Vestgötabreen complex | | | Cataclasite | Cataclasite | Muscovite | Chlorite | Quartz | | | |
| HSF-501 | 230,5 | Vestgötabreen complex | | | Cataclasite | Cataclasite | Muscovite | Chlorite | | | | |
| HSF-501 | 239,55 | St. Jonsfjorden Group | Small peak | Small peak | Sandstone | Sandstone | Quartz | Carbonate | Muscovite | Pyrite | | |
| HSF-501 | 242,2 | St. Jonsfjorden Group | Very small peak | Small peak | Sandstone | Sandstone | Carbonate | Muscovite | Quartz | Pyrite | | |
| HSF-501 | 251,45 | St. Jonsfjorden Group - Alkhornet Fmormation | | | | Carbonate Rock | Carbonate | | | | | |
| HSF-501 | 280,9-281 | St. Jonsfjorden Group - Alkhornet Fmormation | | | | Dirty Limestone | Carbonate | Graphite | Pyrite | | | |
| HSF-502 | 317 | St. Jonsfjorden Group - Alkhornet Fmormation | | | | Quartz-Carbonate Rock | Quartz | Carbonate | Muscovite | Pyrite | | |
| HSF-501 | 320-320,1 | St. Jonsfjorden Group - Alkhornet Fmormation | | | | Limestone | Carbonate | | | | | |

| DH | Meter | Group/Formation from Plot | Au Plot | As Plot | Remarks Plot | Rock Type TS | Mineral TS | Mineral TS | Mineral TS | Mineral TS |
|---|---|---|---|---|---|---|---|---|---|---|
| HSF-303 | 78.75-78.85 | Vestgötabreen Complex | peak | peak | Ag Pb Ca Fe and S peak | Carbonate Rocl | Carbonate | Quatz | Pyrite | Arsenopyrite |
| HSF-303 | 80.5-80.57 | Vestgötabreen Complex | | | | Sandstone | Quatz | Carbonate | Muscovite | Pyrite |
| HSF-303 | 126.95-127 | Vestgötabreen Complex | | | | Carbonate Rock | Carbonate | Quatz | Pyrite | |

| DH | Meter | Group/Formation from Plot | Au Plot | As Plot | Rock Type TS | Mineral TS | Mineral TS | Mineral TS | Mineral TS | Mineral TS | Mineral TS |
|---|---|---|---|---|---|---|---|---|---|---|---|
| HSF-402 | 36.2-36.3 | Bulltinden Conglomerate Member | peak | | Conglomerate | Quatz | Carbonate | Muscovite | Chloritoid | Pyrite | Arsenopyrite |